EFFECTS OF ALTERED GRAVITY ON JUMPING
PERFORMANCE AND INTERMUSCULAR CONTROL

95-004D

APPROVED BY
DISSERTATION COMMITTEE:

Lawrence D. Abraham Co-supervisor

R. Joe Thornhill Co-supervisor

19950517 096

REPORT DOCUMENTATION PAGE

Public reporting burden for this collection of information is estimated to average 1 hour per response, including the time for reviewing instructions, searching existing data sources, gathering and maintaining the data needed, and completing and reviewing the collection of information. Send comments regarding this burden estimate or any other aspect of this collection of information, including suggestions for reducing this burden, to Washington Headquarters Services, Directorate for Information Operations and Reports, 1215 Jefferson Davis Highway, Suite 1204, Arlington, VA 22202-4302, and to the Office of Management and Budget, Paperwork Reduction Project (0704-0188), Washington, DC 20503.

1. AGENCY USE ONLY (Leave blank)	2. REPORT DATE May 95	3. REPORT TYPE AND DATES COVERED

4. TITLE AND SUBTITLE
Effects of Altered Gravity on Jumping Performance & altered Intermuscular Control

5. FUNDING NUMBERS

6. AUTHOR(S)

David P. Carpenter

7. PERFORMING ORGANIZATION NAME(S) AND ADDRESS(ES)

AFIT Students Attending:

Univ of Texas - Austin

8. PERFORMING ORGANIZATION REPORT NUMBER
AFIT/CI/CIA

95-004 D

9. SPONSORING/MONITORING AGENCY NAME(S) AND ADDRESS(ES)

DEPARTNEMT OF THE AIR FORCE
AFIT/CI
2950 P STREET, BDLG 125
WRIGHT-PATTERSON AFB OH 45433-7765

10. SPONSORING/MONITORING AGENCY REPORT NUMBER

11. SUPPLEMENTARY NOTES

12a. DISTRIBUTION/AVAILABILITY STATEMENT

Approved for Public Release IAW AFR 190-1
Distribution Unlimited
BRIAN D. GAUTHIER, MSgt, USAF
Chief Administration

12b. DISTRIBUTION CODE

13. ABSTRACT (Maximum 200 words)

DTIC
SELECTED
MAY 18 1995
B

DTIC QUALITY INSPECTED 6

14. SUBJECT TERMS			15. NUMBER OF PAGES 155
			16. PRICE CODE

17. SECURITY CLASSIFICATION OF REPORT	18. SECURITY CLASSIFICATION OF THIS PAGE	19. SECURITY CLASSIFICATION OF ABSTRACT	20. LIMITATION OF ABSTRACT

Dedication

I am dedicating this effort to my parents, grandparents and godparents.

EFFECTS OF ALTERED GRAVITY ON JUMPING PERFORMANCE AND INTERMUSCULAR CONTROL

by

DAVID R. CARPENTER, B.S., M.S.

DISSERTATION

Presented to the Faculty of the Graduate School of

The University of Texas at Austin

in Partial Fulfillment

of the Requirements

for the Degree of

DOCTOR OF PHILOSOPHY

THE UNIVERSITY OF TEXAS AT AUSTIN

May, 1995

Acknowledgements

First, I wish to acknowledge my committee. I wish to thank Dr. Abraham, Dr. Thornhill, Dr. Spirduso, Dr. Barr, and Dr. Poitrast for all of their time, advise, and assistance. Dr. Abraham and Dr. Thornhill, co-chairmen of my committee, were outstanding. I owe a great debt to the U. S. Air Force for both finical and technical help. This includes John Frazier and Dr. Burton. These two individuals allowed this study to start and then run smoothly. I also wish to thank my laboratory comrades, Jim, Clay, Kristin, Brian and Patrica, for all of their support. I need to thank Roxanne Constable for all of her help. I hope this is just the beginning of our combined research efforts.

Janice, my spouse and my friend, thank you for all of your support not only for the last four years but also the last 16 years. You have both motivated me and helped me keep most aspects of my life in balance. I can't wait to see what we will do in the next 16 years!

EFFECTS OF ALTERED GRAVITY ON JUMPING PERFORMANCE AND INTERMUSCULAR CONTROL

Publication No._____

David R. Carpenter, Ph.D.

The University of Texas at Austin, 1995

Supervisors: Lawrence Abraham and R. Joe Thornhill

The purpose of this study was to determine the effect of altered gravity on human jump performance and intermuscular control. A musculoskeletal model was used to determine jump height, muscle power and energy delivered to the skeletal system (jump performance), and changes in muscle neuroexcitation and activation patterns (intermuscular control) for different values of gravity. The different values of gravity ranged from 0.2 to 1.8 times earth gravity. Prior to analyzing the musculoskeletal model solutions, the model solutions were validated by comparing predicted jump heights, time-required-to-jump, ground reaction force, joint kinematics and muscle neuroexcitations to measured experimental data collected in increased gravitational environments. The increased gravitational environments were achieved by using the Dynamic Environment Simulator, a centrifuge rated for human study, located at Wright-

Patterson AFB, Ohio. Subjects performed non-countermovement squat jumps in environments of 1.0, 1.2, 1.4, 1.6 and 1.8 times earth gravity. Comparison of experimental data to the musculoskeletal model solutions indicated that the four segment, twenty muscle, planar model adequately replicated the major dynamic features of human jumping.

Using all of the simulation solutions, it was found that 1) jump height was inversely related to gravity, 2) the time-required-to-jump increased as gravity increased, and 3) angular joint displacement patterns and muscle neuroexcitation and activation patterns did not change when gravity was altered. Further analysis of the model solutions also indicated that the peak muscle force and peak muscle power generated did not substantially increase as gravity increased. The total energy delivered to the skeletal system increased as gravity increased due to the longer integration time of the power, but at a lesser rate than the changes in gravity. The take-off height of the jump remained constant and take-off velocity decreased as gravity increased. This resulted from the re-distribution of the total energy utilized during the jumps. The potential energy increased directly (constant take-off height) with the increase of gravity but the kinetic energy (take-off velocity) decreased as gravity increased.

Table of Contents

List of Figures

List of Tables

Chapter 1: Introduction

Humans sometimes live and work in altered gravitational environments. Aircrew members of high performance aircraft function in environments where the force due to motion is up to twelve times greater than earth's gravity, while space flight requires astronauts to live and work in micro-gravitational environments. The individual must adjust to the different forces resulting from altered gravity to perform work and sustain life. The aircraft pilot is required to maintain consciousness (Whinnery, 1990; and Moore et al., 1993) and perform specific tasks in high gravitational environments to survive. For the astronaut, prolonged exposure to micro-gravity leads to physiological changes in both bone and muscle (Apseloff et al., 1992; Arnaud et al., 1992; Berry et al., 1993; and Krippendorf et al., 1993). To fully understand how humans perform in altered gravitational environments, the changes in musculotendon forces, and how these changes affect the motion of the body segments in response to altered gravity, need to be quantified.

Musculotendon forces in humans are extremely difficult to determine experimentally. An alternative method to determine musculotendon forces is to estimate musculotendon forces using mathematical models that include an accurate representation of musculotendon dynamics. A combination of optimal control theory (or dynamic optimization techniques) and musculoskeletal computer modeling is potentially the most powerful method for determining

1

musculoskeletal forces during human movement (Hatze 1976; and Davy and Audu, 1987). This form of modeling, in earth gravity, has been used to predict musculotendon forces generated during kicking (Hatze, 1976; and Ziegler 1994), walking (Davy and Audu, 1987) bicycle pedaling (Sim, 1988), vertical jumping (Pandy et al., 1990; Anderson and Pandy, 1993; Fujii and Toshimichi, 1993; and van Soest et al., 1993) and rising from a chair (Heekin, 1991; Garner, 1992; and Daigle 1994).

These models are mathematical descriptions of human movement and are based on approximations of muscle activation dynamics, musculotendon dynamics, and body segment dynamics. Parameters for activation dynamics, maximum isometric force of the muscle, length and intrinsic maximum shortening velocity of muscle relationship, and the attachment sites for the musculotendon actuators are all based on data reported in the literature. Segment parameters (i.e. moment of inertia, mass, length, and center of mass) are also based on literature data. Direct validation of the musculoskeletal model is not possible, i.e. predicted muscle forces cannot be compared directly with measured muscle forces. Therefore, once all of these parameters are combined to create the musculoskeletal model, each parameter is adjusted until an acceptable agreement exists between predicted and experimentally determined kinematics and ground reaction forces (see Pandy et al., 1990; and van Soest et al., 1993 for examples). Recently, an attempt was made to use this modeling approach to predict changes in musculotendon forces during jumping in both hypo- and hyper-gravitational environments (Loveland et al., 1992). Importantly however, these predictions were never validated against appropriate experimental data.

Modeling jumping in altered gravitational environments and verifying the simulation results with experimental data will not only justify the parameters used in the musculoskeletal model, but it will also provide insight into the effects of gravity on human performance. By analyzing the musculoskeletal model solutions, using the same anthropometric parameters at different values of gravity, changes in musculotendon forces, the timing and sequencing of muscles, and the resulting power and energy delivered to the skeletal system can all be estimated.

1.1 RESEARCH QUESTION

The research question is "how do changes in gravitational force affect jumping performance and intermuscular control?"

Jumping performance was divided into two areas, 1) the maximum height reached by the body's center of mass during a non-countermovement jump and 2) the musculotendon power and energy delivered to the skeleton during the propulsion phase of the jump. A non-countermovement jump was a jump that began from a static squatting position, followed by propulsion of the center of mass continuously upward. Intermuscular control referred specifically to the timing and sequencing of the neural excitation of the muscles required to perform a maximal effort jump. Muscle neuroexcitation gave information about the motor control patterns that led to the voluntary musculotendon forces that resulted in movement of the skeletal system.

1.2 DEFINITION OF TERMS

This section contains system language definitions used in this study. This study is multidisciplinary and therefore contains nomenclature from several disciplines including kinesiology, musculoskeletal modeling, mechanical engineering and gravitational research. The nomenclature format used in each discipline is slightly different. Rather than developing a new nomenclature, the different nomenclatures will be used as appropriate. To assist in reading the document, all symbols used in this document are defined in Table 1.1 (page 6).

Bi-articular Muscle: Any muscle that spans two joints.

Dynamic Environment Simulator (DES): A centrifuge located at Wright-Patterson Air Force Base that was used to altered the forces acting on the subject's center of mass.

Gravity: The attractive force between the earth and a body. On the surface of the earth, the gravitational force induces an acceleration on the center of mass of the body equal to 9.806 m/sec^2, directed toward the center of the earth.

G_z: A system term used in centrifuge studies. G_z is the scalar quantity equal to the magnitude of the external force acting on the subject's center of mass in the direction of the line created by the intersection of the frontal and sagittal planes divided by the magnitude of gravity.

HAT: The combination of the trunk, head and arms areas of the body. For modeling purposes, the HAT segment was considered a rigid body.

Musculoskeleton: The combined muscle and skeletal tissues.

Musculotendon: The combined muscle and tendon tissues.

Uni-articular Muscle: A muscle that spans only one joint.

Table 1.1 Abbreviations and Symbols used in this Document

$\underline{AFB}$ - Air Force Base

$\underline{A(\theta)}$ - mass matrix

$\underline{^z\bar{a}_{com}}$ - acceleration of the COM in the z direction

$\underline{^z\bar{a}_n}$ - acceleration of the COM towards the center of rotation

$\underline{\bar{a}_g}$ - acceleration of the COM resulting from gravity

$\underline{a(t)}$ - muscle activation

$\underline{\dot{a}(t)}$ - derivative of muscle activation

$\underline{\alpha}$ - pennation angle of muscle fibers

$\underline{B(\theta)}$ - matrix that contains centrifugal and Coriolis terms

$\underline{\beta}$ - incline in the z x plane of a body in the cab of the DES

$\underline{C}$ - constraint

$\underline{C(\theta)}$ - matrix that contains gravitational terms

$\underline{COM}$ - center of mass

$\underline{^z\bar{d}_{com}}$ - displacement of COM in the z direction

$\underline{D(\theta)}$ - matrix that contains terms to convert joint torques to segment torques

$\underline{DES}$ - Dynamic Environment Simulator

$\underline{E}$ - energy

$\underline{F^{MT}}$ - magnitude of the musculotendon force

$\underline{\dot{F}^{MT}}$ - magnitude of the derivative of musculotendon force

$\underline{\mathbf{F}^T}$ - matrix that contains muscle forces

$\underline{F^T}$ - magnitude of the force in tendon

$\dot{F}^T$ - magnitude of the derivative of tendon force

F_0^M - magnitude of peak isometric muscle force

$\bar{F}_n$ - force exerted on a body due to rotation directed toward the center of rotation

$\bar{F}_r$ - vector sum of gravity and the reaction force resulting from $\bar{F}_n$

GRF - ground reaction force in the z direction

H - height

i - indicator of segment, 1 - foot, 2 - shank, 3- thigh, and 4 - HAT

I_i - moment of interia about the COM of the ith segment

J - performance criteria

j - discrete time step during an integration, $1 \leq j \leq$ # integration steps

K.E. - kinetic energy

l_0^m - optimal fiber length

l_s^t - tendon slack length

L^{MT} - length of musculotendon actuator

l_{ci} - distance of COM from distal end of the ith segment

l_i - length of ith segment

$M(\theta)$ - moment arm matrix

$\bar{M}_o$ - moment about point O directed in the x direction

minang – minimum joint angle prior to assessing hyper-extension penalty

maxang – maximum joint angle prior to assessing hyper-extension penalty

P - instantaneous power

P.E. - potential energy

pen_c - penalty function for countermovement

$\underline{pen_h}$ - **penalty function for joint hyper-extension**

$\underline{SEMG}$ - **surface** electromyography

$\underline{\theta}$ - segment angle

$\underline{\theta_0}$ - foot **angle** where spring-damper system becomes active

$\underline{T\left(\theta, \dot{\theta}\right)}$ - **matrix** that contains ligament and toe torques

$\underline{\tau}$ - torque

$\underline{t_{rise}}$ - rise **time** constant

$\underline{t_{fall}}$ - fall **time** constant

$\underline{u(t)}$ - muscle neuroexcitation

$\underline{V_{max}}$ - **magnitude of maximum muscle shortening velocity**

$\underline{V^{MT}}$ - **magnitude of the musculotendon actuator velocity**

$\underline{^X\bar{V}}$ - velocity of the COM directed toward the center of rotation

$\underline{^z\bar{v}_{com}}$ - velocity of the COM in the z direction

$\underline{\bar{W}}$ - body weight

$\underline{w}$ - width

$\underline{\bar{\omega}}$ - angular velocity of DES, directed in the Z direction

$\underline{X\ Y\ Z}$ - **reference** frame attached to the centrifuge, Z passes through the center of the centrifuge in the same direction as gravity, X is perpendicular to Z and attached to the rotating arm of the centrifuge, and Y is perpendicular to both Z and X.

$\underline{x\ y\ z}$ - reference frame attached to the subject, z is directed along the line created by the intersection of the sagittal plane and frontal plane, x is directed along the line created by the intersection of the frontal plane and transverse plane and y is

directed along the line created by the intersection of the sagittal plane and transverse plane.

1.3 LIMITATIONS

Subjects were required to jump in a spinning centrifuge. For safety reasons, the subjects were required to wear safety equipment designed to prevent injury potentially caused by collisions with the centrifuge structure. The safety equipment could have interfered with the subjects' ability to perform the jump. During the jump, the subjects' movement included a radial component. This resulted in the production of Coriolis acceleration. The Coriolis acceleration was in the Y direction (see Chapter Three and Figure 3.3). The maximum Coriolis acceleration was much less than any other acceleration the subjects experienced and was usually near zero until the very end of the jump. To minimize subject discomfort and reduce the possibility of motion sickness and termination of the test, subjects experienced increases in gravity in a linear step method rather than randomized levels of gravity. This presented the possibility of treatment order effects in the results.

1.4 DELIMITATIONS

All subjects were male, active duty Air Force personnel, experienced centrifuge riders who met minimal United States Air Force physical fitness and medical standards. This implied the subjects were physically active, maintained routine aerobic exercise program, were drug and alcohol free, and were asymptomatic of any musculoskeletal or neurological disease. Generalization of the conclusions from this study to a population with a different physical profile may be unwarranted.

1.5 SIGNIFICANCE

This study demonstrated how musculoskeletal modeling combined with optimal control theory adequately simulated human movement in different gravitational environments. In addition, analysis of the model simulations in altered gravity gave insight into the effect gravity had on jumping performance and intermuscular control. This information was needed in order to understand how muscle coordination, muscle force, power, and energy all changed with gravity. The results of this study can be used to understand the stresses of altered gravitational exposure better and to allow early intervention to prevent injury.

Tasks performed in space require unique tools that allow an interface between humans and machines. By knowing muscle coordination and muscle force requirements prior to entering a micro-gravitational environment, better tool design, work plans, and exercise programs during space flight can be developed. This could lead to a higher probability of mission success and substantial cost savings. Also, exercise strategies could be developed that more effectively load the skeleton and reduce muscle atrophy during space flight. For increased gravitational environments, such as those found in high performance aircraft, understanding the muscle and skeletal loading during high gravitational exposures could lead to better design of the cockpit. This would allow for increased survivability of aircrews and a distinct advantage during adversarial air conflicts.

Chapter 2: Literature Review

The research question, "how do changes in gravitational force affect jumping performance and intermuscular control?" was answered by using a musculoskeletal model. The literature review discusses three general areas related to the research question: 1) altered gravitational environments, 2) musculoskeletal modeling, and 3) jumping.

2.1 ALTERED GRAVITATIONAL ENVIRONMENTS

Until the advent of the airplane, less than 100 years ago, the issue of the effects of altered G_z on human health and performance was of little interest. The only exposure an adult had to altered G_z prior to the airplane was during certain amusement activities, such as roller coaster and Ferris wheels. Many children and some adults have experienced altered G_z effects by hanging upside down from a tree so that the force of gravity acting on the body is directed in the opposite direction. In the 1970's and 80's, hanging from the ankles using "inversion boots" was marketed as an exercise program. Vehrs et al. (1988) investigated the physiological response to inversion and found that during inversion the systolic and diastolic blood pressures increased as well as the systolic/diastolic ratio. Also, heart rate and oxygen consumption increased while inverted. These effects quickly reversed as soon as the subjects were righted. The manufacturers claimed these effects were normal and related to any exercise program, however, Vehrs found that the effects were not permanent and, after five weeks of inversion

exercise, the subjects had the same physiological responses as the first day of the study, thus no physiological conditioning took place. Vehr's findings for the simple system described are an accurate depiction of the problems of altered G_z exposure. Undesirable physiological events that impair the individual begin to occur the instant G_z is altered but are reversed once the individual is brought back to a 1.0 G_z environment. A more detailed description of the overall effects of long term space flight and delivery of health care can be found in Sekiguchi (1994) and Bonde-Petterson (1994).

Prolonged exposure to micro-gravity does have dangerous effects on humans. Muscle tissue atrophies in micro-gravity environments which is progressive with increase time of exposure (Ilyina-Kakueva et al., 1976; and Martin et al., 1982) To simulate a micro-gravity environment, Krippendorf and Riley (1993) suspended the hindquarters of rats for 12 days, then biopsies the muscle after initial reloading of the hindquarters and 48 hours later. They found that significant changes occurred in the muscle morphology after 12 days of suspension, but the effects began to reverse within 48 hours of reloading. Essentially, if the micro-gravity induced muscle atrophy is of a short duration, the muscle atrophy is reversible.

The skeletal system also experiences deleterious effects to micro-gravity exposure. Bone is absorbed during micro-gravity exposure (Morey and Baylink 1978; Berry et al., 1993; and Arnaud et al., 1992). Concerned that long micro-gravity exposures (years) could eventually make re-acclimation to earth gravity impossible, attempts have been made to find drugs that will slow down the bone loss. Unfortunately, drugs that are successfully used for diseases that induce bone

loss (such as Paget's disease) have proven ineffective for bone loss due to micro-gravity environments (Apseloff et al. 1992).

In the 1950's and early 1960's, human exposure to altered gravitational environments was of short duration. Even in the space program, the duration of American space flights were limited to only a few days. In all cases, the individuals exposed were constrained to a sitting position with little room to move about. Therefore, the major research efforts were geared to study the effects of alter gravity on neuromotor activities such as reaching. A common method to achieve an altered gravitational environment was parabolic flight (Beckh, 1954; Gerathewohl et al., 1957; Roman et al. 1963; and Whiteside 1961). In these studies, an aircraft was taken to a high altitude and then placed into a nose dive, followed by flying the aircraft out of the dive into a steep climb. Thus both hypo- and hyper-gravitational environments could be achieved. In these studies, the subjects were able to replicate a pattern or touch a designated point in all environments when the target and hand were visible. However, when the hand was not visible, subject performance degraded substantially in both hypo- and hyper-gravitational environments. The subjects typically aimed high in the hypo-gravitational environments and low in the hyper-gravitational environments.

Parabolic flight does allow both hypo- and hyper-gravitational exposures however, the duration of the exposure is very short (less than thirty seconds). Thus the testing protocol is limited in time as well as the stability of the airframe. Cohen (1970) used a centrifuge to expose subjects to sustained 2.0 G_z environment. This allowed Cohen to observe both the initial performance as well as changes in performance due to repetition. Using a mirror projected image

(therefore the subject could not see his hand) the subjects were directed to touch the target in the hyper-gravitational state. Initially, the subjects missed the target low. After several repetitions, the subjects started to miss the target high. Cohen concluded that with minimal number of repetitions, humans can accommodate to altered gravitational environments.

The studies to date indicate that many tasks can be performed in a range of different gravitational environments. Eventually, the load due to increase gravity inhibits the performance. Hyper- G_z environments impair reaching capabilities. Astronauts experience increased G_z environments on lift-off and re-entry. During these phases of flight, the astronauts are required to wear specialized life support suits. The combination of the life support suits and G_z levels greater than 3.0 G_z leads to a decreased reach distance (Schafer and Bagian, 1993; and Bagian and Schafer, 1992). At present, astronauts experience a maximum of 3.0 G_z during take-off but, in the future, astronauts will need to withstand in excess of 6.0 G_z during take-off. This means the entire cockpit will need to be redesigned because of the reaching limitations induced on man by increased G_z environments.

In the 1970s and 1980s, astronauts stayed longer in space and performed many activities that required more than reaching. Thus, the effect of micro-gravity on posture became an important research issue. Specifically, how is the muscle coordination associated with a task changed by the lack of gravity. Several researchers have studied the SEMG signals from the arms, back and legs associated with posture in simulated micro-gravity environments and compared the results to 1.0 G_z environment (Layne and Spooner, 1990; Clement et al.,

1985; and Horstmann and Dietz 1990). Posture was disturbed by either having the subjects perform rapid arm movement or the use of a tilt floor. The results of these studies were similar. The surafce electromyography, SEMG, activity (SEMG magnitude, frequency, and sequencing) in the arms and back did not change as gravity was reduced however, the SEMG activity in the legs ceased in a micro-gravity environment. One possible explanation for the loss of leg SEMG activity in a micro-gravity environment is that in a micro-gravity environment, unless the subjects feet are constrained to the floor, a subject cannot fall (torque at the feet would be zero) therefore, leg action is not required.

The United States and Russia have sent astronauts and cosmonauts into space for long duration. Both astronauts and cosmonauts experienced significant loss of muscle and bone tissues and it became apparent that intervention during flight was necessary. This lead to an expansion of the research in the altered gravity to include full body motion. Numerous devices were built to simulate alter- gravitational environments. In general, these devices included drop towers, elevators, sled/track, aircraft, water submersion and vertical cable suspension (Davies and Cavanagh, 1993). The Americans tried several different exercise programs (Thornton and Rommel, 1977). Initially, a stationary bicycle was placed on the skylab for the astronauts to use. The results of using the bicycle were disappointing. Even the astronauts who rigorously used the bicycle experienced significant loss of muscle mass. On skylab 4, a treadmill was used for exercise. A bungee cord, that produced equivalent force near body weight, pulled the astronaut toward the surface of the treadmill. It was found that the astronauts that routinely used the treadmill system did not lose muscle mass

during the mission. The cosmonauts also used a treadmill similar to the Americans (Hargens, 1994). The bungee cords on the Russian treadmill generated only 65 percent body weight. The cosmonauts who used the treadmill still experienced significant muscle mass loss. These experiences seem to indicate substantial loading of the lower mass during space flight is required to prevent muscle tissue loss. Whalen (1993) concluded that a device that was designed to abate the orthostatic pressure loss (lower body negative pressure, LBNP) due to micro-gravity could also be used to load the lower extremities during space flight. By placing a treadmill inside the LBNP device, the negative pressure acting on the astronaut's lower body would force the legs onto the treadmill. The astronaut could then walk or jog on the treadmill resulting in loading forces similar to those found on earth.

The effect of altered gravity on whole-body movement (running and jumping) have also been experimentally simulated (He et al. 1991; and Cavagna et al., 1972). In both studies, the simulated gravitational environments were achieved by a system of pulleys and weights. SEMG data were not collected in either study and the results of the two studies were similar. As gravity was increased, the ground contact time increased and flight time decreased. For running at a constant speed, the stride length decreased and frequency increased as gravity increased. For jumping, the take-off velocity decreased as gravity increased. In both cases, the GRF pattern, once normalized in time, remained constant between different gravitational environments. The results of both studies indicate that the muscle coordination associated with the activities does not

change with gravity rather, the observed performance changes are due to the changing external load resulting from the altered gravity.

2.2 MUSCULOSKELETAL MODELING

Altered G_z environments affect human performance, cause short term illness and have long term negative physiological effects on humans. These problems can only be alleviated by proper physiological training and engineering controls. To solve the musculoskeletal problems, understanding how the muscle and skeletal forces change with G_z is imperative. Unfortunately, these forces cannot be easily measured, therefore, musculoskeletal models need to be used.

Modeling of human motion can be divided into two general areas, forward dynamics and inverse dynamics (Zajac and Gordon, 1991; Winter, 1990; and Happee, 1994). Inverse dynamics is the process of using measured external forces, such as ground reaction force and seat force, and kinematic data combined with estimates of the subject's anthropometric parameters to assess the resultant joint torques during movement. Once the resultant joint torques are found, estimates of the muscle forces that created the net torques can be made. A forward dynamics solution involves estimating the muscle neuroexcitations that lead to muscle force and muscle movement. The muscle force and movement create power and energy that are transferred to the skeletal system and produce motion. For both inverse and forward dynamics, simplifications of the skeletal system are made (Winter, 1990; and Rim and Chao, 1969). These simplifications

include reducing the number of degrees of freedom of the skeletal system, assuming the body to be comprised of rigid links, and using approximations for the dynamic properties of bone. For forward dynamics, additional approximations for muscle neuroexcitation and activation, maximum muscle force production, muscle length, shortening velocity, tendon parameters and path the muscle follows are also made (Zajac and Gordon 1991).

The inverse dynamics approach requires the input of experimental data while the forward dynamics approach does not require experimental data to produce a result. However, experimental data are needed for the validation of the forward dynamic solution. Normally in the formulation of a forward dynamic problem, some type of controller or optimizer is needed to achieve a final solution. One method to control the inputs to the model is optimal control theory (Rim and Chao, 1969; Hatze, 1976; and Davy and Audu, 1987). Based on an initial guess and some performance standard, a better set of controls is found. This process is repeated until no improvement in performance can be made (Gill et al., 1981). A second method of controlling the forward dynamic model is a hybrid approach (Cholewicki and McGill, 1994). Optimal control theory is combined with SEMG data to find the best solution for the problem. This method has the advantage that the solution is at least partially based on actual data while the former method is based solely on how well the performance criteria mimic the actual system.

2.3 JUMPING

In 1921, Sargent proposed that vertical jumping was a measure of man's strength or ability to generate power (in Vanderewalle et al., 1987). Jump height is a function of the velocity and height of the center of mass at take-off. Both velocity and height of the center of mass at take-off can be calculated from the ground reaction force (Davies and Rennie, 1968; and Offenbacher, 1970). To achieve a successful jump, the subject must possess sufficient strength to overcome the gravitational force and achieve an airborne state.

Strength is difficult to define. Operational definitions of strength usually take one of two forms; 1) the maximum individual force that can be obtained from a muscle or group of muscles (Kulig et al., 1984) or 2) the maximum resultant torque created at a joint by the muscle(s) spanning that joint (Cabri, 1991). The maximal isometric force produced by muscle has been related to the muscle cross-sectional area (Brenton et al., 1981; Buckle et al., 1979; Haggmark et al., 1978; Termote et al., 1980; and Klitgaard et al., 1990). The maximum tension produced in muscles of young and middle aged men varies between 40 to 100 N/cm^2. The variability in reported muscle tension is in part due to the method of estimating muscle forces. Muscle force is calculated by measuring joint torque and dividing the torque by an approximation for the muscle moment arm. The best estimate of isometric muscle force is limited by the accuracy of measuring joint torque and estimating moment arm length. The largest relative error exists in determining the length of the moment arm of a muscle. The moment arms created between muscles and the skeletal system have not been determined extensively in humans.

The few researchers that have measured moment arms in humans used x-ray and cadaver studies (Spoor and van Leeuwen, 1992; Spoor et al., 1990; and Smidt, 1973). The reported measured moments arms in the lower extremities have a coefficient of variation no better than 25%, therefore, the reported muscle forces, based on joint torques, have at best a coefficient of variation of 25%. Reports describing nominal strength values are abundant, based on joint torques, for a variety of different populations (Kannus et al., 1991; Osternig et al., 1977; Scudder, 1980; Olsen et al., 1972; Knapik et al., 1983; and Murray and Sepic 1970). Using the reported strength values, a four-fold difference exist in reported muscle force between the most physically fit population and physically inactive populations.

Several studies have verified the relationship between isometric muscle force and muscle cross-sectional area. However, no such relationship has been demonstrated between isokinetic muscle force and muscle cross-sectional area (Schantz et al., 1983; Maughan et al., 1983; Herzog et al., 1991; and Brand et al., 1986). Jumping is affected by the isokinetic properties of muscle rather than the isometric properties. Thus, knowledge of isometric muscle force alone is not sufficient to predict jumping performance.

Numerous attempts have been made to correlate jump height to isometric joint torques and subject anthropometric data. Most researchers have found a weak relationship, $r < 0.40$ (Grassi, 1991; Sipila et al., 1991; Mayhew and Salm, 1990; Colliander and Tesch., 1992; and White and Johnson, 1993). Other researchers have found a moderate relationship, $r = 0.45$, between jump height, joint torque and anthropometrics (Hortobagyi et al., 1990; Nutter and Thorland,

1987; and Ball et al., 1992). In a few studies, the two extremes were reported. Hakkinen (1991) found a strong relationship, r = 0.84, while Ball et al. (1992) and Callister et al. (1990) reported no relationship among jump height, isometric joint torques, and anthropometric data. The wealth of information in the literature seems to indicate that knowledge of isometric muscle force, joint torque and anthropometric data alone cannot be used to predict jump height.

One possible reason that a definitive correlation cannot be found between jump height, isometric joint torques, and anthropometric data is that no one has included the nervous system parameters, even though the nervous system controls and coordinates muscle activities. Several researchers (Bobbert et al., 1988; Bobbert et al., 1986; and Gregoire et al., 1984) using SEMG data concluded that during jumping, muscles are activated in a proximal to distal direction. Also, the activation and deactivation times for muscles vary among individuals. The time needed to achieve maximum force is dependent upon the neural activation of muscle (Edwards, 1977, Young et al., 1983; and Murray et al., 1977). Muscles that can develop full force quickly can provide more power to the skeletal system. As with all anthropometrics, the activation and de-activation dynamics for muscles vary among individuals and therefore the power available to perform a maximum height jump also varies among individuals.

A major issue that continues to be discussed in the literature is the role of uni-articular and bi-articular muscles. Numerous researchers have studied different types of motions to understand the role these muscles better (Bobert and van Schenau, 1988; Zajac, 1993; Jacobs and van Ingen Schenau, 1992; Fujii and Moriwaki, 1993; and Suzuki et al., 1982). The general, but not universal, opinion

is that bi-articular muscles transfer energy between segments while the uni-articular muscles are the prime movers. In all cases, the energy analysis is actually limited to translational energy while the rotational energy is considered to be or assumed to be inconsequential.

Inverse and forward dynamic methods have been used to study jumping (Komi and Bosco, 1978; Bobbert and van Ingen Schenau, 1988; and Pandy and Zajac, 1991). The conclusions about the role of particular muscle groups reached by the inverse modeling technique were different from the conclusions reached by using the forward modeling technique. These differences have been attributed to the approximations made in each type of modeling (Van Leeuwen and Spoor, 1991; Zajac and Pandy; 1991; van Soest et al., 1993; and Anderson and Pandy, 1993). One issue stands out in each argument: neither modeling technique actually validates the actual muscle forces; thus, neither modeling method has been proven to be more accurate. Therefore, the type of modeling technique used in a study should probably be driven by the research question rather than by a perceived superiority of one modeling technique.

The present study was designed to model the effects of jumping in both hypo- and hyper-gravitational environments. It was not possible to collect hypo-gravitational jumping data. Also, predicting the changes in individual muscle force, muscle power and muscle energy related to changes in gravity was desired. Therefore, the forward dynamics modeling technique was selected.

Chapter 3: Methods

The purpose of this study was to answer the research question "How do changes in gravitational force affect jumping performance and intermuscular control?". To answer this question, four actions were taken: 1) experimental data were collected while subjects jumped in increased G_z environments, 2) a model was used to find solutions to a maximal height jumping problem in both hypo- and hyper-gravitational environments, 3) the experimental data were used to validate the musculoskeletal model solutions for hyper-gravitational environments, and 4) all musculoskeletal model solutions were analyzed to determine how changes in gravity affected jump performance and intermuscular control. In this chapter, the subjects will be described along with the research design, experimental methods, musculoskeletal model, optimal control problem, and validation methods.

3.1 SUBJECTS

The eight subjects who participated in this study were all members of the Wright-Patterson Sustained Acceleration Panel. Panel members were given routine medical examinations and were medically evaluated prior to each ride on the DES. All subjects were male; mean age 30.6 ± 5.5 years; mean height 179.0 ± 3.0 centimeters; and mean mass 87.1 ± 13.2 kg. The subjects were drug and alcohol free and had no history of serious muscle or joint injury. Subjects maintained a routine cardiovascular exercise program and were all experienced

24

DES riders. All subjects were required to read and sign a Subject Consent Form (Appendix A). This study, including the Subject Consent Form, was approved by the Human Use Review Committee located at Wright-Patterson AFB.

Subjects were required to ride the DES on four different occasions. The first ride was to orient the subjects to whole body movement in increased G_z environments. During the orientation ride, the subjects were required to sit, stand, rise from a chair, and jump at five different G_z levels (1.0, 1.2, 1.4, 1.6, and 1.8 G_z). Data were not collected during the orientation ride but were collected during the following three rides on the DES. For data collection, SEMG electrodes and reflective markers were attached to the subjects.

During all rides, subjects were required to wear safety equipment that consisted of a crash helmet and a safety harness specifically designed for this study (combined mass of 5.0 kg). The safety harness was a parachute harness with five adjustable tethers attached to the ceiling, floor, and side wall. This configuration allowed the subject free motion from a squatting position to a fully extended position five centimeters off the floor before the safety harness would become active and prevent any further motion. Thus, if the subject lost consciousness or if the cab inverted, the subject would have been protected from crashing into the cab structure. The safety helmet was used for head protection and communication with control room personnel.

3.2 RESEARCH DESIGN

This research design consisted of 1) collecting experimental data, 2) modeling jumping at different G_z levels, 3) validating the musculoskeletal model solutions by comparing predicted and experimental data qualitatively and quantitatively, and 4) analyzing the musculoskeletal model solutions to answer the research question (see Figure 3.1). The data collection, musculoskeletal modeling and validation processes are described in detail in the following sections of this chapter.

3.3 EXPERIMENTAL APPARATUS AND METHODS

The experimental apparatus and methods included the following components; DES, data acquisition system, ground reaction force, SEMG, video system, and experimental data analysis. In this section, each of these elements will be discussed.

3.3.1 Dynamic Environment Simulator

The DES consisted of rotating and fixed components, a total weight of 1.6 x 10^6 N, driven by three 110.0 volt dc electric motors (Figure 3.2). The cab, where subjects were placed, was a sphere of diameter 3.05 m and the center of the cab was 5.94 m from the center of rotation of the DES. A subject in the cab experienced a resultant force, $\bar{F}_r$, in the negative z direction (Figure 3.3). $\bar{F}_r$ was the vector summation of gravity, $\bar{W}$, and the centrifugal force, $-\bar{F}_n$, related to the centripetal force, $-\bar{F}_n$. $-\bar{F}_n$ resulted from the spinning motion of the DES. Based
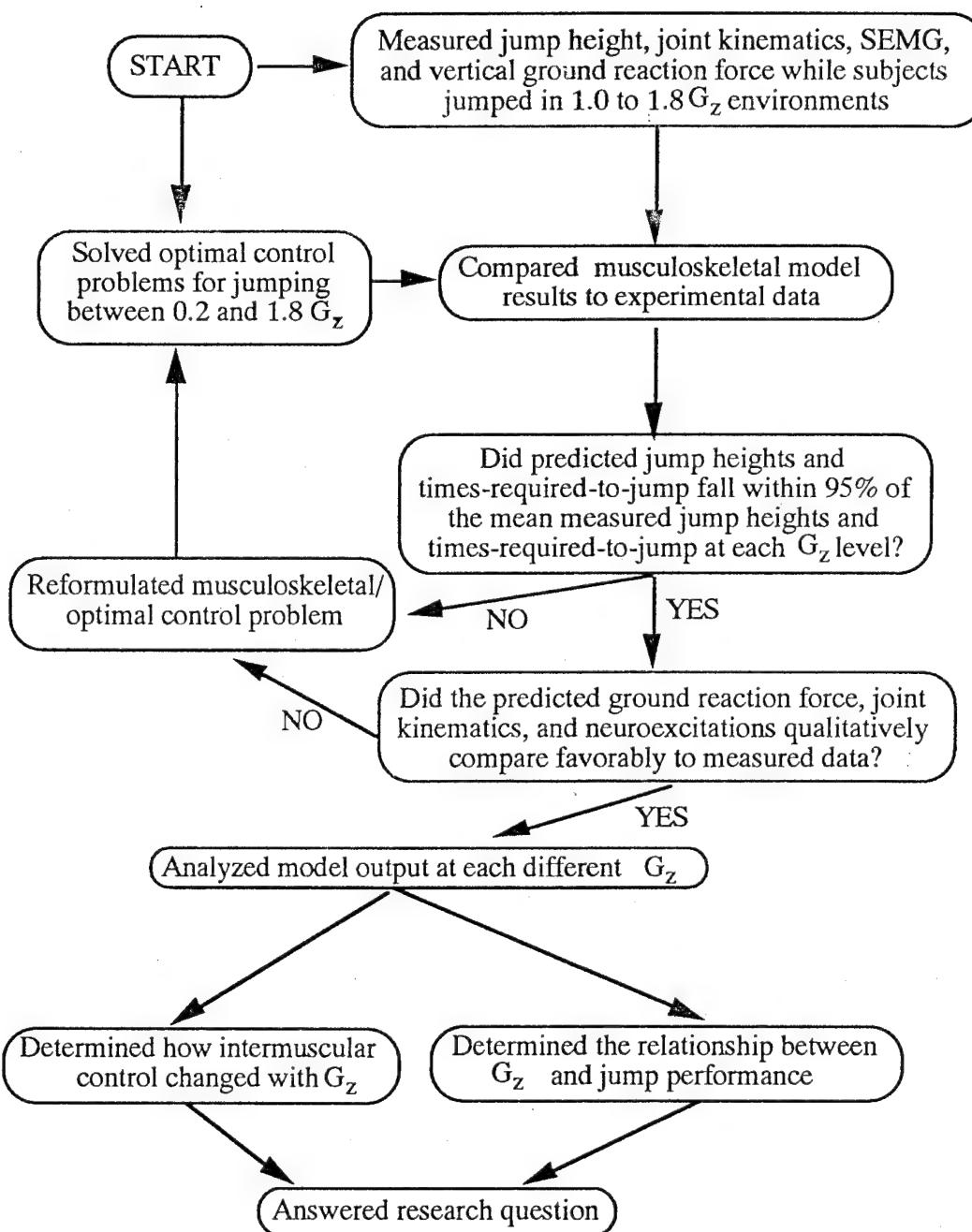
Figure 3.1   Experimental Design.
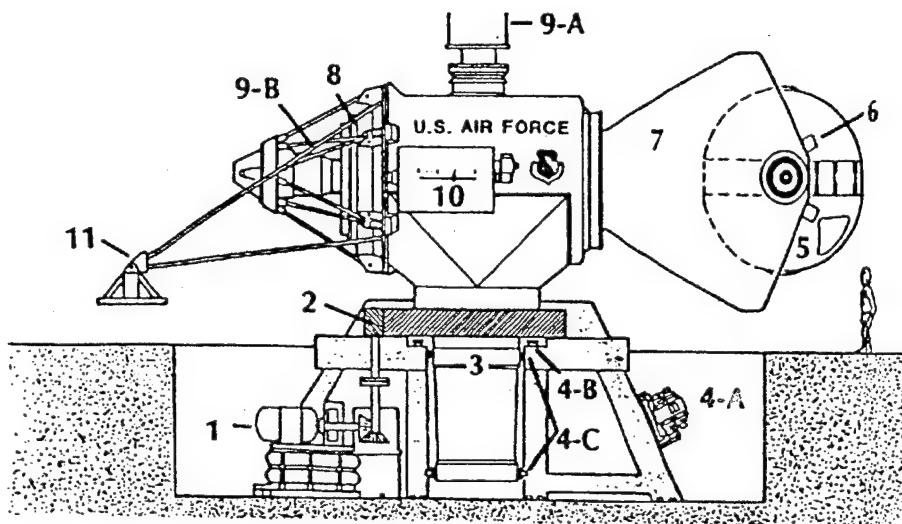
Figure 3.2 Dynamic Environment Simulator Major Assemblies

The major components of the DES include 1) main arm drive motor, 2) drive pinion, 3) main rotating trunion and bull gear, 4) hydrostatic bearing system (a-hydrostatic bearing system, b-thrust pad, c-radial pads), 5) cab, 6)cab drive motor, 7) fork, 8) fork drive motor, 9) slip ring assemblies (a-main arm axis, b-fork axis), 10) motor driven counterweight, and 11) aft-mounted experimental platform (Raytheon Service Company).
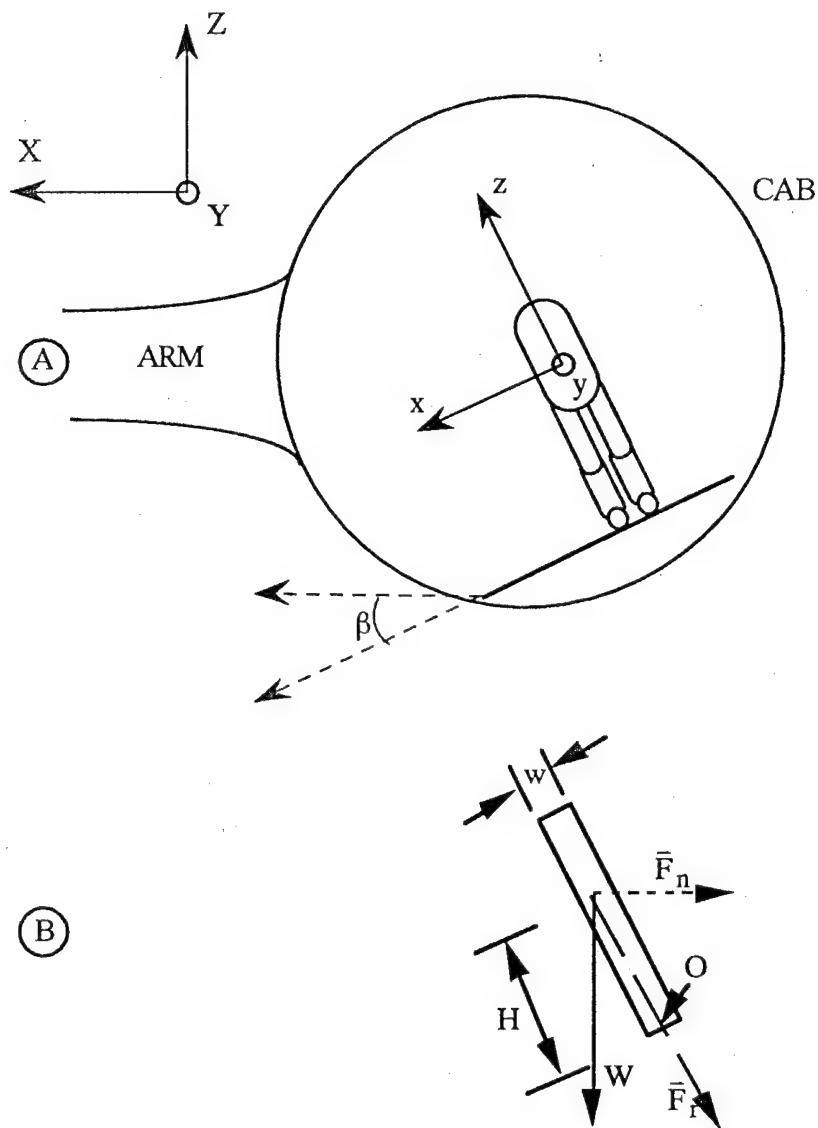
Figure 3.3 Forces Acting on Subject.

Top figure, A, orientation of subject in cab, bottom figure, B, forces that produce a non-zero moment about point O. Short dashed line is effective force and long dashed line is resultant force

on Newton's third law of motion, an equal and opposite effective force was produced in response to $-\bar{F}_n$. It was desired not to have motion in the x direction. Assuming w was small compared to H, the sum of the moments about O (the point of contact between the subject and the cab) needed to be zero. Only two forces created a non-zero moment about O, $-\bar{F}_n$ and $\bar{W}$. Intuitively, for a non-zero $-\bar{F}_n$ the subject needed to be tilted an amount β such that the resulting moment about O would be zero. To determine β,

$$\sum M_O = H\cos(90-\beta)|\bar{W}| - H\sin(90-\beta)|\bar{F}_n|$$

$$0 = H\cos(90-\beta)|\bar{W}| - H\sin(90-\beta)|\bar{F}_n|$$

$$H\cos(90-\beta)|\bar{W}| = H\sin(90-\beta)|\bar{F}_n|$$

$$\sin(\beta)|\bar{W}| = \cos(\beta)|\bar{F}_n|$$

$$\frac{\sin(\beta)}{\cos(\beta)} = \frac{|\bar{F}_n|}{|\bar{W}|}$$

$$\tan(\beta) = \frac{\text{mass}|\bar{a}_n|}{\text{mass}|\bar{a}_g|}$$

$$\beta = \tan^{-1}\left(\frac{|\bar{a}_n|}{|\bar{a}_g|}\right) \tag{3.1}$$

$\bar{a}_g$ was constant at 9.806 m/sec^2 in the Z direction and $\bar{a}_n$ was

$$\bar{a}_n = \left(\text{radius} \cdot \bar{\omega}^2\right) \text{ in the X direction} \tag{3.2}$$

where $\bar{\omega}$ was the angular velocity of the DES about the Z axis. Thus, β and $\bar{\omega}$ could be set to obtain a desired $\bar{F}_r$. In the discipline of altered gravitational studies the $\bar{F}_r$ is not normally reported, rather, the magnitude of $\bar{F}_r$ normalized to earth gravitational force (i.e. G_z) is used. G_z is always directed along the z axis and has the magnitude

$$G_z = \frac{\sqrt{\bar{a}_n^2 + \bar{a}_g^2}}{|\bar{a}_g|}$$

(3.3)

In this study, five different G_z levels were used. The DES settings used to achieve the desired G_z levels are summarized in Table 3.1.

Table 3.1 DES Settings

The DES settings used to achieve the desired different G_z values

G_z	$\bar{\omega}$, degrees/s	$\bar{a}_n$, m/s^2	β, degrees
1.0	0.0	0.0	0.0
1.2	59.6	6.5	33.6
1.4	72.8	9.6	44.4
1.6	82.5	12.2	51.2
1.8	90.0	14.7	56.3

During rotation, one additional acceleration exists, Coriolis acceleration that acts in the Y direction. The Coriolis acceleration is produced if a body on a rotating structure has a radial velocity. During jumping, the radial velocity, $^X\bar{V}$, was

$$^{X}\bar{V} = {}^{z}\bar{v} \cdot \cos\beta \tag{3.4}$$

Thus, at time zero, $^{z}\bar{v}$ was zero and it did not maximize until near the end of the jump. The Coriolis acceleration was not directed in the Z or z directions and the magnitude of the peak effective force created by the Coriolis acceleration was less than 20 percent of the resultant force created by $\bar{a}_g$ and $\bar{a}_n$ accelerations. For these reasons the Coriolis acceleration was not a factor in this study.

3.3.2 Data Acquisition System

The data acquisition system consisted of a Macintosh® Quadra 950 computer, two National Instrument computer boards, and LabVIEW® software. The computer boards were a NBIO-16XL used to convert analog data to digital data and a NBDMA-8 that directly transferred all collected data to computer memory. Ground reaction force and SEMG analog signals were analog lowpass filtered at 2000 Hz, digitized at 4000 Hz, and collected for 3.0 sec. All software and analog filters (fourth order Sallen-Key filter) used were developed at Brooks AFB.

The selected sampling time and rate were much higher than necessary to study jumping. However, other investigative efforts involving these data required the selected sampling time and rate. Also, the oversampling reduced the chances aliasing and the analog filters reduced noise and spurious signals.

3.3.3 Ground Reaction Force

The ground reaction force in the z direction (GRF), was measured by the use of a force plate. The major commercial manufacturers of force plates would not certify that their product would work properly in the DES. To circumvent this problem, a force plate was designed and constructed that would measure the GRF at a variety of G_z levels. The surface of the force plate was made from a 1.27 cm thick, 1648.3 cm^2 square aluminum plate. Load cells (strain gauge, Sensotec Inc. AA223 rated at 1,000 pound) were placed under the corners of the aluminum plate. Power to the load cells and signal amplification were accomplished with an external amplifier-power source (Sensotec Inc. AE321) located in the cab. Information about the frequency response and calibration of the force plate can be found in Appendix B.

3.3.4 Surface Electromyography

The SEMG electrodes (IOMED, ML220, 4.0 cm center-to-center distance, 13 mm diameter, nominal gain of 350, CMRR 100 dB and a bandpass of 8.0 Hz to 32 kHz) were attached to the skin over the following muscles: gastrocnemius (ankle plantar flexor and knee flexor), vastus lateralis (knee extensor), semitendinosus (knee flexor and hip extensor), and gluteus maximus (hip extensor). A more detailed description of the SEMG electrode placement can be found in Appendix C. After the SEMG electrodes were attached to the subject for the first time, the placement sites were annotated and used for each subsequent run.

3.3.5 Video System

Kinematic data were obtained by using a video system. Jumping is often considered a planar activity and therefore only one camera, non-colinear with respect to the motion, is required to collect kinematic data. The CCD camera was positioned perpendicular to the plane of motion of the subjects, 89.5 centimeters above the floor. The video signal was passed to a video recorder located in the control room. The video signal was synchronized with the analog data by the use of a multiplexor switch, controlled by the computer, located in the video line. When analog data were being collected, the multiplexor switch was activated and the video signal was allowed to pass to the video recorder. When analog data were not being collected, the multiplexor switch was de-activated and no video signal was passed to the video recorder. The video recorder continuously ran during the experiment. Thus, the video tape was blank except for 3.0 sec time periods corresponding to the analog data collection.

Spherical reflective markers attached to the subjects were used to identify the selected joint centers on the video tape. The location of the reflective markers were the lateral surfaces over the fifth metatarsophalangeal joint, lateral malleolus, lateral epicondyle, greater trochanter, and glenohumeral joint. The reflective markers that covered the lateral malleolus, lateral epicondyle, greater trochanter, and glenohumeral joint had a diameter of 3.5 cm and the reflective marker on the fifth metatarsophalangeal had a diameter of 2.5 cm. For calibration, a rectangular grid, 170 cm by 80 cm, was constructed and video taped.

3.3.6 Experimental Data Analysis

The collected video and digitized data were transported to the Biomechanics Laboratory at The University of Texas at Austin for processing and analysis. The video data were analyzed using the Motion Analysis Expert Vision® system software and the digital data were analyzed using LabVIEW®. The digital data were processed first to determine each subject's highest non-countermovement jump for each G_z level. The corresponding video data for the highest jump were then analyzed.

The GRF data were twice filtered by the same digital, fourth order low-pass Butterworth filter (20 Hz cutoff). On the second pass through the filter, the data were sent in reverse order (last point first to first point last). This process removed any potential time or phase shift resulting from filtering the data. The filtered data were used to determine the start and end of the jump. The end of the jump was defined as the point in time where the GRF became zero. The start of the jump was defined as the point in time, prior to peak GRF, that the GRF was continuously greater than body weight. The difference between final time and start time was defined as the time required to jump.

In this study, SEMG data were used only for qualitative comparison with predicted muscle neuroexcitation. The SEMG data were twice passed through a highpass (20 Hz cut-off) Butterworth filter. As with the GRF data, this was accomplished to remove any potential time and phase shift problems due to the filtering process. The method of simulating muscle neuroexcitations in the model used in this study allowed muscle neuroexcitation to have a value between 0.02

and 1.0. Also, the jumping movement can introduce movement artifact into the SEMG signal up to 15.0 Hz. To keep the SEMG data always positive, the SEMG data were zero meaned and then full wave rectified. This resulted in a doubling of the frequencies contained in the SEMG data, i.e. 15 Hz would go to 30 Hz. To remove potential movement artifact, the SEMG data would have needed to been high pass filtered at 30 Hz. However, in doing so some actual SEMG data would have been lost. The decision was made to high pass filter at 15 Hz and keep the actual SEMG data in the 7.5 to 15 Hz range, realizing the data could have been contaminated with movement artifact. A subset of the processed SEMG data was then taken that corresponded to the jump sequence. This subset for each muscle was scaled such that the maximum SEMG signal was 1.0.

The kinematic data were analyzed using the Expert Vision® system. After digitizing the two dimensional data, the software package was used to generate the time histories of segment and joint angles. The kinematic data was smoothed using the "smoo" routine (a 2-D moving average filter) available in the Expert Vision software. The "smoo" routine is a very simple routine that averages consecutive data points, thus it acts as a very simple low pass filter. The actual filter characteristic was not known. This was not a major concern. The kinematic data were used for comparison with predicted joint and segment displacements only. The experimental kinematic data were not used for inverse dynamics nor determining jump height (see section 3.5.3 and equation 3.15).

3.4 MUSCULOSKELETAL MODEL

The musculoskeletal model used in this study was produced by Frank Anderson and Dr. James Ziegler, both members of the University of Texas, Department of Kinesiology Biomechanics Laboratory. The musculoskeletal model consisted of four body segments joined together by frictionless revolutes and actuated by twenty musculotendon units (Figure 3.4). The toes were hinged to the ground and the foot-ground contact was modeled by placing a torsional spring and damper at the toes. The musculoskeletal model was divided into three major components: skeletal dynamics, musculotendon dynamics, and muscle excitation-contraction dynamics. The skeletal dynamics were used to calculate segment accelerations in response to the forces acting on the body segments. Musculotendon actuation was used to calculate the forces generated by each of the musculotendon units in response to a level of muscle activation. Muscle excitation-contraction dynamics transformed the incoming neuroexcitation signals to the muscle into muscle activation.

The musculoskeletal model was not solved for jumping in a centrifuge, rather, $\bar{a}_g$ was directly altered resulting in an increase or decrease in $\bar{F}_r$ (Z and z colinear). In contrast, the experimental data were collected with $\bar{a}_g$ constant with the increase in $\bar{F}_r$ being achieved by increasing $\bar{\omega}$ and β. In either case, the resulting G_z acting on the COM indicates that the same $\bar{F}_r$ was being applied.
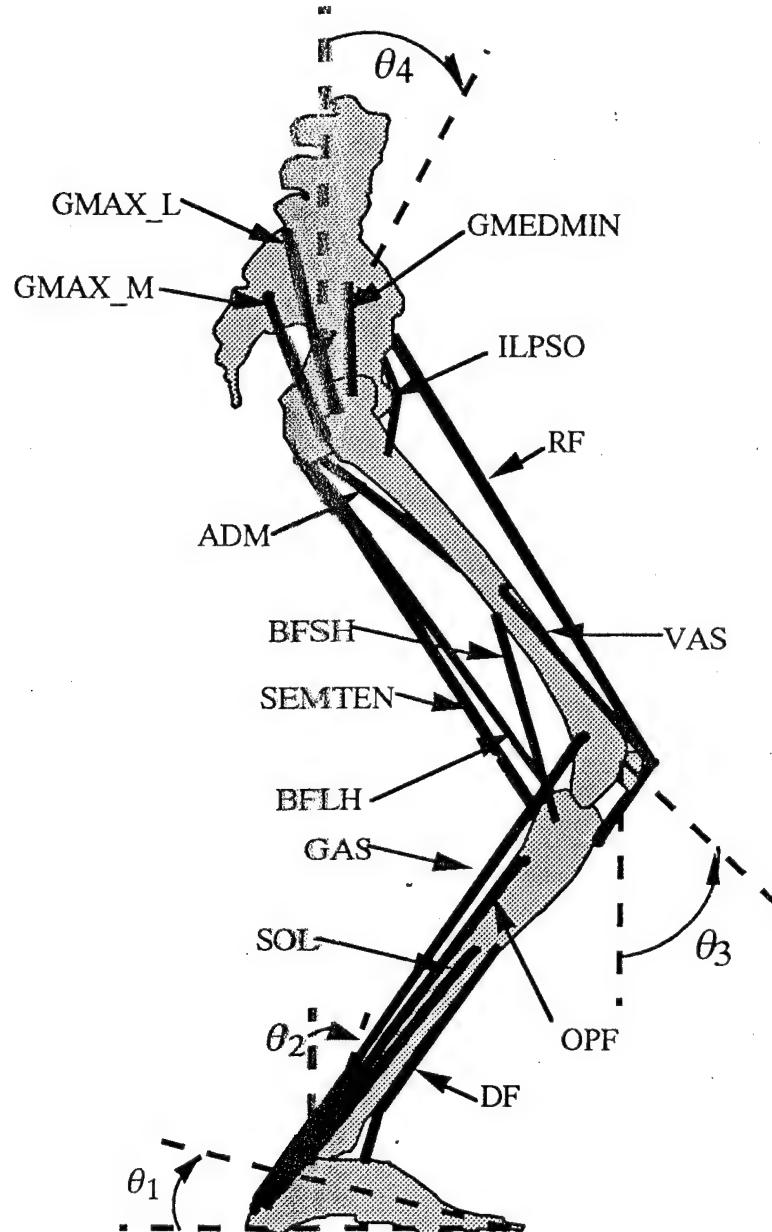
Figure 3.4 Musculoskeletal Model

The 17 muscles that can be easily viewed in the sagittal plane are presented in this figure, see Table 3.3 for abbreviations.

3.4.1 Skeletal Dynamics

Movement of the body segments was described using Newton's laws (Pandy et al., 1990). The mathematical representation of body-segmental dynamics, in vector-form, was

$$\mathbf{A}(\theta)\begin{bmatrix} \ddot{\theta}_1 \\ \ddot{\theta}_2 \\ \ddot{\theta}_3 \\ \ddot{\theta}_4 \end{bmatrix} = \mathbf{B}(\theta)\begin{bmatrix} \dot{\theta}_1^2 \\ \dot{\theta}_2^2 \\ \dot{\theta}_3^2 \\ \dot{\theta}_4^2 \end{bmatrix} + \mathbf{C}(\theta) + \mathbf{DM}(\theta)\mathbf{F}^T + \mathbf{T}(\theta,\dot{\theta})$$

(3.5)

The segment angles (θ_i), segment angular speeds ($\dot{\theta}_i$), and the magnitudes of the segment angular accelerations ($\ddot{\theta}_i$) are vector components corresponding to the four body segments. The subscript i indicates the segment (1-foot, 2-shank, 3-thigh, 4-HAT). $\mathbf{A}(\theta)$ is a 4 X 4 mass matrix; $\mathbf{B}(\theta)$ is a 4 X 4 matrix containing the centrifugal and Coriolis terms; $\mathbf{C}(\theta)$ is a 4 X 1 matrix containing the gravitational terms; and $\mathbf{D}$ is a 4 X 3 matrix that transformed joint torques into segmental torques. The ligament torques and toe torque are included in $\mathbf{T}(\theta,\dot{\theta})$, a 4 X 1 matrix. The musculotendon forces are in $\mathbf{F}^T$, a 20 X 1 matrix. The moment arm matrix $\mathbf{M}(\theta)$, a 3 X 20 matrix, is used to transform applied musculotendon forces into joint torques.

The anthropometric properties of the segments are listed in Table 3-2 (Winter, 1990; Whitsett, 1963; and Santschi et al., 1963).

Table 3.2 Anthropometric Parameters Included in the Model

This table presents the mass of each segment, distance of each segment's COM from distal end (l_{ci}), length of each segment,(l_i), and each segment's moment of inertia about the mass center (I_i). The mass of the safety equipment (5.0 kg) worn by the subjects was included in the value shown for the HAT segment mass during the jumping simulations.

Segment	mass(kg)	l_{ci}(meter)	l_i(meter)	I_i(kg-m^2)
Foot	2.2	0.147	0.25	0.016
Shank	7.5	0.274	0.435	0.13
Thigh	15.15	0.251	0.40	0.252
HAT	51.22	0.343	0.343	1.814

The foot-ground contact was modeled using a spring-damper system that produced a torque about the X axis at the toes. The magnitude of the torque produced at the toe was

$$\tau_{toe} = \tau_{toe,spring} + \tau_{toe,damper} \tag{3.6}$$

where

$$\tau_{toe,spring} = 0.75\left[120.0\,(\theta_0 - \theta_1)\right]^{1.5}; \qquad \theta_0 > \theta_1$$
$$\tau_{toe,spring} = 0.0; \qquad\qquad\qquad\qquad \theta_0 \leq \theta_1 \tag{3.7}$$

and

$$\tau_{toe,damper} = 11.13\,\dot{\theta}_1; \qquad\qquad \theta_0 > \theta_1 \text{ and } \dot{\theta}_1 \leq 0.0$$
$$\tau_{toe,damper} = 0.0; \qquad\qquad\quad \theta_0 \leq \theta_1 \text{ or } \dot{\theta}_1 > 0.0 \tag{3.8}$$

$\tau_{toe,spring}$ was the torque generated at the toes by the spring and $\tau_{toe,damper}$ was the torque generated at the toes resulting from damping element. θ_0 was

determined during static optimization. The damper was only active if θ_1 was less than θ_0 and if the velocity of the foot was negative (directed toward the ground). All numerical constants used in equations (3.7) and (3.8) were determined analytically so that the desired spring-damper system would 1) not allow oscillation of the foot while the foot remained flat on the ground, 2) kept the foot from penetrating the ground, and 3) allowed the foot to freely leave the ground.

Anderson (1992), working with an eight musculotendon model, concluded that ligaments at the knee and hip joints were needed in order to control joint hyper-extension when simulating jumping. Audu and Davy (1985) created ligament models for both the knee and hip joints. Audu's model was incorporated into the musculoskeletal model used in this study. These models are similar to the spring-damper system used to control the foot. The ligaments are considered exponential springs in series with a damping element. The damping element is only active when the joint is moving. The torque created at the knee joint resulting from ligaments was modeled using

$$\tau_{\text{lig,knee}} = 3.1^{-5.9(\theta_3 - 1.91)} - 10.5^{11.8(-0.035 - \theta_3)} - 3.17\,\dot{\theta}_3 \tag{3.9}$$

where $\tau_{\text{lig,knee}}$ was the knee torque created by the ligaments and was a function of knee angle and knee angular velocity. The torque created at the hip joint resulting from ligaments was modeled using

$$\tau_{\text{lig,hip}} = 2.6^{-5.8(\theta_4)} - 8.7^{1.3(0.95 - \theta_4)} - 1.09\,\dot{\theta}_4 \tag{3.10}$$

where $\tau_{lig,hip}$ was the hip torque created by the ligaments and was a function of both hip angle and hip angular velocity.

3.4.2 Musculotendon Model

The musculotendon model used in this study consisted of muscle in series with tendon. A Hill-type, three element muscle model was used to model muscle's mechanical behavior. The three elements included a series elastic element that simulated muscle's short range stiffness, a parallel elastic element that simulated muscle's passive properties, and a contractile element that simulated muscle's force-length and force-velocity properties (see Zajac, 1989; and Pandy et al., 1990 for a detailed description of the muscle and tendon models).

The unique force-length-velocity curve for each musculotendon unit (F^T) was defined by the muscle's peak isometric force (F_0^m), optimal fiber length (l_0^m), peak shortening velocity ($V_{max} = 10 \ l_0^m$ for all actuators), pennation angle (α), and tendon slack length (l_0^m). The muscle parameters used in this study to define F^T are listed in Table 3.3. Musculotendon actuator origin and insertion sites were defined on the basis of data adapted from Delp (1990) and Yamaguchi et al. (1991).

The time rate of change of musculotendon force, $\dot{F}^T$, was related through a first-order, non-linear, differential equation to musculotendon length and velocity ($\dot{F}^T$ and V^{MT}), muscle activation (a(t)), and musculotendon force (F^T, that is

Table 3.3 Musculotendon Parameters used in the Model for Jumping

The numerical values for the musculotendon parameters were derived from the literature (Brand et al., 1986; Delp, 1990; Wickiewicz et al., 1983; Jensen et al., 1971; Haggmark et al., 1978; Sipila et al., 1991; Schantz et al., 1983; McCullagh et al., 1983; Friederich and Brand, 1990; and Termote et al., 1980).

Muscle	abbreviation	F_0^m (Newton)	l_0^m (meter)	l_s^t (meter)	α (degree)
soleus	SOL	4260	0.060	0.233	25
other PF	OPF	4000	0.032	0.310	12
dorsiflexor	DF	1630	0.100	0.219	5
gastrocnemius	GAS	2330	0.050	0.402	17
biceps femoris - short head	BFSH	600	0.173	0.050	23
vasti	VAS	6750	0.087	0.140	3
rectus femoris	RF	1170	0.134	0.288	5
biceps femoris - long head	BFLH	1260	0.099	0.328	0
semimembranosus	SEM/TEN	1800	0.201	0.252	5
gracilis	GRA	195	0.352	0.140	3
tensor fascia lata	TFL	280	0.095	0.435	3
sartorius	SAR	190	0.579	0.040	0
gluteus maximus lateral	GMAXL	1880	0.153	0.122	2
gluteus maximus medial	GMAXM	660	0.144	0.175	5
gluteus medius	GMED/MIN	3440	0.126	0.023	8
adductor magnus	ADM	1960	0.148	0.079	4
adductor longus	ADLB	1235	0.128	0.042	6
iliopsoas	ILPSO	1500	0.104	0.135	8
pectineus	PECT	320	0.001	0.133	0
piriformis	PICT	535	0.110	0.030	10

$$\dot{F}^{T} = f(F^{T}, L^{MT}, V^{MT}, a(t)) \tag{3.11}$$

The musculoskeletal model used in this study allowed for direct calculation of $\dot{F}^{T}$ at discrete time intervals during the simulation. Therefore, the force in the musculotendon actuator at any discrete time (F_{j}^{T}) during the simulated jump was calculated by using F_{j}^{T} (determined during static optimization procedure) and numerically integrating $\dot{F}^{T}$.

3.4.3 Excitation-contraction Dynamics

The voluntary generation of musculotendon force began with neural excitation ($u(t)$) of the muscle. Muscle excitation was allowed to vary between 0.02 and 1.0 where $u = 1.0$ indicated that all motor units were maximally recruited and $u = 0.02$ indicated essentially that no motor units were recruited (note: $u(t)$ equal to 0.0 could lead to division by zero in the muscle model). The excitation signal to the muscle eventually led to muscle activation. These activities required time and resulted in a time delay between muscle excitation and muscle activation (see Pandy et al., 1990). The relationship between excitation and the change in activation ($\dot{a}(t)$) was modeled as a first-order differential equation,

$$\dot{a}(t) = \left[\left(\frac{1}{t_{rise}}\right)u + \left(\frac{1}{t_{fall}}\right)(1-u)\right](u-a) \tag{3.12}$$

The model was developed using a rise time constant, t_{rise}, of 22 msec, and a fall time constant, t_{fall}, of 200 msec. Edwards et al. (1977) measured voluntary muscle contractions and reported similar rise and fall times for muscle force.

Similar to determining F_j^T, the musculoskeletal model used in this study allowed for direct calculation of $\dot{a}(t)$ at discrete time intervals during the simulation. Therefore, the muscle activation at any discrete time (a_j) during the simulated jump was calculated using $a_{initial}$ (determined during static optimization procedure) and numerically integrating $\dot{a}(t)$.

3.4.4 Musculoskeletal Model Scaling

To achieve the highest level of confidence in the musculoskeletal model solution, the muscle parameters (F_0^m, l_0^m, V_{max}, α, l_s^t) and the segment parameters (mass, l_{ci}, l_i, I_i) used in the musculoskeletal model should have reflected the actual values of the subject population. However, it was not feasible to measure these parameters for each subject. Therefore, nominal values for these parameters (reported in the literature for a similar subject population) were used.

Different methods have been used to scale a musculoskeletal model. One method was to measure the subjects' isometric joint torques and then adjust the muscle parameters until the same isometric joint torques were achieved by the musculoskeletal model (Ziegler 1994). Another method was to compare the isometric joint torques produced by the model to isometric torques reported in the literature (see Delp, 1990; and van Soest et al., 1993). In the present study, no reliable method was available to measure any muscle or segment parameters nor

isometric joint torques. However, the test population consisted of active duty military personnel. The anthropometric and isometric joint torque data for this population has been studied extensively.

The musculoskeletal model was first scaled to produce similar isometric torque angle curves, both magnitude and shape, reported in the literature (Perrine and Edgerton, 1978; Wickiewicz et al., 1984; Mendler, 1967; Campney et al., 1965; Olson et al., 1972; Kulig et al., 1984; Knapik et al., 1982; Stokes et al., 1983; Kannus et al., 1991; Wennerberg, 1991; Scudder, 1980; Murray et al., 1977; and Herzog et al., 1991). Several of these studies included military personnel as subjects. Then, the musculoskeletal model was more precisely adjusted to produce the same jump height as the subjects in this study at 1.0 G_z. To determine if the final parameters used in this study were reasonable with respect to other musculoskeletal modeling studies, the maximum isometric torques used in this study were compared to similar studies (Pandy et al., 1990; Anderson, 1992; and Ziegler, 1994) to ensure no major deviations existed between the present model and other modeling efforts. The maximum isometric extensor torques reported in the literature and maximum isometric extensor torques produced by the musculoskeletal model are summarized in Table 3.4; the general shapes of the torque-angle curves are presented in Figure 3.5.
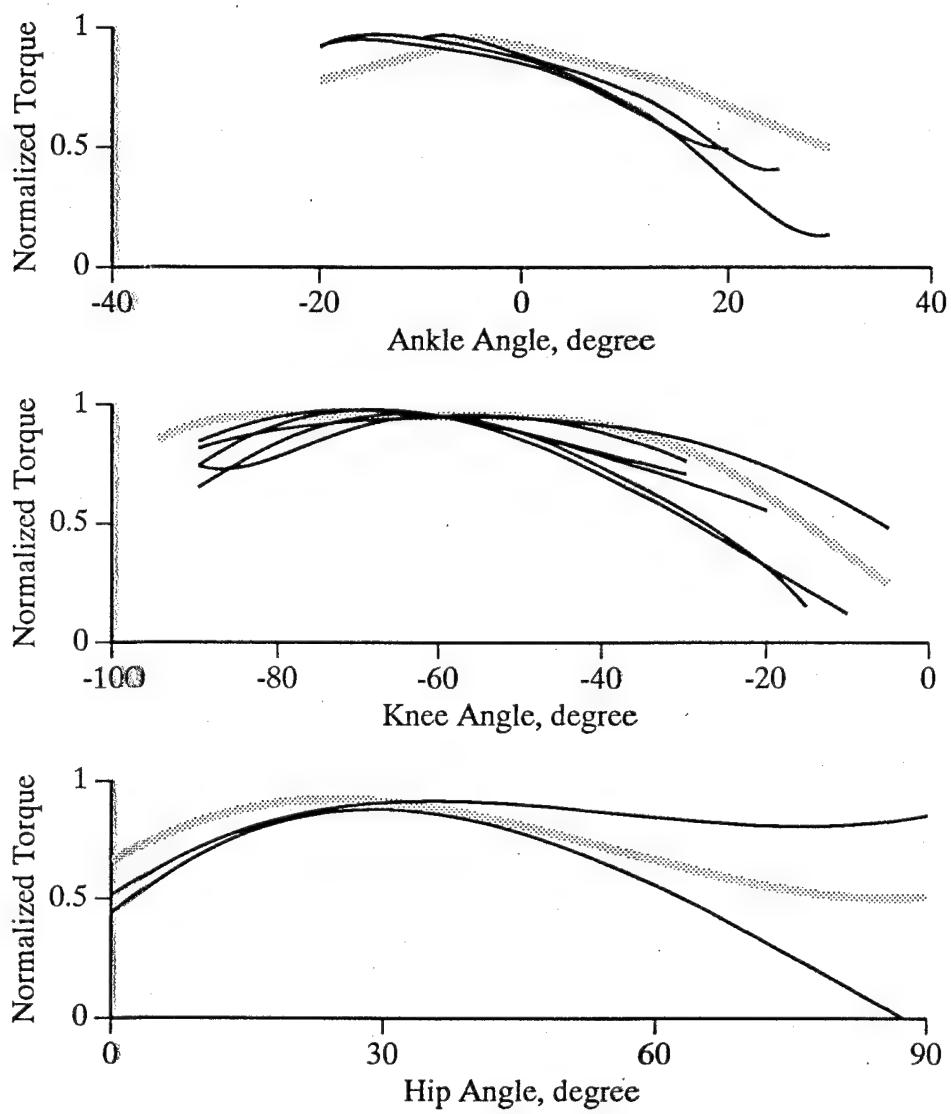
Figure 3.5 Isometric Torque-Angle Curves:

The gray line represents the model and the thin lines values found in the literature. Torque was normalized by dividing each torque value by the maximum torque. See Table 3.4 for actual maximum isometric torque values and text for references.

Table 3.4 Maximum Isometric Torques

Maximum isometric torque developed by the model and range of joint torques reported in the literature, see text for references. See Fig. 3.5 for the general shape of each torque-angle curve.

joint	Isometric peak torque used in model (N-m)	Range of peak isometric torque values reported in literature (N-m)	Peak isometric torques values reported in other models (N-m)
ankle	210	100-210	266
knee	275	160-380	320
hip	320	182-245	389

The model's isometric torque-angle curves were generated by summing the extension torques produced about each joint by each individual muscle. The predicted isometric joint torques in this study and other musculoskeletal modeling studies were greater than those isometric torques based on human studies. It has been reported that ankle and hip torques are difficult to measure and the accuracy of the reported experimental joint torques about the hip and ankle joints and have been questioned (Cabri, 1991; Bovens et al., 1990 and Wennerberg, 1991).

3.5 OPTIMAL CONTROL PROBLEMS

The number of musculotendon units spanning each joint in the body is greater than the number of degrees-of-freedom that each joint possesses; therefore, an infinite number of combinations of muscle forces can create the same resultant joint torque. This means muscle forces cannot be determined directly using inverse techniques, since more unknowns exist than equations describing the motion. One method to determine individual muscle forces is

optimal control theory. Using optimal control theory, unique musculotendon force histories can be determined that achieve a desired movement pattern based on a selected performance criterion subject to certain constraints (Rim and Chao, 1969; Hatze 1976; Davy and Audu, 1987; and Koopman, 1989). A performance criterion is a single measure of performance that is to be optimized; and the constraints are limits on the acceptable values of variables in the problem (Gill et al., 1981). For jumping, the performance criterion is to maximize jump height.

3.5.1 Parameter Optimization

For jumping, the optimal control problem was converted into a parameter optimization problem (Hull, 1991 and Pandy et al., 1992). The conversion was accomplished by approximating the continuous time histories of the controls by a set of discrete control nodes that became the independent variables in the resulting optimization problem. Solving the optimization problem required four steps: 1) making an initial guess of the controls; 2) determining the performance based on the initial guess; 3) calculating the partial derivatives of the performance and constraints with respect to the controls; and 4) using all of this information in the optimization routine. The optimization routine was used to produce a better set of controls based on the partial derivatives (Figure 3.6). For jumping, the variables selected for parameterization were the muscle neuroexcitations (Figure 3.7). The partial derivatives of the performance and constraints were determined numerically by perturbing each control individually by a small amount (10^{-7}),

Initial Guess for Muscle Excitation Histories

Nominal Forward Integration and
Evaluation of Performance and Constraints

Derivatives of Performance and Constraints
With Respect to Each Control

Parameter Optimization Routine

Convergence? Yes Stop

No

Improved Set of Controls
(muscle excitation histories)
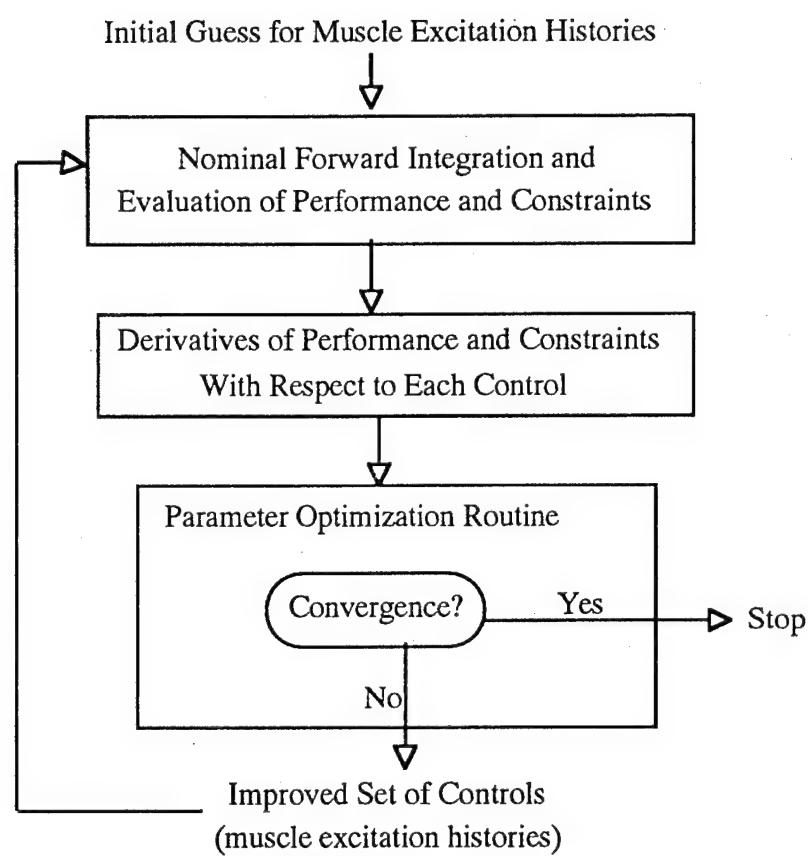
Figure 3.6 Flowchart of Parameter Optimization Algorithm
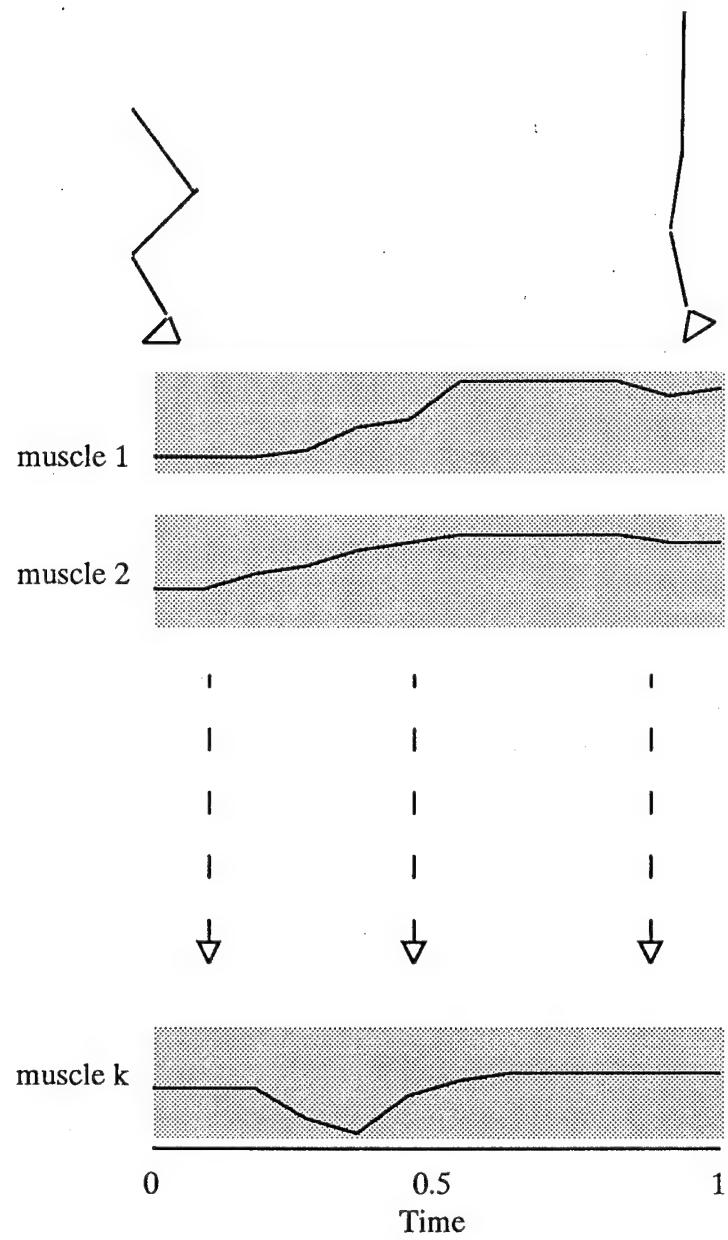
Figure 3.7 Parameterized Controls of Muscle Neuroexcitations

The continuous neuroexcitation history for each muscle is reduced to discrete time intervals, k is the total number of muscles used in the model.

repeating the integration, and determining the changes in performance and constraints.

Two optimization problems needed to be solved to find a set of musculotendon forces for squat jumping. First, the muscle forces and activations required to maintain the static equilibrium for the initial position of the squat jump were found. Second, the muscle neuroexcitations required to perform a maximum height jump were determined.

3.5.2 Static Optimization

The jump began from a static squat position ($\theta_1 = 23.0°$, $\theta_2 = 27.0°$, $\theta_3 = -75.0°$ and $\theta_4 = 90.0°$). This initial position, rather than a full squat, was selected for safety reasons; at 1.8 G_z, the effective body weight was almost double with a corresponding increase in joint stresses. All joint angular speeds were set to zero. To determine initial muscle forces, it was assumed muscles were activated to produce minimal muscle stress. Therefore:

$$ J = \sum_{k=1}^{20} \left(F_k^T \middle/ F_k^{T,max} \right)^2 \tag{3.13}$$

where F_k^T is the force in the kth muscle, $F_k^{T,max}$ is the isometric maximum force of the kth muscle, and J is the performance criteria (total muscle stress). The magnitude of the joint accelerations were constrained to be zero under conditions of static equilibrium and muscle excitations were bounded between 0.02 to 1.0 where $u(t) = 1.0$ represents full excitation of the muscle.

Once the muscle forces were found, θ_0 (the foot angle where the spring-damper system became active) was calculated. θ_0 was selected such that the torque created by the spring-damper system about the toe was equal in magnitude and opposite in direction to the torque created about the toe resulting from gravity acting on the COM.

3.5.3 Dynamic Optimization

Once the musculotendon forces required to maintain the static squat position were determined, the optimization solution for jumping was found. The performance criterion was to maximize the vertical displacement of the COM while not allowing countermovement nor joint hyper-extension. The non-countermovement and hyper-extension requirements were handled as penalty functions added to the performance criteria (Gill et al., 1981; Anderson, 1992; and Ziegler, 1994). The hyper-extension penalty function was included because it was found that with ligaments in the model, the joints would still slightly hyper-extend. Performance was calculated as

$$J = -(\text{jump height}) + \text{pen}_h + \text{pen}_c \qquad (3.14)$$

where J was the performance, pen_h was the penalty for joint hyper-extension and pen_c was the penalty for countermovement. Note that performance improved as J became more negative. Jump height was defined as

$$\text{jump height} = {}^z\bar{d}_{\text{take-off}} + \frac{0.5\ {}^z\bar{v}^2_{\text{take-off}}}{\left|\bar{a}_g\right|} - {}^z\bar{d}_{\text{standing}}$$

(3.15)

where ${}^z\bar{d}$ is the displacement of the COM in the z direction and ${}^z\bar{v}$ is the velocity of the COM in the z direction. Thus, jump height was defined as the maximum height of the COM above the standing height of the COM.

The penalties were defined as

$$\text{pen}_h = 10.0 \cdot \sum_{j=1}^{\#\text{ of steps}} \sum_{i=1}^{4} \left[\min\left(0, \theta_{i,j} - \text{minang}_i\right) - \max\left(0, \theta_{i,j} - \text{maxang}_i\right) \right]^2$$

(3.16)

and

$$\text{pen}_c = -0.05 \cdot \sum_{j=1}^{\#\text{of steps}} \left[-\min\left(0, \dot{\theta}_{3,j}\right) + \max(0, \dot{\theta}_{4,j}) \right]$$

(3.17)

If θ_i was greater than minang$_i$ or less than maxang$_i$, the assessed penalty was zero. Otherwise, a non-zero value was returned. By squaring the returned value, the penalty value was always equal to or greater than zero. The minang$_i$ and maxang$_i$ are listed in Table 3.5. To prevent countermovement, the hip and knee joints were required to always extend. Due to the sign convention, a negative velocity at the hip indicated the hip was extending while a positive velocity at the knee indicated the knee was extending. If the knee or hip flexed, a negative value was returned, and by multiplying by a negative constant the penalty function was

always equal to or greater than zero. In both cases, any hyper-extension of the joints or countermovement at any time step resulted in an increase in J resulting in a decrease in performance.

Table 3.5 Hyper-extension Angles

The following table lists the angles where joints hyper-extension began

joint	i	minang (degree)	maxang (degree)
foot	1	-23.0	37.0
ankle	2	-67.0	30.0
knee	3	-120.0	0.0
hip	4	-10.0	140.0

The final GRF was required to be zero at the time of lift-off. This was achieved by making the final GRF an equality constraint (Gill et al. 1981; Anderson, 1992; and Ziegler, 1994.).

$$C_{equality} = {}^{z}\bar{a}_{com,\,final\,time} + \bar{a}_{g} \tag{3.18}$$

The equality constraint was met when the constraint's value was equal to zero.

The requirement that the neuroexcitations be between 0.02 and 1.0 was initially handled as a set of inequality constraints (Anderson, 1992; and Ziegler, 1994.). The number of inequality constraints in this problem, 320, seemed to inhibit the optimization algorithm. The performance improved initially followed by very little improvement. This problem was also noted by Anderson (1992) and Ziegler (1994). Normally, once this occurred, the optimization process was stopped and the final set of controls were considered the optimized solution.

One task in this study was to compare the results obtained from several optimization problems with the only difference between the problems being the value of gravity. For the comparisons to be valid, each optimization problem had to converge to the same criterion. For reasons mentioned in the previous paragraph, none of the solutions converged to the same criterion. This problem was assumed to be related to the number of inequality constraints. The inequality constraints were required to bound the muscle excitations between 0.02 and 1.0. To circumvent this problem, the inequality constraints were removed, allowing the controls to take on any value. To bound the muscle neuroexcitations between 0.02 and 1.0, a transfer function was developed. Using a generic function that produced the desired relationship, the numerical constants were fixed such that the greatest change in the bounded controls took place between -1.0 to 1.0 for the unbounded controls (Figure 3.8). This range was selected to maintain the magnitude of the unbounded controls near a value of 1.0 for numerical accuracy. The transfer function transformed the unbounded controls into bounded controls.

$$u_{bounded} = \frac{0.98}{\left(1 + 64^{-u_{unbounded}}\right)} + 0.02$$

(3.19)

To test the reliability of not using the inequality constraints, the initial guess used for the optimization problem using inequality constraints was used as the initial guess for the same optimization problem using unbounded controls. The

Bounded Control
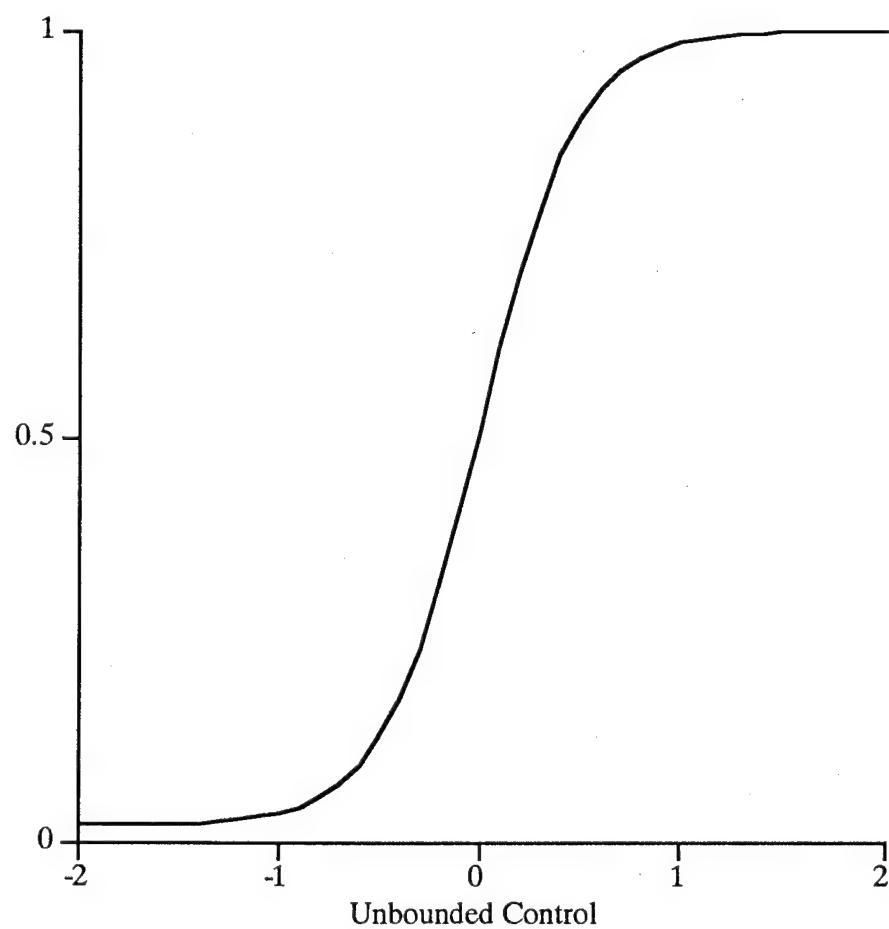
Figure 3.8 Bounded and Unbounded Controls

unbounded control problem converged while the constrained problem did not. This converged solution was then used as the initial guess for the constrained problem. The constrained problem did not improve the performance (reached convergence on the first iteration). To ensure that controls near the boundary were not "stuck", one not fully activated control was turned completely on and another turned completely off. The unconstrained problem was then solved. The same converged solution was achieved. The use of unbounded controls for all simulations in this study led to converged solutions.

3.5.4 Altered Gravity Problem

All optimal control problems were identical (initial static position, performance criterion, equality constraint, and penalty functions) with the exception of the value of gravity ($\bar{a}_g$). $\bar{a}_g$ was varied from 0.2 to 1.8 times earth gravity in steps of 0.2 G_z. Static optimization was repeated for each different G_z level prior to finding an optimal control solution for jumping. Each optimal control problem was run until convergence was achieved.

3.6 VALIDATION OF MUSCULOSKELETAL MODEL SOLUTIONS

The solutions of the musculoskeletal model were validated by comparing experimental data to equivalent predicted quantities and comparing the musculoskeletal model solution from this study to other similar musculoskeletal studies in the literature. The experimental data were compared on both qualitative and quantitative bases.

The validation and eventual discussion of the results required the calculation of the acceleration of the COM, $^z\bar{a}_{com}$, from the vertical ground reaction force, GRF, velocity of the COM, $^z\bar{v}_{com}$, displacement of the COM , $^z\bar{d}_{com}$, power transferred to the COM, Pcom, and energy transferred to the COM, E_{com}. The following derivations were based on Offenbacher (1970), Davies and Rennie (1968), and Davies (1971).

$$^z\bar{a}_{com} = \left(\frac{GRF}{mass}\right) - \left|\bar{a}_g\right| \cdot G_z \tag{3.20}$$

$$^z\bar{v}_{com} = \int {}^z\bar{a}_{com}dt \tag{3.21}$$

$$^z d_{com} = \int {}^z\bar{v}_{com}dt \tag{3.22}$$

$$p_{i,k} = mass \cdot {}^z\bar{a}_{i,k} \cdot {}^z\bar{v}_i$$
$$= mass \cdot {}^z\bar{a}_{com} \cdot {}^z\bar{v}_{com} \tag{3.23}$$

$$E_{com} = \int P_{com}dt \tag{3.24}$$

Also used during the analysis of the model solutions was the power and energy delivered to each segment by each muscle, $P_{i,k}$ and $E_{i,k}$.

$$p_{i,k} = mass \cdot {}^z\bar{a}_{i,k} \cdot {}^z\bar{v}_i \tag{3.25}$$

$$E_{i,k} = \int p_{i,k}dt \tag{3.26}$$

where $^z\bar{a}_{i,k}$ was the muscle induced segment vertical acceleration of the ith segment by the kth muscle and $^z\bar{v}_i$ was the velocity of the ith segment.

3.6.1 Quantitative Validation

For each subject, the best jump (highest jump) was selected for each G_z. The mean and standard deviation for the eight jump heights and times required to jump were calculated and compared to the predicted jump heights and times-required-to-jump. It was decided a priori that if the predicted jump heights and times-required-to-jump were within two standard deviations (95 %) of the experimental data for each value of G_z, the modeling simulations would be considered adequate.

3.6.2 Qualitative Validation

The qualitative comparison of the experimental and predicted data included GRF, segment and joint displacements, and SEMG data to neuroexcitations. Only the experimental data from the best jumps at each G_z level were compared to predicted values. The modeling simulations were considered acceptable if the predicted values followed the same general time history patterns as observed in the experimental data.

3.7 SUMMARY

In this chapter, the research design, subjects, data collection, modeling techniques and validation procedures were presented. The musculoskeletal model solutions could only be validated for 1.0 G_z to 1.8 G_z levels. If the musculoskeletal model solutions for greater than 1.0 G_z were validated with the

experimental data, it was assumed that the less than 1.0 G_z solutions were also correct and would also be used to answer the research question.

Chapter 4: Validation Results

To answer the research question "how do changes in gravitational force affect jumping performance and intermuscular control", a musculoskeletal model was used. Using the methods outlined in Chapter 3, the musculoskeletal model was scaled to match the anthropometric features of the subjects. Optimal control solutions were obtained for jumping in 0.2 G_Z to 1.8 G_Z environments. Prior to analyzing the optimal control solutions to answer the research question, the musculoskeletal model/optimal control solutions for 1.0 G_Z to 1.8 G_Z were validated by the methods outlined in Chapter 3. In this chapter, the validation results will be presented.

4.1 QUANTITATIVE VALIDATION

The quantitative validation of the musculoskeletal model solutions included comparing predicted and measured time required to jump and jump height for 1.0 G_Z, 1.2 G_Z, 1.4 G_Z, 1.6 G_Z and 1.8 G_Z.

4.1.1 Time Required to Jump

The measured and predicted time required to jump are presented in Figure 4.1 and Table 4.1. The error bars represent one standard deviation about the mean measured time required to jump for the best jump of each subject at each G_Z level. The predicted time required to jump was generally within one standard deviation for each G_Z level measured. The predicted time required to jump

62
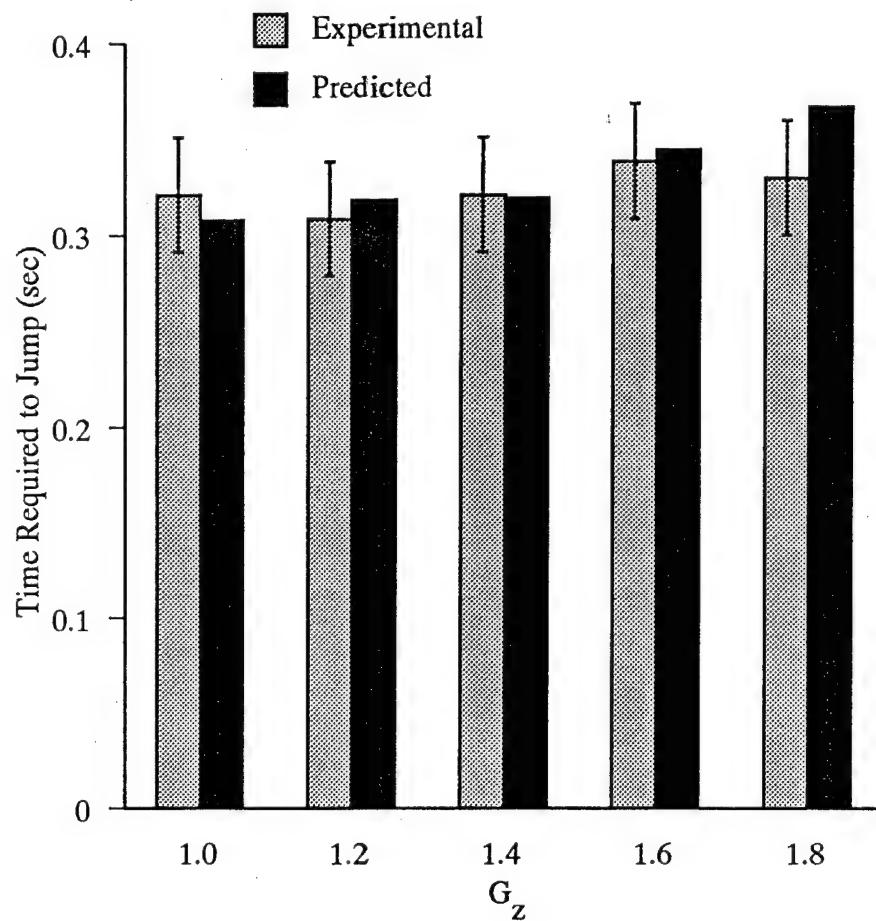
Figure 4.1 Comparison of Measured and Predicted Time Required to Jump

The predicted time required to jump (black bars) fall within one standard deviation of the measured time required to jump (gray bars) for 1.0, 1.2, 1.4, and 1.6 G_z. At 1.8 G_z, the predicted time required to jump falls within two standard deviations.

Table 4.1 Experimentally Determined and Predicted Time Required to Jump at Different G_z Values

The predicted time to jump is within one standard deviation of the experimentally determined time to jump with the exception of 1.8 G_z. At 1.8 G_z the predicted time to jump is within 1.5 standard deviations of the experimentally determined time to jump. Time has units of seconds.

	1.0 G_z	1.2 G_z	1.4 G_z	1.6 G_z	1.8 G_z
Subject 1	0.310	0.290	0.310	0.320	0.320
Subject 2	0.310	0.290	0.300	0.320	0.290
Subject 3	0.330	0.300	0.320	0.330	0.320
Subject 4	0.330	0.310	0.320	0.370	0.310
Subject 5	0.330	0.320	0.340	0.330	0.340
Subject 6	0.310	0.320	0.360	0.380	0.390
Subject 7	0.300	0.280	0.310	0.320	0.320
Subject 8	0.370	0.360	0.310	0.340	0.350
Group mean	0.326	0.309	0.321	0.339	0.330
Standard Deviation	0.025	0.025	0.020	0.024	0.030
Mean +/- One Standard Deviation	0.301 to 0.376	0.284 to 0.334	0.301 to 0.341	0.315 to 0.363	0.300 to 0.360
Model	0.308	0.319	0.320	0.345	0.367

increased with increased G_z while the measured time required to jump appeared to be independent of G_z. The lack of a clear relationship between the measured time required to jump and G_z was probably due to the small sample size (Mandel, 1984). However, the predicted time required to jump did fall within two standard deviations of the measured time required to jump, therefore, the predicted time required to jump adequately replicated the measured time required to jump at each G_z level.

4.1.2 Jump Height

The measured and predicted jump heights for each level of G_z are presented in Figure 4.2 and Table 4.2. The symbols represent the individual subjects' jump heights and the gray line represents the predicted jump heights. The predicted jump heights were within two standard deviations of the measured jump heights at each G_z level. The change in jump height was not linearly related to a change in G_z. As expected, jump height decreased with increasing G_z. The predicted jump height adequately replicated the actual measured jump heights at each level of G_z.

4.2 QUALITATIVE VALIDATION

The qualitative validation of the musculoskeletal model solutions included comparing predicted and measured time histories of the GRF, segment and joint displacements and SEMG data for 1.0 G_z, 1.2 G_z, 1.4 G_z, 1.6 G_z, and 1.8 G_z.
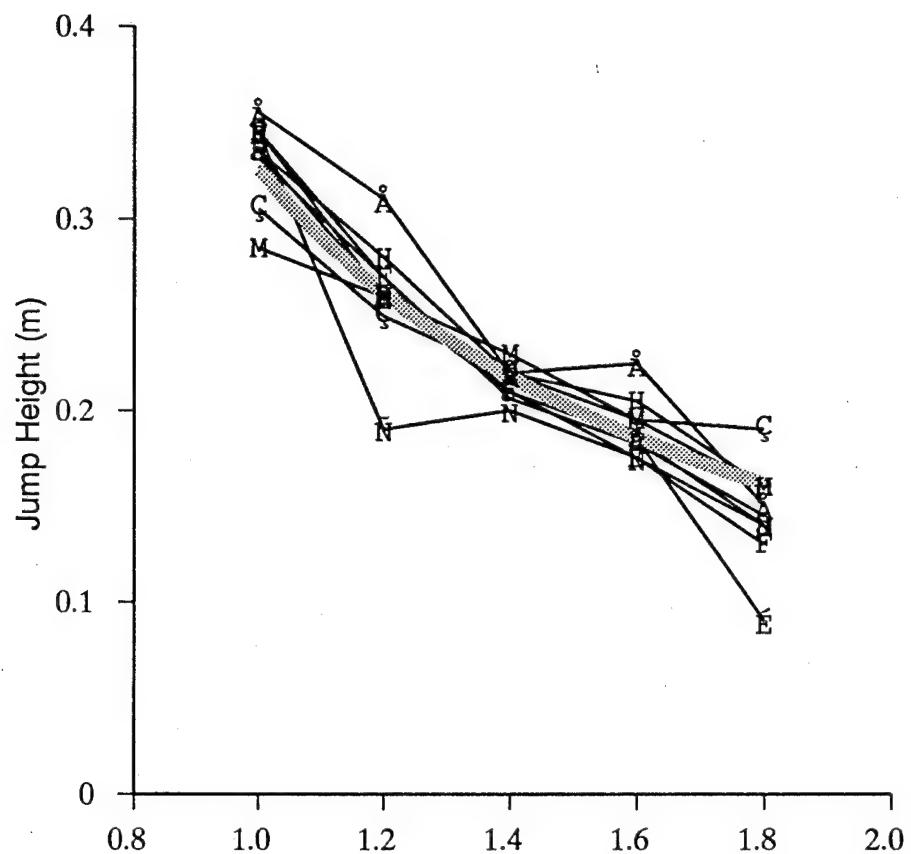
Figure 4.2 Comparison of Measured and Predicted Jump Heights for Different G_z Levels

The predicted jump height is represented by the gray line. The thin lines represent the individual jump heights. The mean jump height at each G_z fall within two standard deviations of the experimental data.

Table 4.2 Experimentally Determined and Predicted Jump Height at Different G_z Values

The predicted jump height is within one standard deviation of the experimentally determined jump height for all values of G_z. The coefficient of variation ranges from four to twenty percent. The unit of jump height is meter .

	1.0 G_z	1.2 G_z	1.4 G_z	1.6 G_z	1.8 G_z
Subject 1	0.335	0.280	0.220	0.205	0.160
Subject 2	0.345	0.270	0.210	0.175	0.130
Subject 3	0.345	0.190	0.200	0.175	0.140
Subject 4	0.345	0.260	0.220	0.185	0.090
Subject 5	0.305	0.250	0.220	0.195	0.190
Subject 6	0.355	0.310	0.220	0.225	0.150
Subject 7	0.285	0.260	0.210	0.185	0.14
Subject 8	0.327	0.261	0.215	0.185	0.160
Group Mean	0.331	0.260	0.216	0.193	0.145
Standard Deviation	0.024	0.034	0.009	0.017	0.029
Mean +/- One Standard Deviation	0.355 to 0.307	0.294 to 0.226	0.225 to 0.207	0.210 to 0.176	0.174 to 0.116
Model	0.327	0.261	0.217	0.186	0.162

4.2.1 Ground Reaction Force

To compare the measured and predicted GRFs, each GRF was normalized to body weight and time was normalized to the time required to jump. The measured and predicted GRF, $^z\bar{a}_{com}$, $^z\bar{v}_{com}$, and $^z\bar{d}_{com}$ are presented in Figures 4.3 and 4.4 ($1.0\,G_z$ and $1.8\,G_z$). For both the experimental and predicted data, the peak $^z\bar{a}_{com}$, normalized GRF, and take-off $^z\bar{v}_{com}$ decreased as G_z was increased (note: the actual GRF, GRF * body weight, increased as G_z was increased). Take-off $^z\bar{d}_{com}$ did not substantially change with G_z. The predicted GRF, $^z\bar{a}_{com}$, $^z\bar{v}_{com}$, and $^z\bar{d}_{com}$ at all G_z levels replicated the major features of the measured data.

4.2.2 Segment and Joint Displacement

The predicted joint and segment angular displacements (Z Y plane for the musculoskeletal model) adequately replicated the major features of the subjects' joint and segment angular displacements (z y plane for the subjects), Figures 4.5 - 4.8. The initial and final predicted angles were within 10.0 degrees of the observed angles. Also, for both the observed and predicted cases, the time required for the joints and segments to fully extend increased with increased G_z. This observation was consistent with studies involving load compensation (Bock, 1990; and Shadmehr, 1993). These researchers, working with the upper extremities, reported the relative joint trajectories remained constant as load was increased. However, the time required to complete the motion increased. Increasing G_z was equivalent to increasing body weight or
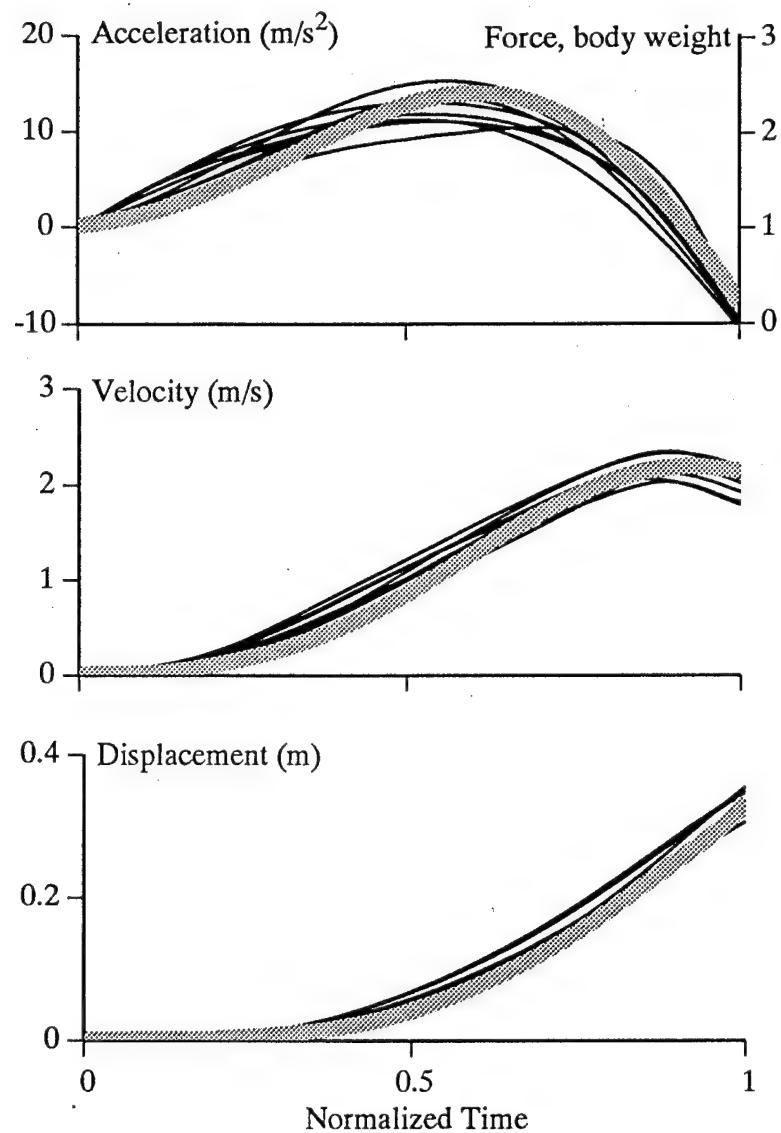
Figure 4.3 Movement of the Center of Mass at 1.0 G_z

The solid black lines represent the measured values and the gray line represents
the predicted value.
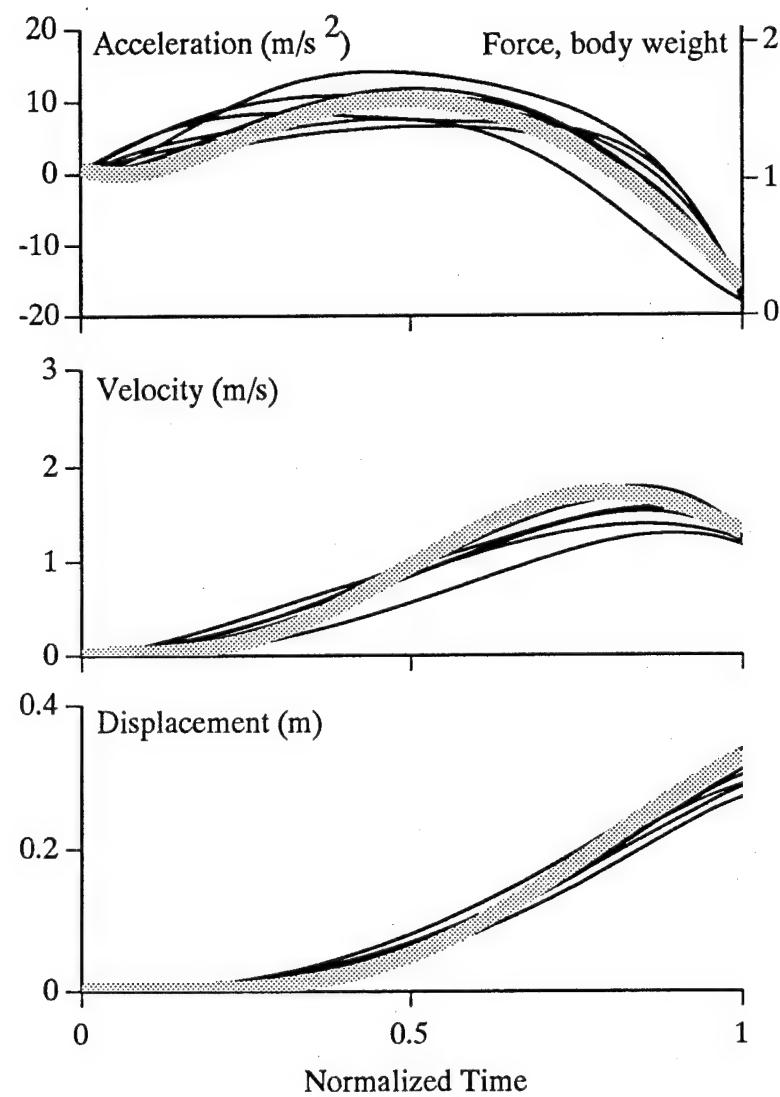
Figure 4.4 Movement of the Center of Mass at 1.8 G_z

The solid black lines represent the measured values and the gray line represents the predicted value.
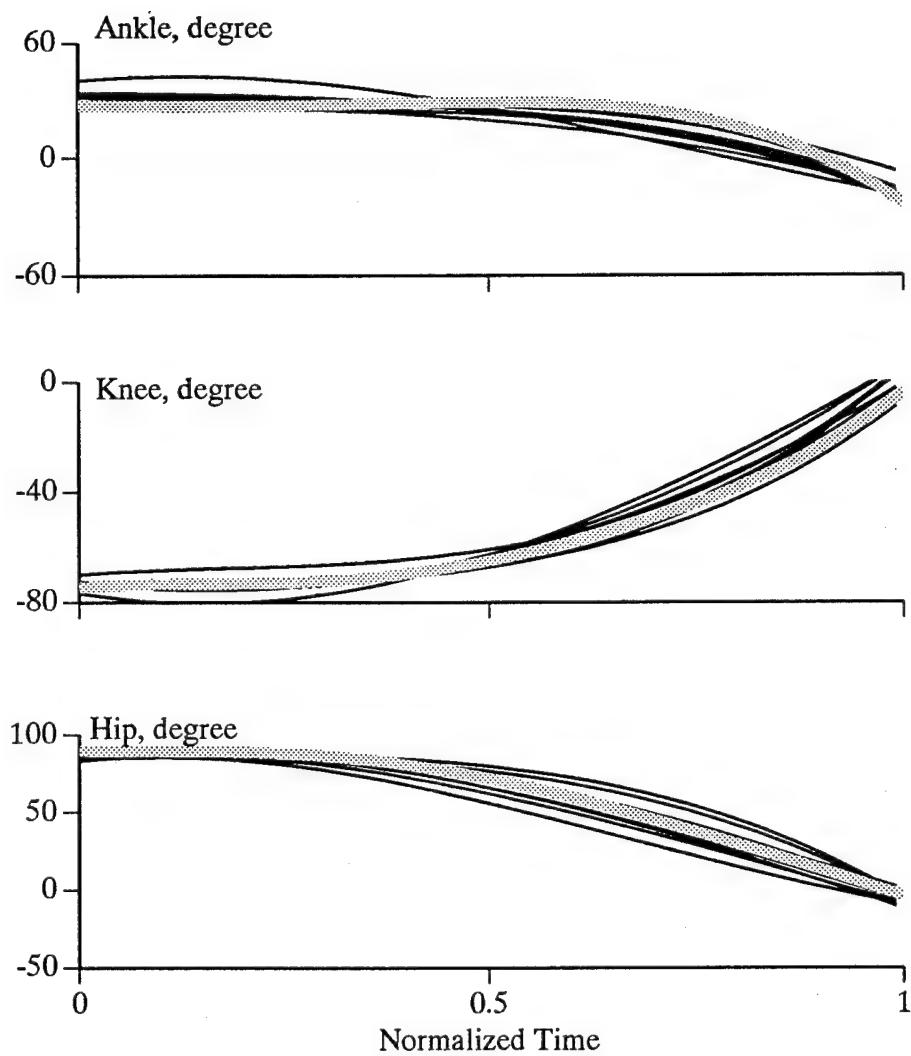
Figure 4.5 Joint Displacements at 1.0 G_z

The solid black lines represent the measured values and the gray line represents the predicted value.
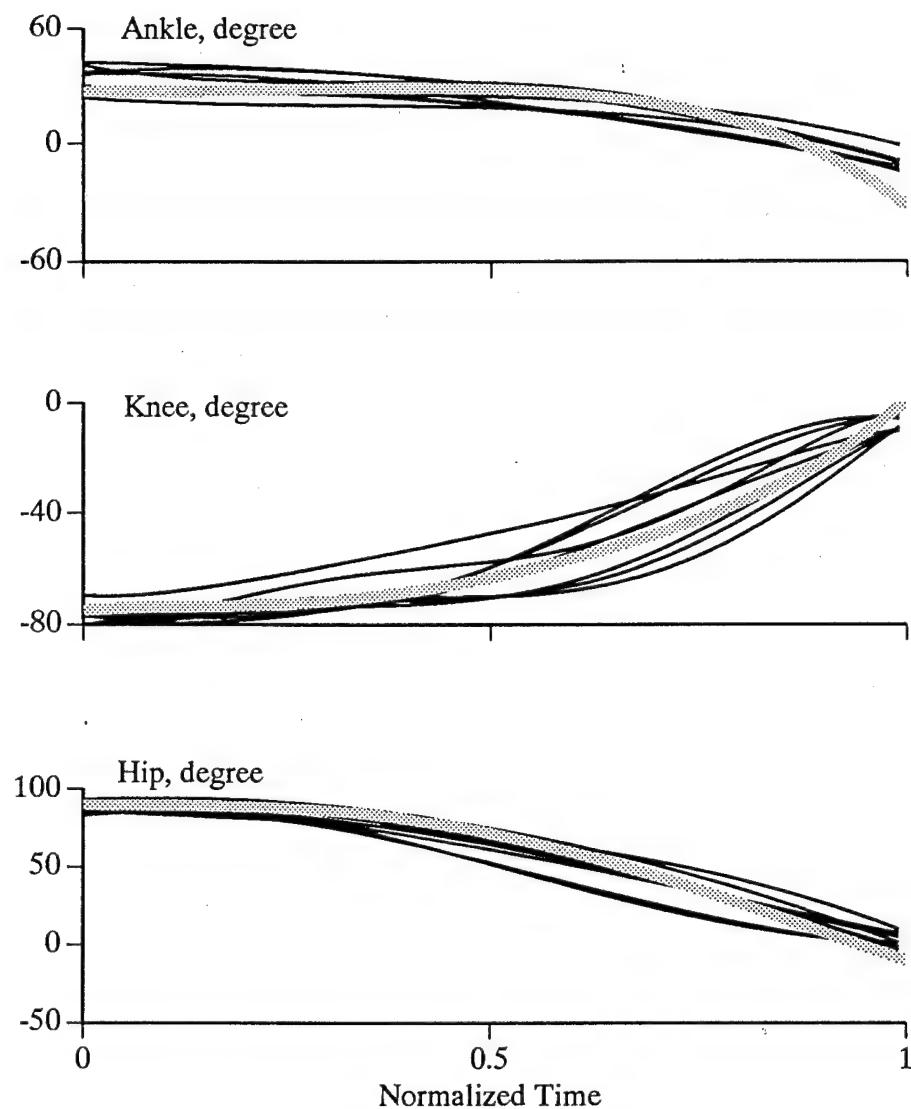
Figure 4.6 Joint Displacements at 1.8 G_z

The solid black lines represent the measured values and the gray line represents
the predicted value.
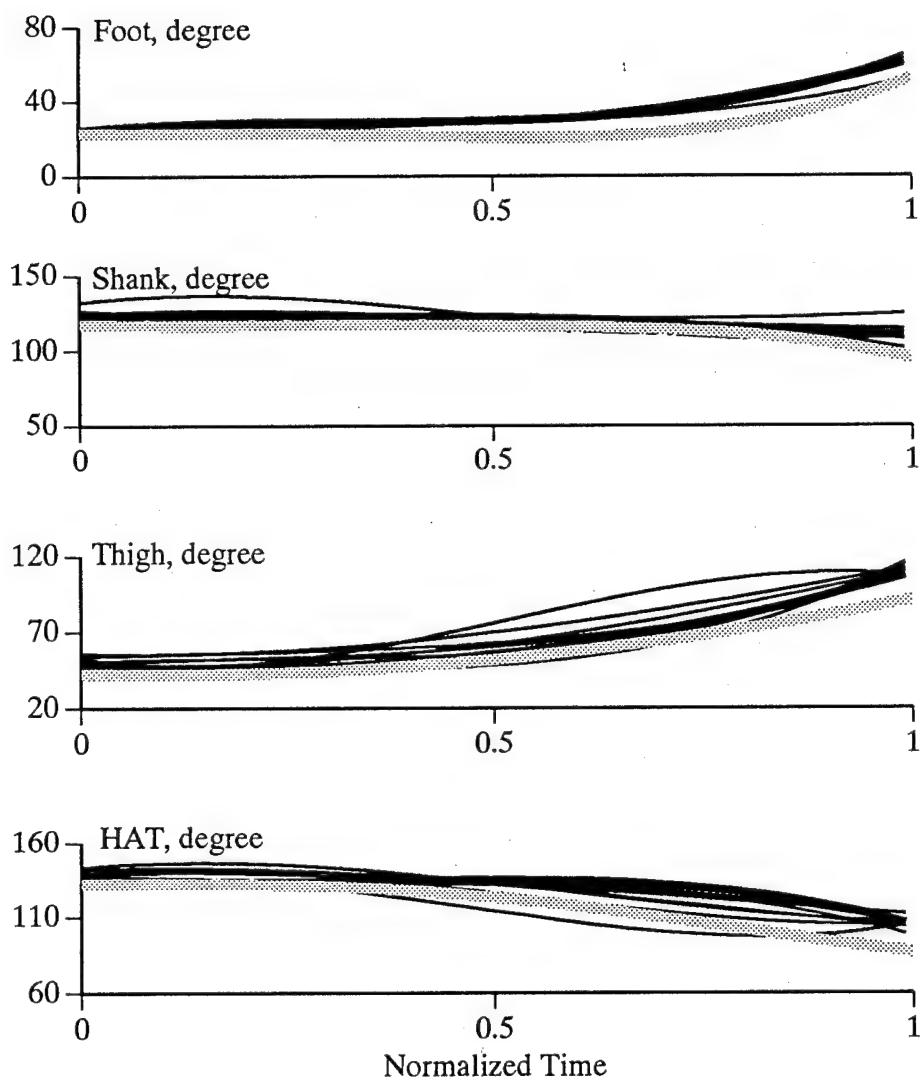
Figure 4.7 Segment Displacements at 1.0 G_z

The solid black lines represent the measured values and the gray line represents the predicted value.
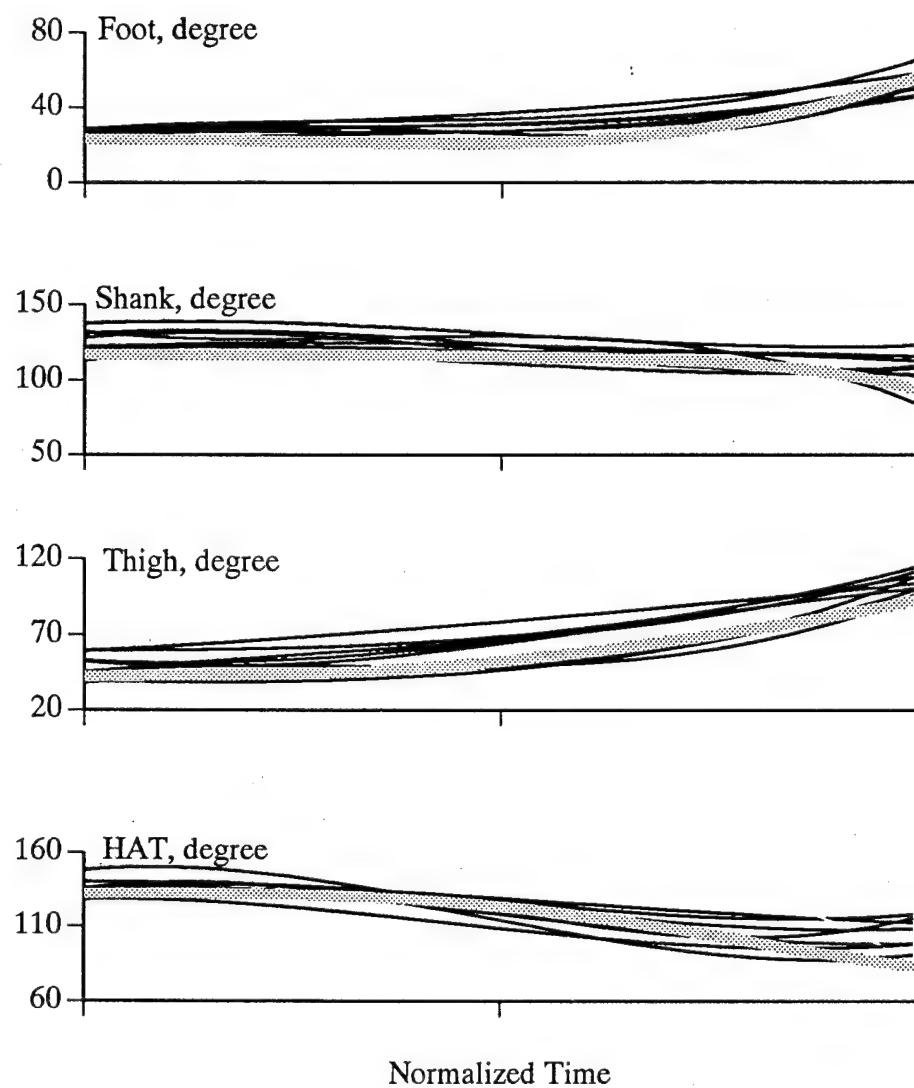
Figure 4.8 Segment Displacements at 1.8 G_z

The solid black lines represent the measured values and the gray line represents the predicted value.

increasing load. The predicted joint and segment trajectories followed the same path and took longer to complete as load increased. The similarities between predicted and observed joint and segment movements and the similar results to increased load as reported by other researchers indicated the musculoskeletal model replicated the major features of joint and segment displacements of humans jumping in increased G_z environments.

4.2.3 SEMG and Neuroexcitation

SEMG is a differential measurement of the electrical activity on the skin above a specific muscle. Previous musculoskeletal modeling studies (Anderson, 1992; Ziegler, 1994; and Pandy et al., 1990), assumed the SEMG signals were related to the predicted muscle neuroexcitations. In these studies, the SEMG data were full wave rectified and compared qualitatively to the predicted muscle neuroexcitations. The comparisons were in terms of the muscles being on or off and the general shape of the time history of the SEMG signal. Direct comparison of SEMG and predicted neuroexcitations is not possible. The SEMG signal is a composite of hundreds of motor units while the predicted neuroexcitation represents the whole muscle as a single unit. Therefore, the frequency content of SEMG will be dramatically different from the predicted neuroexcitation. At best, the SEMG magnitude and frequency would increase as predicted neuroexcitation increases.

SEMG data for four muscles (GMAX, SEM/TEN, VAS, and GAS) collected from one subject while jumping and the predicted neuroexcitations at
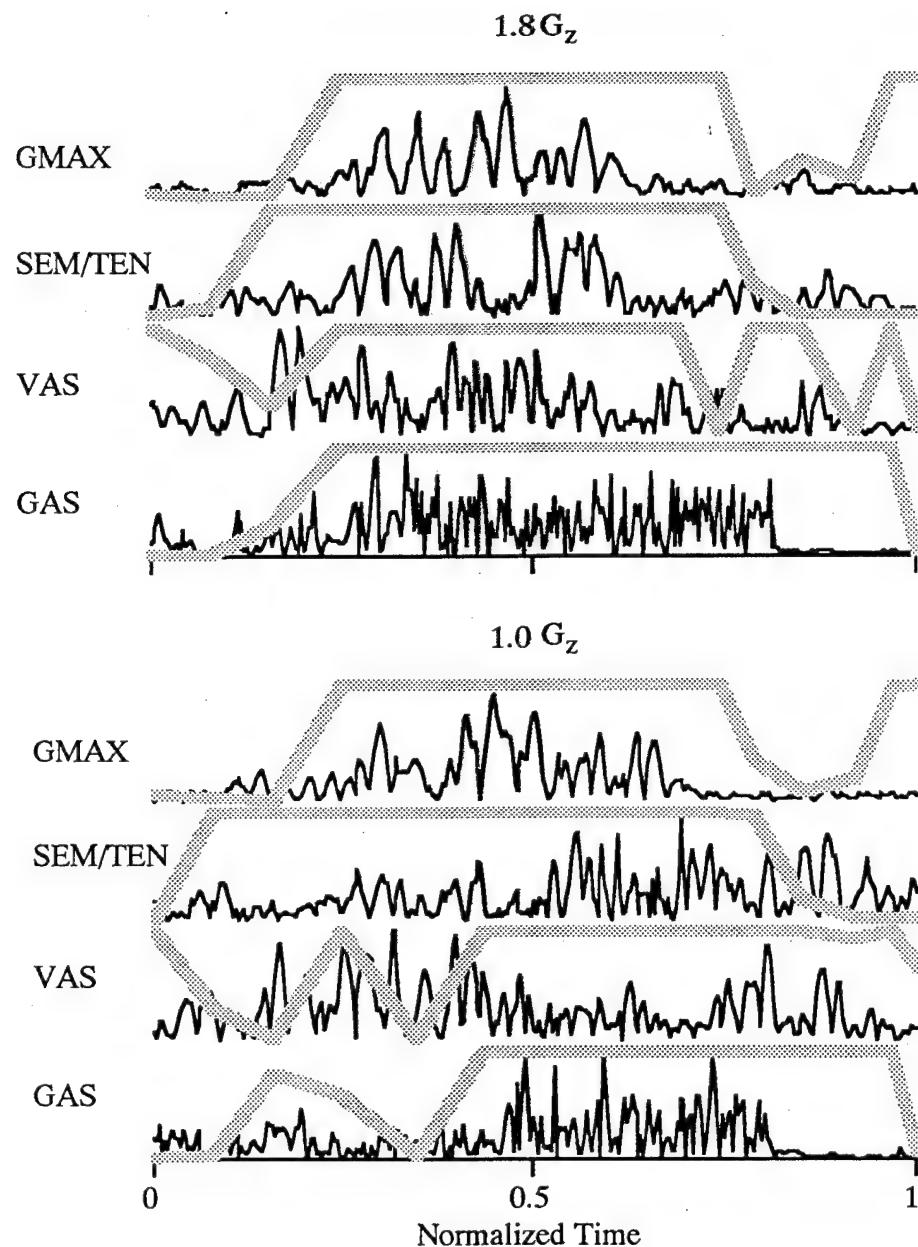
Figure 4.9 SEMG from Subject One and Neuroexcitation for 1.0 G_z and 1.8 G_z

The thin black lines represent measured data and the thick gray lines represent the predicted muscle neuroexcitations.

1.0 G_z and 1.8 G_z are presented in Figure 4.9. The SEMG data for GAS and predicted neuroexcitation for five different G_z levels are presented in Figure 4.10. No strong relationship or pattern exists between the neuroexcitations and SEMG data. No strong common SEMG data patterns between subjects were observed for any muscle. Each subject's SEMG data were qualitatively slightly different. The intra-subject SEMG individual muscle patterns and peak voltages appeared to be consistent for different levels of G_z (Table 4.3). The subjects used the same muscle SEMG patterns for each level of G_z. This same trend was observed with the predicted neuroexcitations.

In terms of the SEMG patterns observed across G_z, the model adequately predicted subject SEMG activity. Intra-subject muscle SEMG patterns did not change with G_z. However, based on the SEMG data, the subjects used slightly different muscle activation patterns to achieve a successful jump. This could have been the result or combination of two possibilities. Possibly, the subjects could have achieved higher jumps by using different activation patterns or, due to slight differences between the subjects, slightly different activation patterns were required to achieve maximum performance. In general, the SEMG data and predicted muscle neuroexcitations indicate a proximal to distal muscle activation pattern. The muscles spanning the hip were activated prior to the muscles spanning the ankle. The predicted neuroexcitation patterns adequately predicted the general trends in muscle SEMG patterns observed.

Measured SEMG and Predicted
Neuroexcitation of GAS
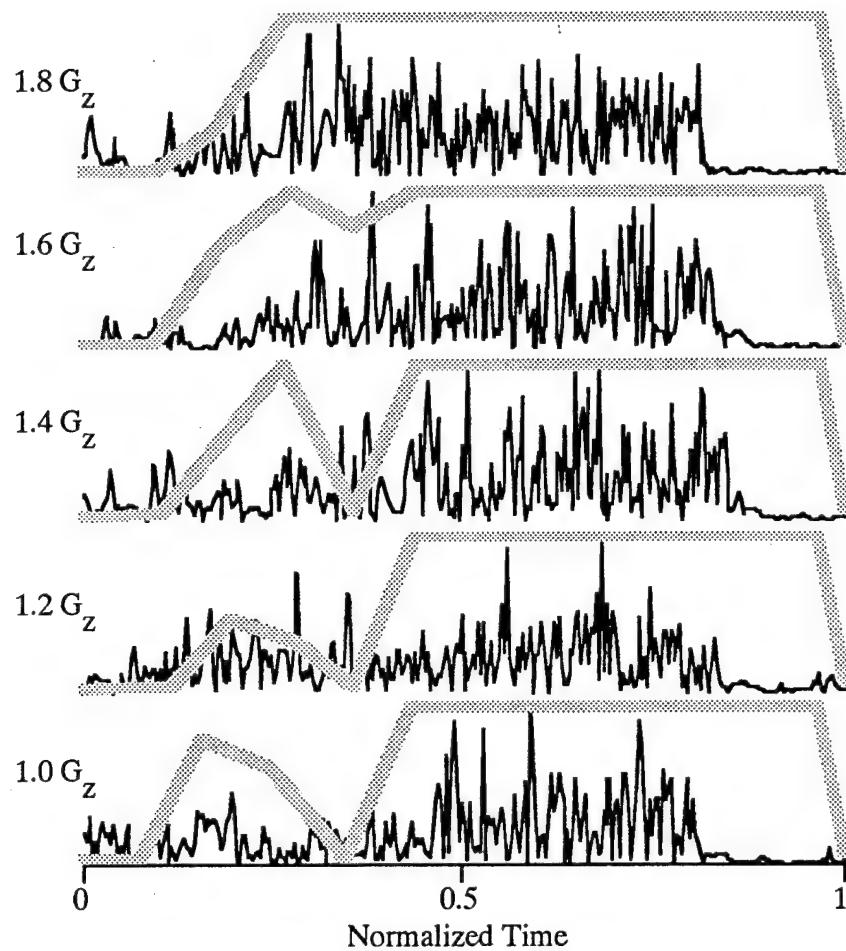
Figure 4.10 Measured SEMG (GAS) from Subject One and Predicted Muscle
Neuroexcitation for all G_z Values

The thin black lines represent measured data and the thick gray lines represent the
predicted muscle neuroexcitations.

Table 4.3 Peak Voltages After Filtering and Rectifying EMG Signal

Changing G_z does not significantly change the peak voltage of the processed
EMG signals. The peak voltages of the processed EMG signals are significantly
different between subjects. Reported values are in volts after being amplified by a
factor of 350.

Subject	Muscle	1.0 G_z	1.2 G_z	1.4 G_z	1.6 G_z	1.8 G_z
1	GAS	0.19	0.15	0.14	0.14	0.23
2	GAS	0.33	0.30	0.32	0.36	0.36
3	GAS	0.05	0.09	0.09	0.11	0.24
4	GAS	0.12	0.07	0.11	0.10	0.11
5	GAS	0.12	0.08	0.11	0.17	0.13
6	GAS	0.12	0.15	0.23	0.19	0.22
7	GAS	0.19	0.24	0.17	0.20	0.13
8	GAS	0.05	0.06	0.05	0.11	0.04
1	VAS	0.33	0.30	0.16	0.14	0.33
2	VAS	0.27	0.23	0.21	0.18	0.19
3	VAS	0.20	0.19	0.14	0.20	0.18
4	VAS	0.38	0.36	0.60	0.26	0.49
5	VAS	0.21	0.15	0.15	0.18	0.17
6	VAS	0.20	0.31	0.21	0.35	0.15
7	VAS	0.39	0.47	0.49	0.43	0.34
8	VAS	0.21	0.15	0.24	0.10	0.20

Table 4.3 Peak Voltages After Filtering and Rectifying EMG Signal - continued

Subject	Muscle	1.0 G_z	1.2 G_z	1.4 G_z	1.6 G_z	1.8 G_z
1	HAMS	0.04	0.04	0.18	0.14	0.06
2	HAMS	0.07	0.07	0.16	0.06	0.06
3	HAMS	0.10	0.09	0.10	0.12	0.10
4	HAMS	0.05	0.05	0.04	0.07	0.04
5	HAMS	0.09	0.08	0.10	0.10	0.13
6	HAMS	0.15	0.14	0.14	0.13	0.08
7	HAMS	0.19	0.18	0.13	0.16	0.14
8	HAMS	0.06	0.07	0.07	0.05	0.06
1	GMAX	0.23	0.15	0.24	0.11	0.18
2	GMAX	0.10	0.07	0.08	0.11	0.08
3	GMAX	0.29	0.22	0.22	0.23	0.11
4	GMAX	0.06	0.09	0.11	0.17	1.03
5	GMAX	0.92	0.92	0.09	0.32	0.27
6	GMAX	0.16	0.20	0.19	0.12	0.09
7	GMAX	0.42	0.25	0.22	0.35	0.41
8	GMAX	0.07	0.09	0.10	0.08	0.08

Some muscles appeared to have a lower frequency response compared to other muscles. These muscles were located in areas of the body that normally had thicker fat storage and the fat may have acted as lowpass filters.

4.3 COMPARISON OF MODELING RESULTS WITH REPORTS IN THE LITERATURE

Other researchers have used this type of modeling technique to simulate jumping in a 1.0 G_z environment (Anderson, 1992; Ziegler 1994; Fujii and Toshimichi, 1993; and van Soest et al., 1993). Differences in the initial static position and subject population made direct numerical comparison of the reported results with the present study unwarranted. However, it was expected that the predicted time histories of accelerations and powers from this study should be of the same order of magnitude as reported in the earlier studies.

The power transferred to each segment during jumping at 1.0 G_z is presented in Figure 4.11. The predicted time history and peak power delivered to the skeletal system and to each segment determined in this study are very similar to previous jumping studies using forward dynamics. The predicted peak power delivered to the skeletal system normally occurred near the 70 percent mark and had a magnitude between 3500 to 4000 watts. The peak power delivered to the HAT segment occurred prior to the peak power to the total skeletal system and had a magnitude near 3000 watts.

Similarly, the predicted muscle power delivered to the HAT segment in this study was consistent with the previous studies. VAS provided more power to the HAT segment than any other muscle. The uni-articular hip extensors muscles,

Instanteous Segment Power, watts
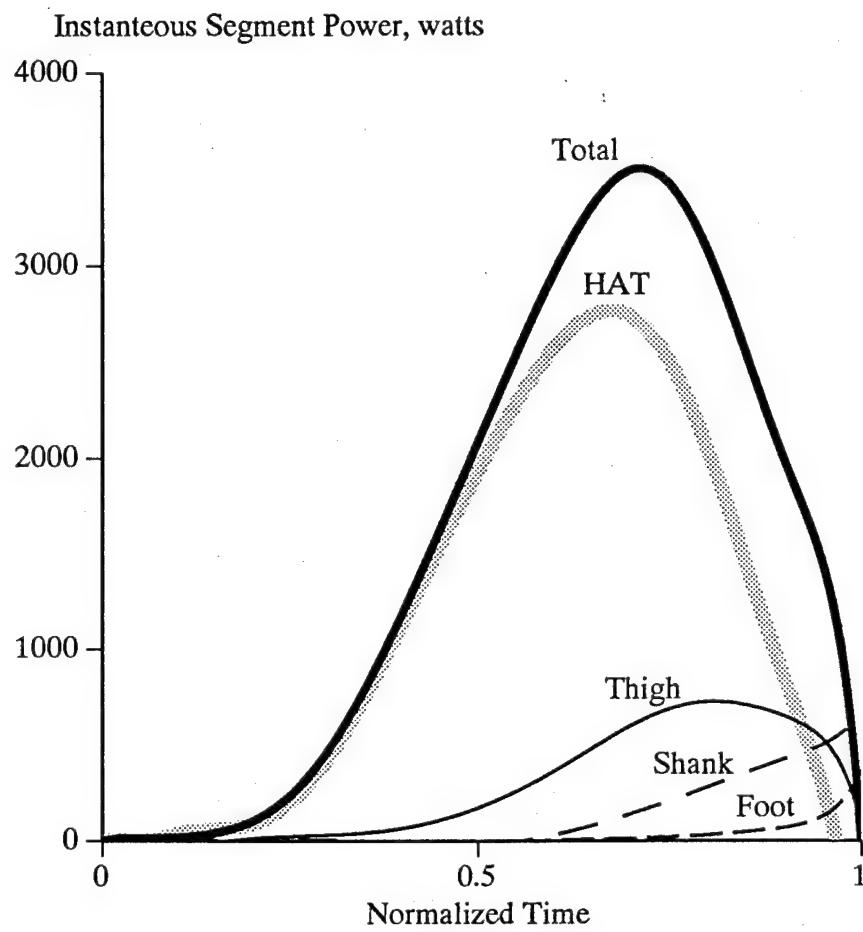
Figure 4.11 Predicted Power Delivered to Each Segment During a Jump at 1.0 G_z

Muscle Power Delivered to HAT, watts
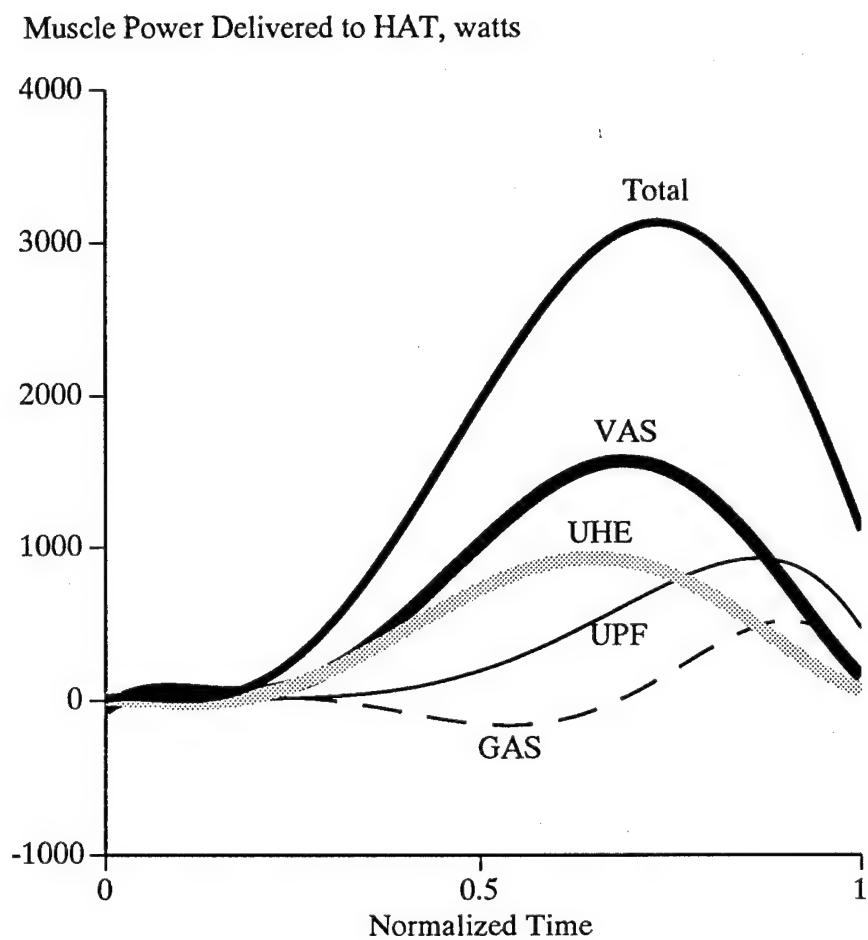
Figure 4.12 Predicted Muscle Power Delivered to the HAT Segment at 1.0 G_z

UHE, and uni-articular plantar flexors, UPF, provided the majority of the remaining power that was delivered to HAT (Figure 4.12).

The predicted neuroexcitations from this study were somewhat difficult to compare to previous studies. Most of the researchers used six to eight muscles with the exception of Ziegler that also used 20 musculotendon units. However, Ziegler had a much more sophisticated knee joint model. Still, the predicted muscle neuroexcitations found in this study agreed with the previous efforts. In fact, Ziegler used the 1.0 G_z optimal control solution found in this study as the initial guess used in his study.

4.4 CONCLUSION

Verification of the musculoskeletal model solution was accomplished by comparing measured quantities (jump height, time required to jump, GRF, joint kinematics, and SEMG) to the corresponding predicted quantities. Also, at 1.0 G_z, the musculoskeletal model solution was verified by comparing predicted quantities to previously verified musculoskeletal model solutions. All comparisons indicated the musculoskeletal model adequately predicted the measured data. Therefore, it was concluded the musculoskeletal model adequately predicted human jumping in altered G_z environments. It was assumed that since the musculoskeletal model adequately predicted performance in the increased G_z environment that results from simulations of decreased G_z environments were also valid.

Chapter 5: Musculoskeletal Model Results

The research question, "how do changes in gravitational force affect jumping performance and intermuscular control?" was answered by analyzing the musculoskeletal model solutions for jumping in altered G_z environments. In previous chapters, the experimental methods were described and musculoskeletal model validated. In this chapter, the effect of altered G_z on jumping performance and intermuscular control is discussed.

5.1 JUMPING PERFORMANCE

Jumping performance was divided into the following areas: jump height, power and energy transferred to the COM of the skeletal system, the muscle forces generated, and the power and energy transferred to the skeletal system during the jump. In this section, each of these areas will be discussed. The musculoskeletal model was solved using nine values for gravity (nine G_z levels). By changing the force acting on the COM by altering the value of gravity rather than using a centrifuge, the X, Y, Z axis were aligned with x, y, z axis, or alternatively, $\beta = |\bar{\omega}| = 0.0$.

5.1.1 Effect of Gravity on Jump Height

The predicted jump height for each value of G_z simulated is presented in Figure 5.1. Jump height decreased as G_z increased. The relationship between jump height and G_z was non-linear (appeared to be a power relationship). This

85

Jump Height, cm

G_z

Jump Height, cm

$1/G_z$
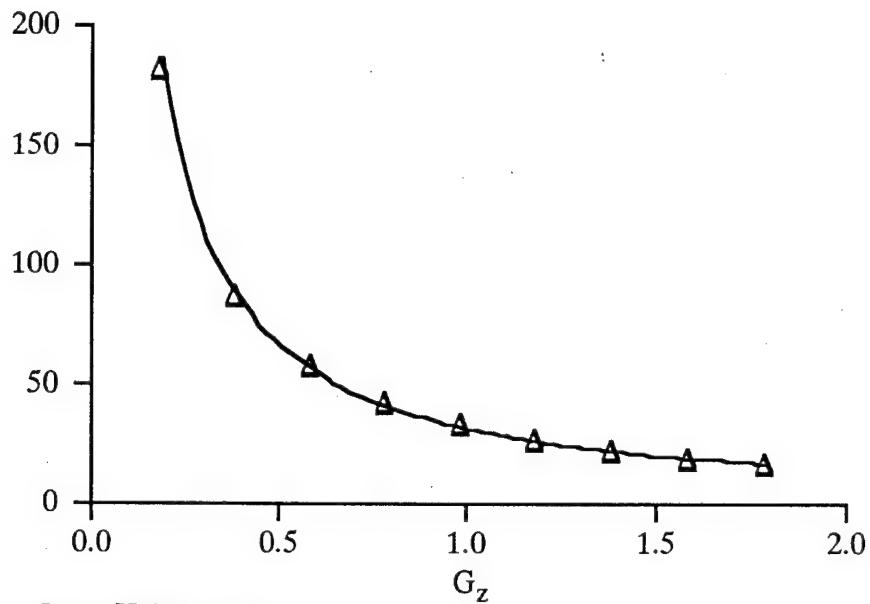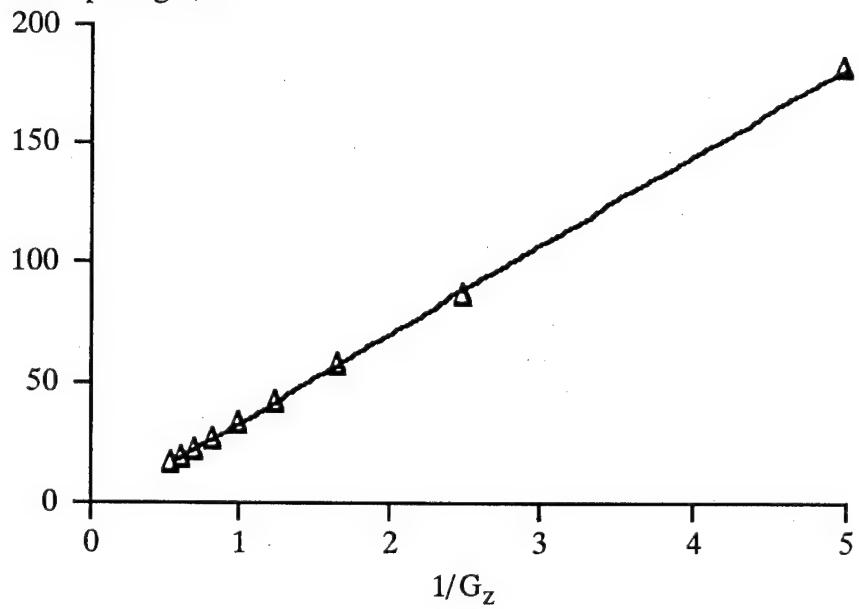
Figure 5.1 Jump Height Versus G_z and $1/G_z$

observation suggested a linear relationship could have existed between the reciprocal of G_Z and jump height (Figure 5.1). In fact, the relationship between $1/G_Z$ and jump height was linear in the range studied (r > 0.99). Changing G_Z led to a change in weight. Using this observation, a linear relationship was hypothesized to exist between 1/weight and jump performance. A similar conclusion, jumping performance was linearly related to strength-to-weight ratio, was reached by Zajac and Pandy (1989). Therefore, it was concluded that jump height was linearly related to $1/G_Z$.

5.1.2 Motion of Center of Mass

Jumping requires energy to be expended to push the COM upward. The total energy expended during jumping is the sum of potential and kinetic energies at the time of take-off. Thus, by knowing the take-off $^Z\bar{v}_{com}$ and $^Z\bar{d}_{com}$, the change in total energy utilization related to altered G_Z could be investigated. To determine the potential, kinetic, and total energies, $^Z\bar{a}_{com}$, $^Z\bar{v}_{com}$, and $^Z\bar{d}_{com}$ were calculated.

The $^Z\bar{a}_{com}$, $^Z\bar{v}_{com}$, and $^Z\bar{d}_{com}$ were calculated from the predicted GRF. Figure 5.2 is a graph of the GRF and $^Z\bar{a}_{com}$ for three different G_Z environments. The initial (body weight) and peak GRF increased as G_Z increased. The peak $^Z\bar{a}_{com}$ decreased as G_Z increased. Also, the $^Z\bar{a}_{com}$ passed through zero earlier in the jump as G_Z was increased. Thus, the COM began to slow down sooner ($^Z\bar{a}_{com}$ became negative sooner) in the jump as G_Z increased.
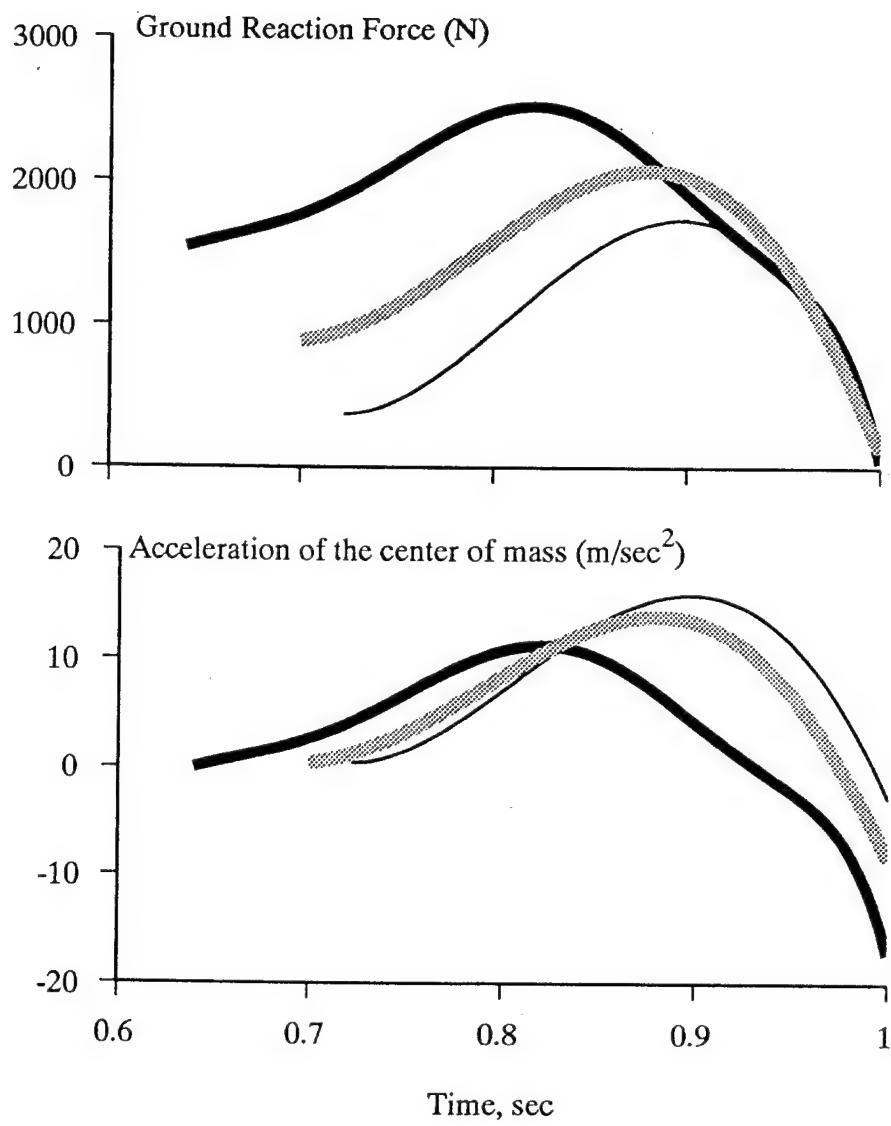
Figure 5.2 GRF and $^z\bar{a}_{com}$ for Different G_z Levels

Gray line 1.0 G_z, light black line 0.4 G_z and heavy black line 1.8 G_z

The $^z\bar{a}_{com}$ was dependent upon the G_z level therefore, it was expected that $^z\bar{v}_{com}$ and $^z\bar{d}_{com}$ would also change with altered G_z (Figure 5.3). The take-off $^z\bar{v}_{com}$ decreased as G_z increased while the take-off $^z\bar{d}_{com}$ remained relatively constant. Since the take-off $^z\bar{d}_{com}$ did not change with G_z, the change in jump height was related to the change in take-off $^z\bar{v}_{com}$ resulting from altering G_z. The peak $^z\bar{v}_{com}$ did not occur at take-off, rather it occurred earlier (the same time the $^z\bar{a}_{com}$ passed through zero) and declined from that point on. Therefore, as the G_z level increased, the peak $^z\bar{v}_{com}$ decreased and occurred earlier in the jump (longer before take-off); both events reduced the take-off $^z\bar{v}_{com}$. During the flight phase of the jump, the only force which acted on the body was gravity. In a decreased G_z environment, the force due to gravity was reduced and therefore, the decline in the flight velocity was reduced. Both the increase in take-off $^z\bar{v}_{com}$ and the decrease in gravity related to decreased G_z resulted in increased flight time. This allowed the COM to rise longer and achieve a higher jump as G_z decreased.

5.1.3 Energy Delivered to the Center of Mass

Total energy is composed of potential energy, P.E., and kinetic energy, K.E. The K.E. can be further divided into translational and rotational energy. The net rotational energy delivered to the HAT segment was small (section 5.1.4 and Figure 5.6). Therefore, the following energy analysis about the COM was restricted to translational movement of the COM in the z direction. The total
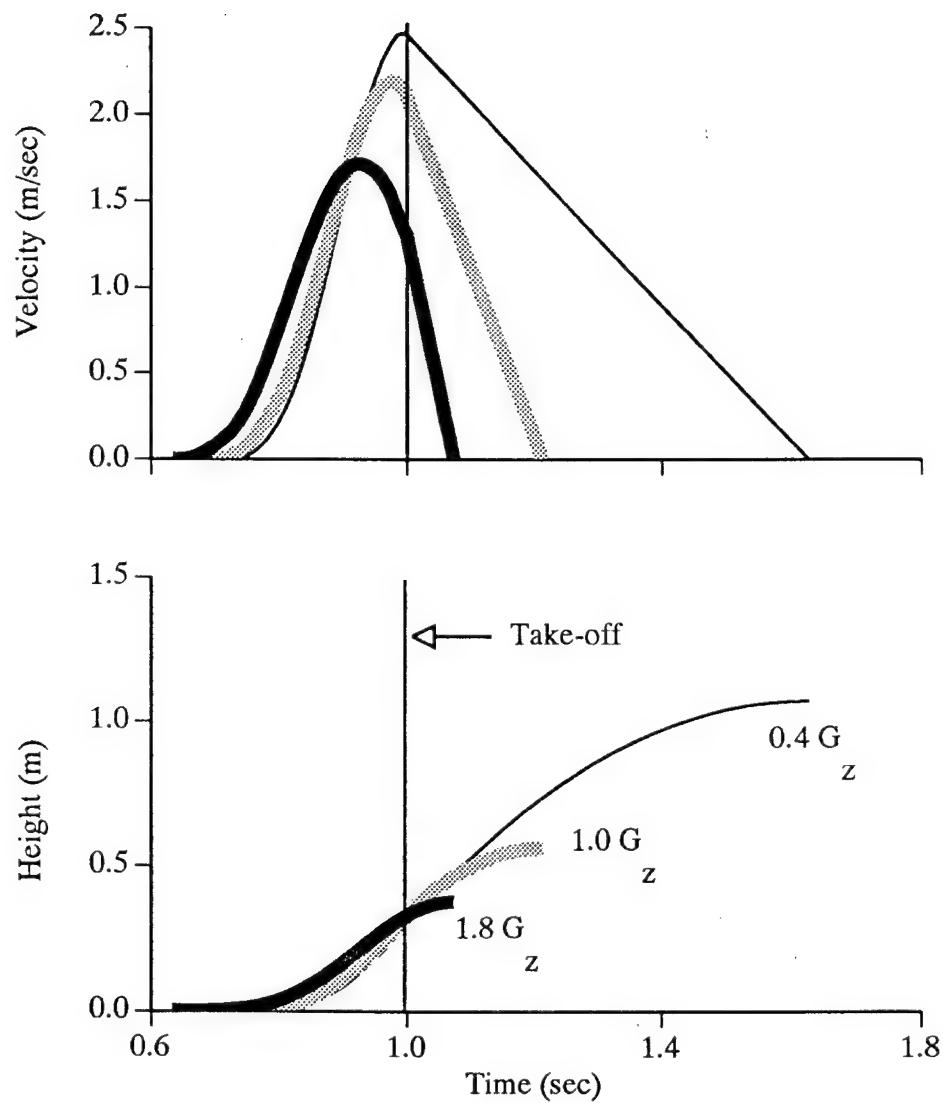
Figure 5.3 $^Z\bar{v}_{com}$ and $^Z\bar{d}_{com}$ at Different G_Z Levels

Thick black line represents 1.8 G_Z, gray line 1.0 G_Z, and thin black line 0.4 G_Z

energy generated in the jump could be found by determining the P.E. and K.E. at take-off. Selecting the datum point at the height of the COM in the static position:

$$P.E. = mass \cdot \bar{a}_g \cdot {}^{z}\bar{d}_{take\text{-}off}$$ (5.1)

$$K.E. = 0.5 \cdot mass \cdot \left({}^{z}\bar{v}_{take\text{-}off}\right)^2$$ (5.2)

The total energy (including P.E. and K.E.) expended at take-off during jumping in different G_z environments is presented in Figure 5.4. For a nine-fold increase in G_z, the total energy expended doubled while the jump height decreased almost 20 fold. If the total energy expended were directly related to jump height, then it would be expected that the jump height would have decreased only five-fold over this G_z range. The reason that the jump height changed was that the distribution of K.E. and P.E. also changed as G_z was altered.

From equation 5.1, the P.E. is a function of $\bar{a}_g$ and ${}^{z}\bar{d}_{take\text{-}off}$. The ${}^{z}\bar{d}_{take\text{-}off}$ changed very little with increased G_z while $\bar{a}_g$ is directly related to G_z. Therefore, the change in the P.E. was the same as the change in $\bar{a}_g$, i.e. a nine fold increase in G_z resulted in a nine fold increase in P.E. The K.E. also varied in a linear mode with G_z but decreased rather than increased with increased G_z. K.E. was a function of mass and ${}^{z}\bar{v}_{com}{}^2$. Mass was held constant therefore, K.E. was directly related to $({}^{z}\bar{v}_{com})^2$. A nine-fold increase in G_z resulted in a three fold decrease in $({}^{z}\bar{v}_{com})^2$, or slightly less than a two fold decrease in ${}^{z}\bar{v}_{com}$. Jump height decreased because the K.E. generated decreased.
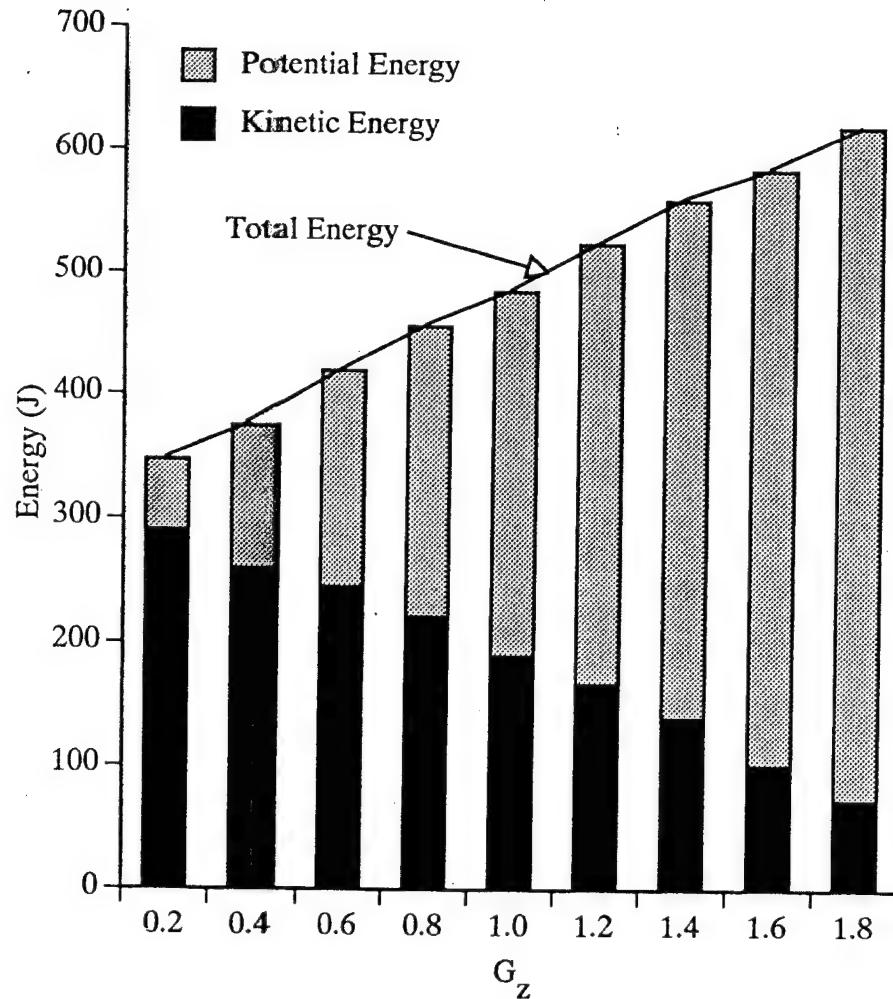
Figure 5.4 Predicted Energy at Take-off in Different G_z Environments

The potential and kinetic energies presented in this graph were calculated at take-off. The datum was selected as the height of the COM in the squat position.

Altering G_z resulted in a change in the total energy (P.E. and K.E.) developed during jumping. The only forces acting on the COM besides gravity are the muscle forces. Since energy is a function of power (equation 3.25) and power is a function of acceleration (equation 3.24) analysis of the forces developed by muscle and muscle power and energy transferred to the skeletal system is required to complete the analysis of jumping performance.

5.1.4 Muscle Force, Power, and Energy

Muscles provided the energy required to jump. Analysis of the energy each muscle provided to each segment of the musculoskeletal model during jumping in different G_z environments indicated that a majority, greater than 70%, of the energy was transferred to the HAT segment. After review, it was decided to classify the muscles into groups based on function and neuroexcitation patterns. The functional groups were: uni-articular plantar flexors (UPF), bi-articular plantar flexor and knee flexor (GAS), uni-articular knee extensor (VAS), bi-articular knee extensor and hip flexor (RF), bi-articular hip extensors and knee flexors (HAMS), and uni-articular hip extensors (UHE). The grouped muscles had similar neuroexcitation patterns (Figure 5.5a and Figure 5.5b) with two exceptions, TFL and GMED/MIN. These two muscles probably act more in joint adduction and abduction rather than joint extension and flexion. VAS, GAS and RF were not combined with any other muscles.

Total energy is also the sum of rotational energy and translational energy. The total, translational and rotational energies transferred to the HAT segment by
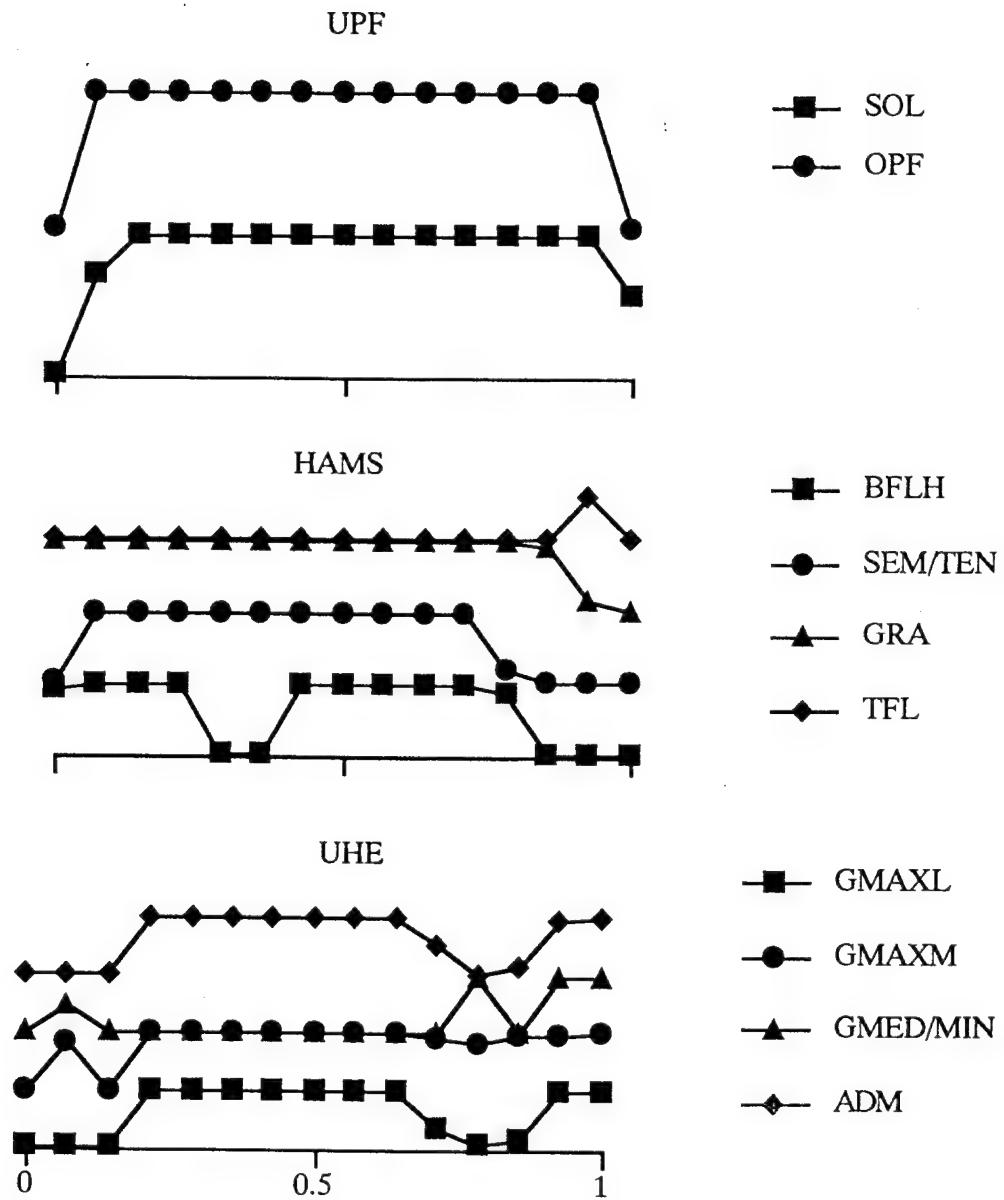
Figure 5.5a Muscle Groups

Predicted neuroexcitations of grouped muscles for 1.0 G_z.
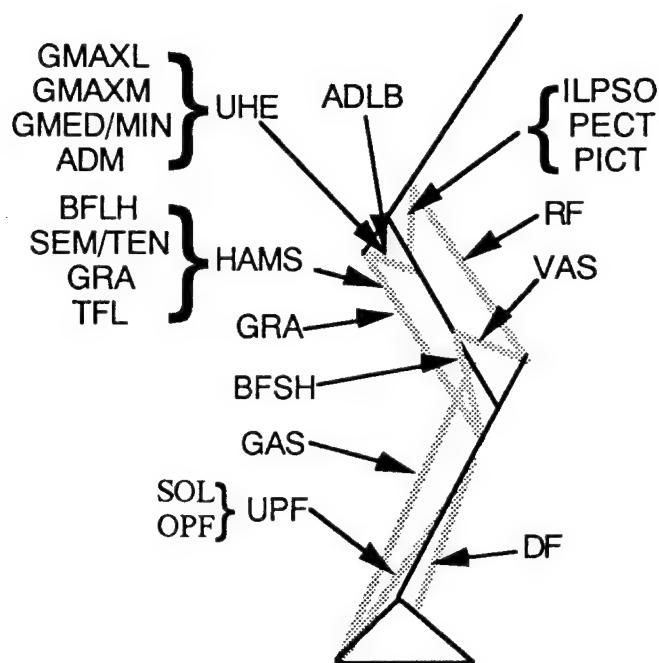
Figure 5.5b Muscle Grouping by Function

All muscles used in the model are represented in this figure. The primary role of
SAR, PICT, PICT, ADLB, and GRA do not include extension/flexion of the joints
or only provide minimal power. Therefore, these muscles were not grouped with
the remaining muscles that did provide the majority of power and energy to the
skeletal system.

each muscle group is presented in Figure 5.6. In general, the muscle energy delivered to the HAT segment increased as G_z increased, but the distribution of the total, translational and rotational energies between muscles remained relatively constant. Therefore, the analysis of the muscle energies transferred to the HAT segment for 1.0 G_z will be presented and will be generally true for every G_z level studied. The distribution of energy between muscles is presented in Table 5.1.

With reference to Figure 5.6 and Table 5.1, the total muscle energy transferred to the HAT segment was comprised of mostly translational energy, with more than 95% of the translational energy being in used for movement in the z direction. The sum of the rotational energies transferred to the HAT segment was much smaller than the translational energy. The uni-articular muscles provided the majority of translational energy to the HAT segment during jumping.

The uni-articular muscles always provided more translational energy than rotational energy while the bi-articular muscles always provided more rotational energy than translational energy to the skeletal system. The uni-articular muscles provided most of the necessary energy for translation of the HAT segment at all G_z levels. Conversely, the bi-articular muscles provided half of all the rotational muscle energy transferred to and absorbed from the HAT segment.
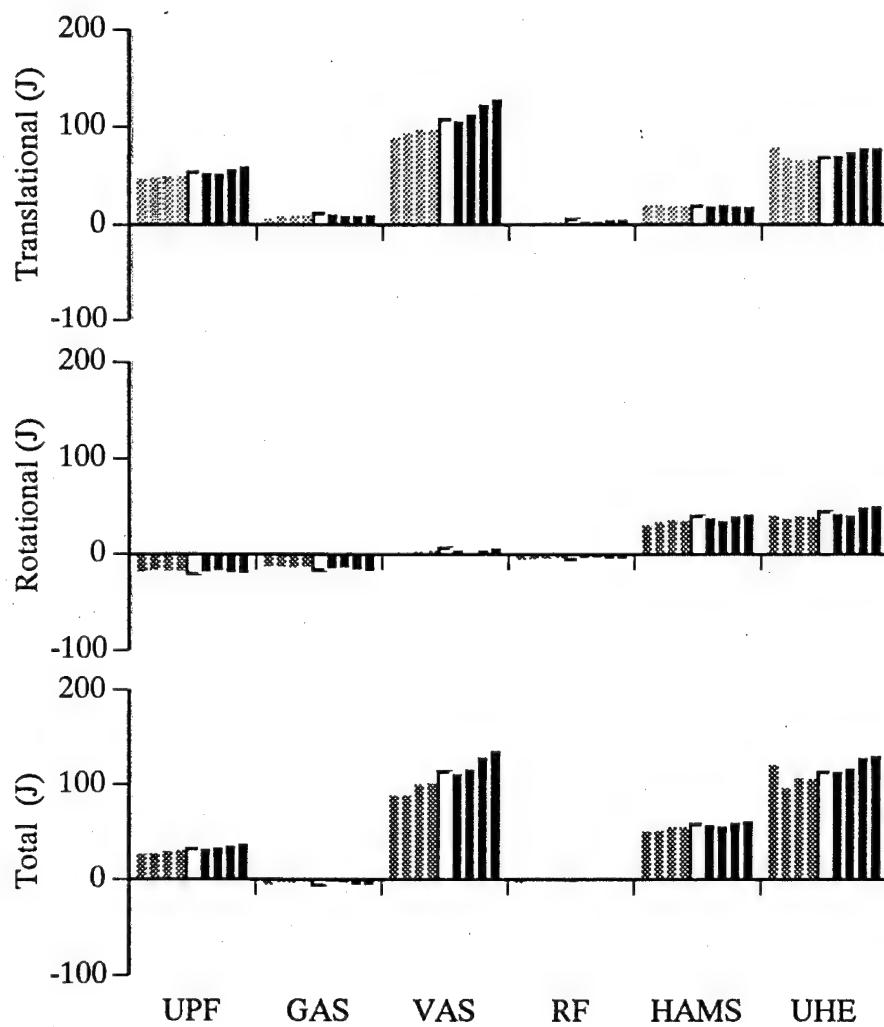
Figure 5.6 Total, Translational and Rotational Muscle Energies Delivered to the HAT Segment for Different G_z Levels

The gray bars represent hypo-gravity (0.2 G_z - 0.8 G_z), the clear center bar represents 1.0 G_z, and the black bars represent hyper-gravity (1.2 G_z to 1.8 G_z)

Table 5.1 Distribution of Muscle Energies

The energy delivered by each muscle to the HAT segment increased as G_z increased but, the distribution of the energies between the different muscles did not vary as G_z was increased. The approximate percentage of muscle energies transferred to the HAT segment for 1.0 G_z level are presented in this table. The [*] represents muscles that absorbed (negative energy) from the HAT segment.

	Translational Energy	Rotational Energy	Total Energy
UPF	21%	13%[*]	10%
GAS	3%	13%[*]	2%[*]
VAS	41%	4%	36%
RF	2%	4%[*]	0%
HAMS	7%	33%	16%
UHE	26%	33%	35%

Translational energy was utilized to move the HAT segment upward, i.e. jump height while rotational energy was used to position (rotate) the HAT into position. At the time of lift-off, the net rotational energy transferred to the HAT segment was about 26 joules. This was a small amount of rotational energy thus the HAT segment had very little rotation at lift-off.

It could be hypothesized that during jumping the uni-articular muscles provided the translational energy to the HAT segment and in doing so caused the HAT segment to rotate. The bi-articular muscles' role was to provide the necessary negative energy to control the HAT segment rotation such that the HAT was optimally positioned during the entire ground contact phase and at take-off.

Energy is the integration of power. Thus, energy is a single measure of the net power transferred over the entire event. Therefore, to understand fully how energy was distributed to the body segments by the muscles, patterns of power distribution must be examined. It is possible for a muscle to provide substantial positive and negative power during the jump such that the net power (energy) would be minimal. The power transferred (total, translational and rotational) by each muscle group for different G_z levels is shown in Figures 5.7 through 5.12.

During jumping, three muscles provided both positive and negative power to the HAT segment. VAS provided all positive translational power and both negative and positive rotational power. The sum of the rotational power provided by VAS during the jump was nearly zero for all G_z levels. RF provided very little translational power but, as did VAS, provided equal amounts of both positive and negative rotational power at different times during the jump for all G_z levels. GAS provided both positive and negative translational power to the HAT segment and all negative rotational power (absorbed rotational power from the HAT segment).

The majority of the muscle power transferred to the HAT segment was translational and was provided by the uni-articular muscles at all G_z levels. The peak , translational and rotational powers did not vary greatly over the G_z range studied. The length of time that the power was applied increased with G_z. Therefore, the increase in muscle energy transferred to the HAT segment as G_z increased was the result of an increased integration time rather than an increase in the peak magnitude of the muscle power transferred to the HAT segment.
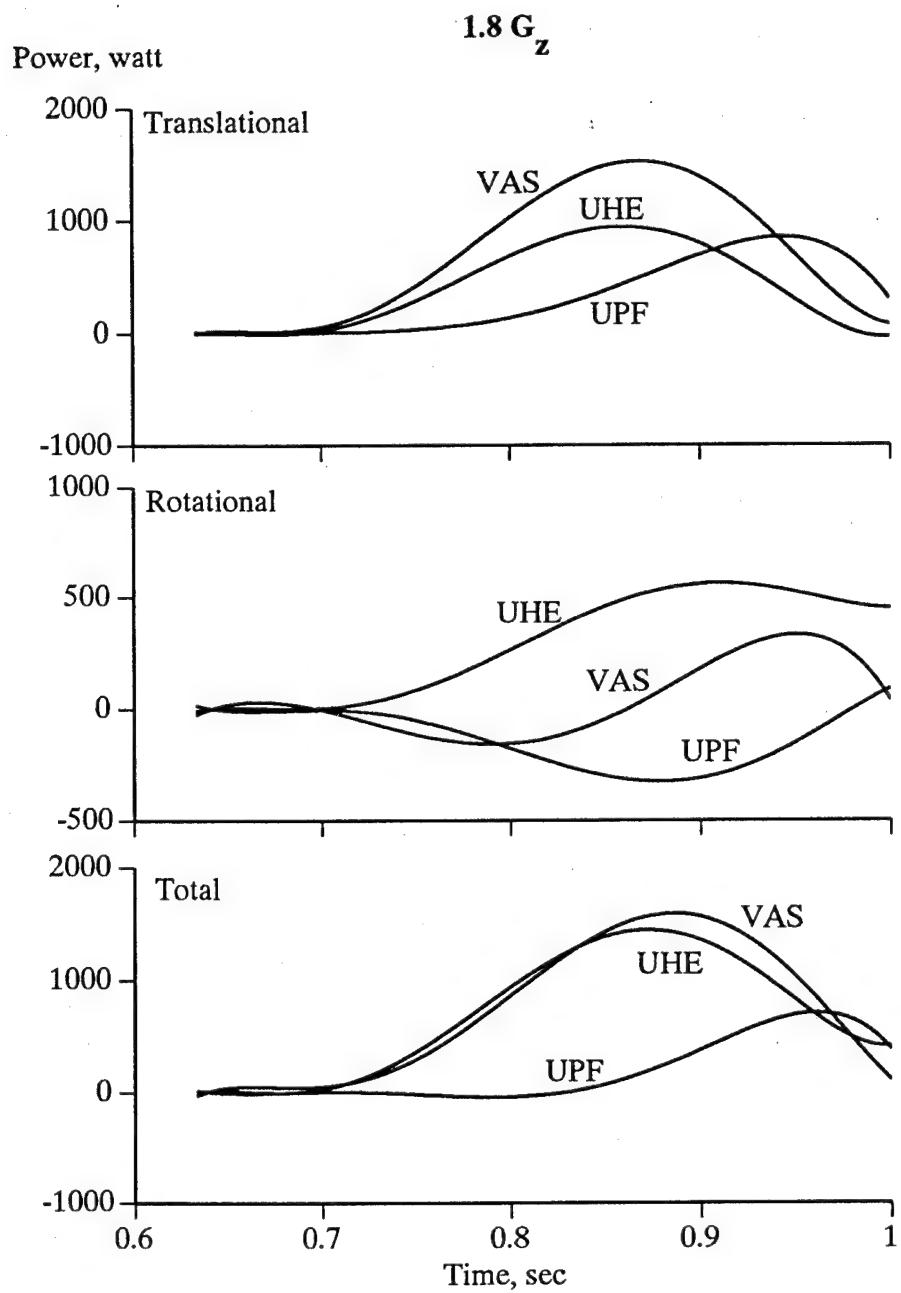
Figure 5.7 Uni-articular Muscle Power Transferred to HAT Segment at 1.8 G_z
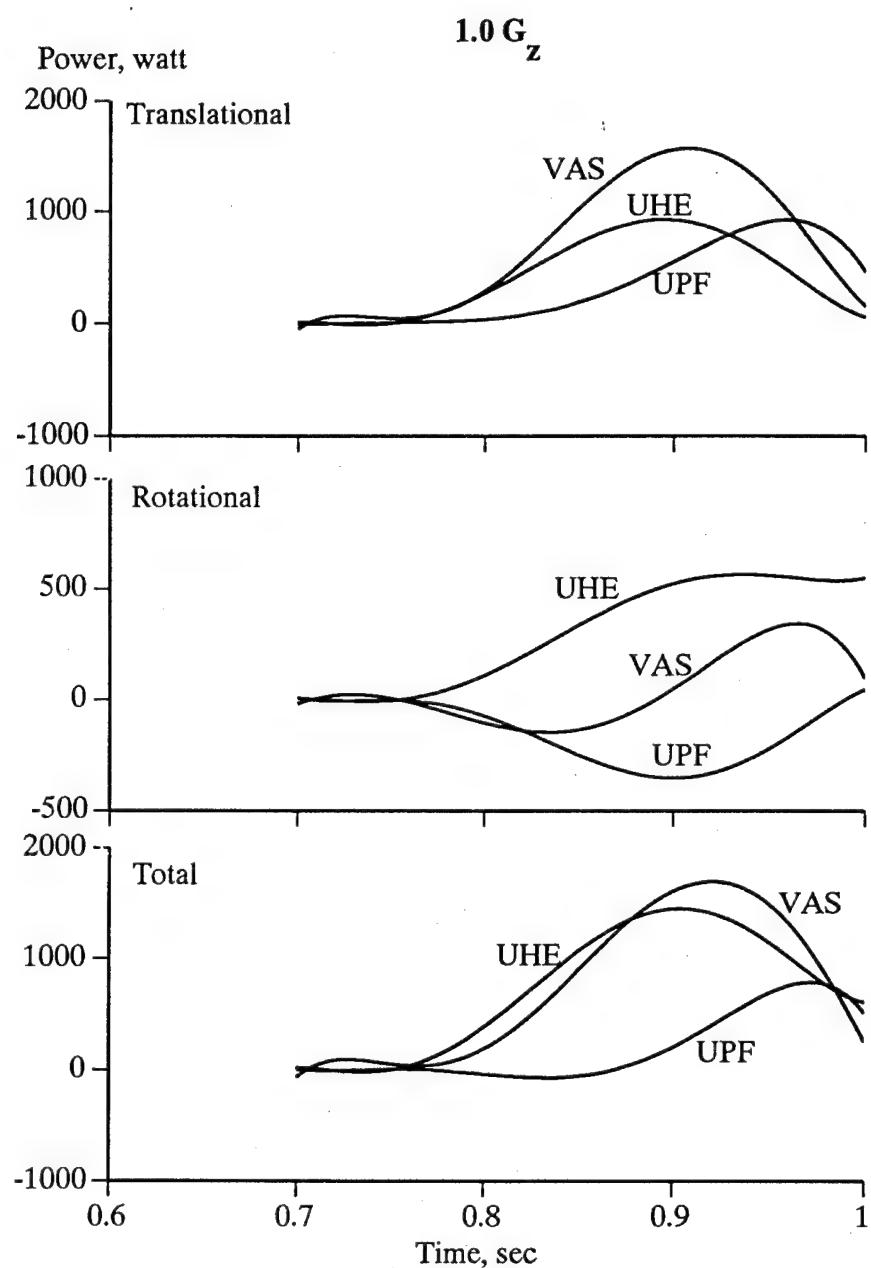
Figure 5.8 Uni-articular Muscle Power Transferred to HAT Segment at 1.0 G_z
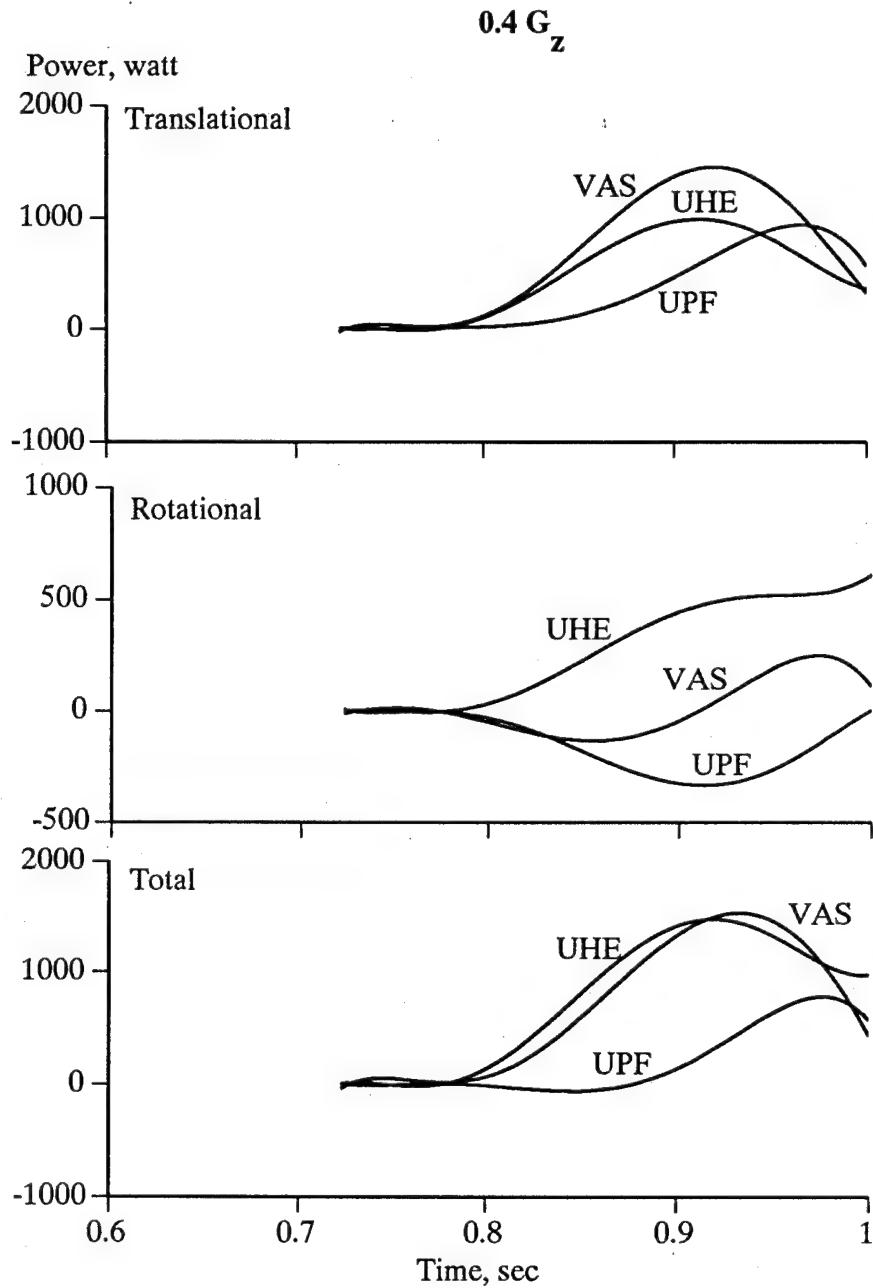
Figure 5.9 Uni-articular Muscle Power Transferred to HAT Segment at 0.4 G_z
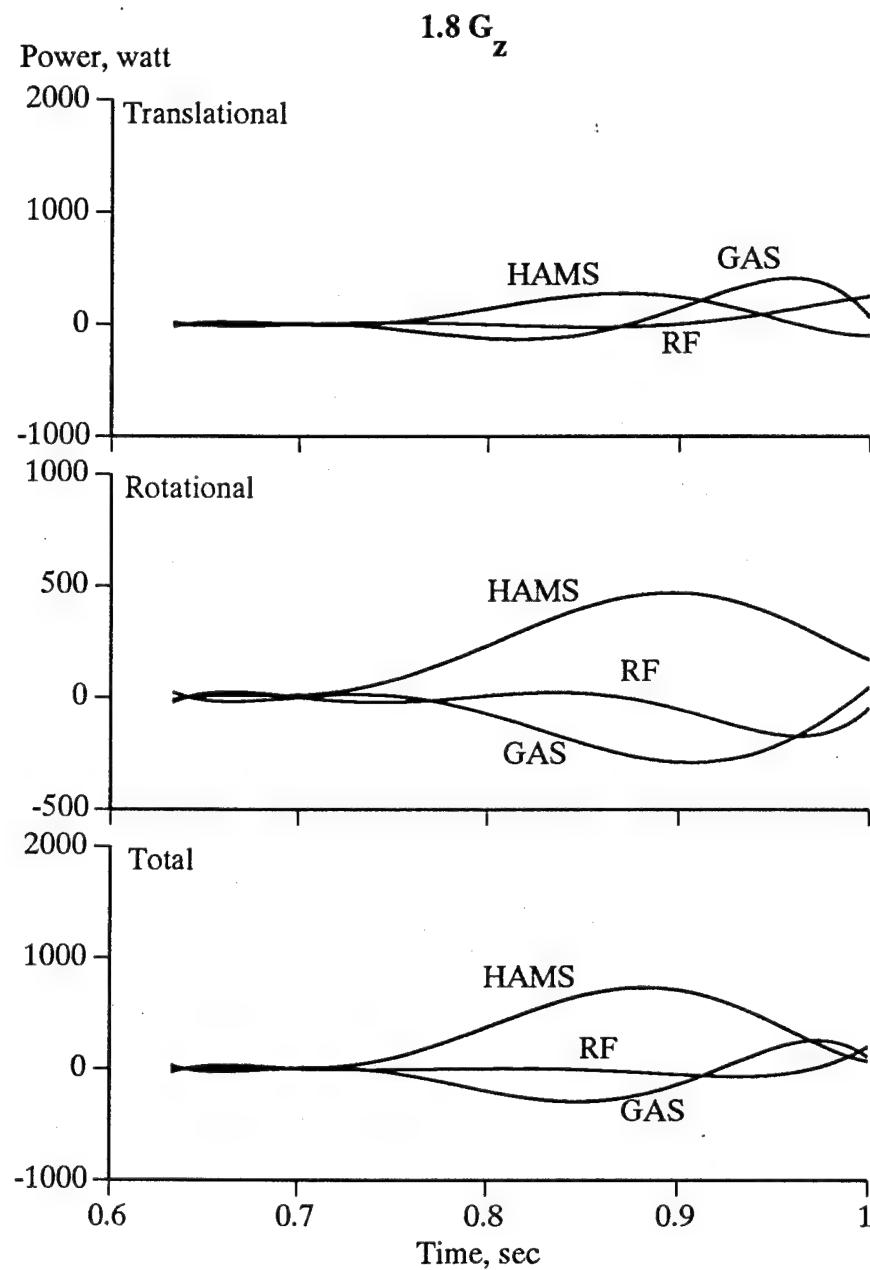
Figure 5.10 Bi-articular Muscle Power Transferred to HAT Segment at 1.8 G_z
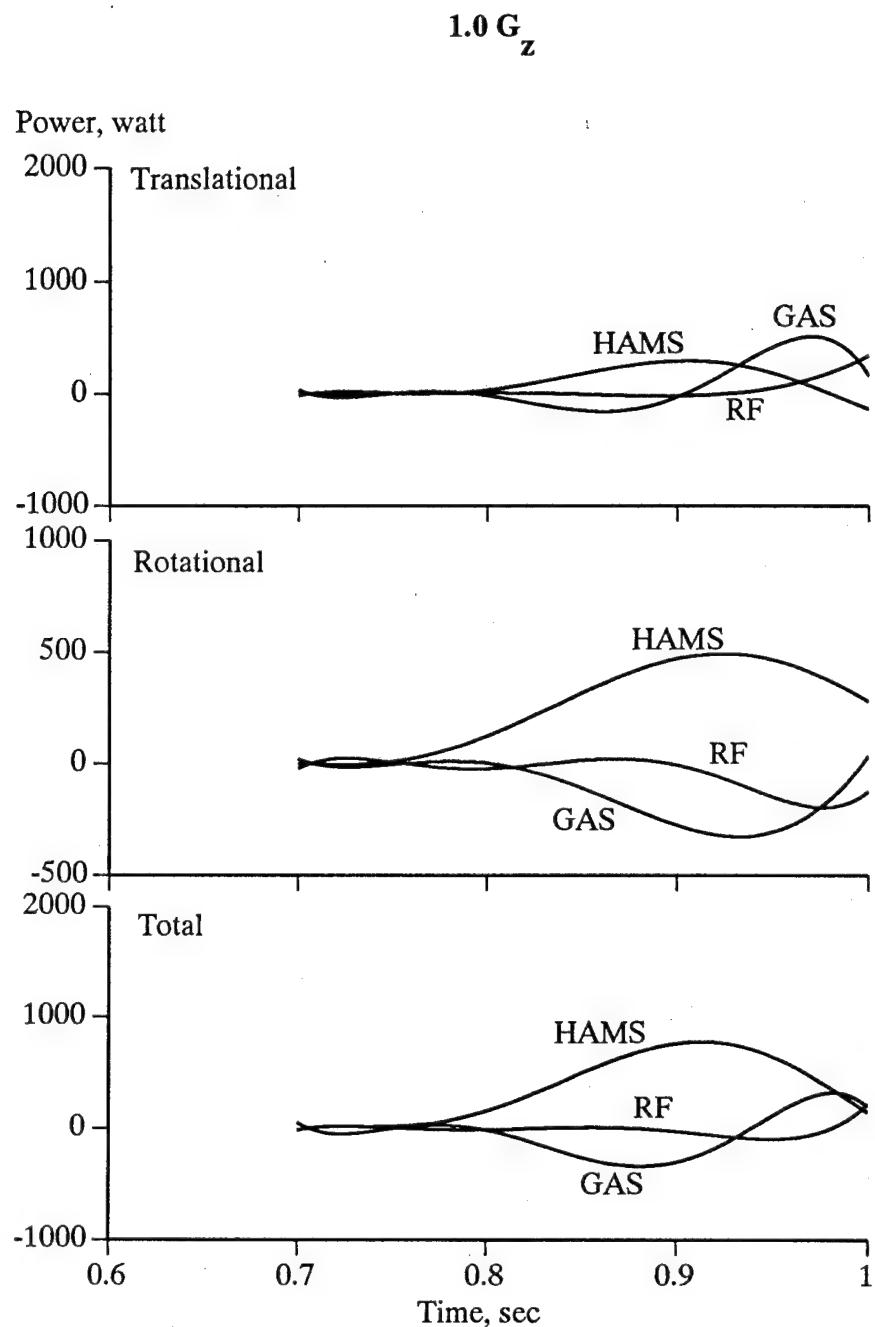
$$1.0\ G_z$$

Power, watt

Figure 5.11 Bi-articular Muscle Power Transferred to HAT Segment at 1.0 G_z
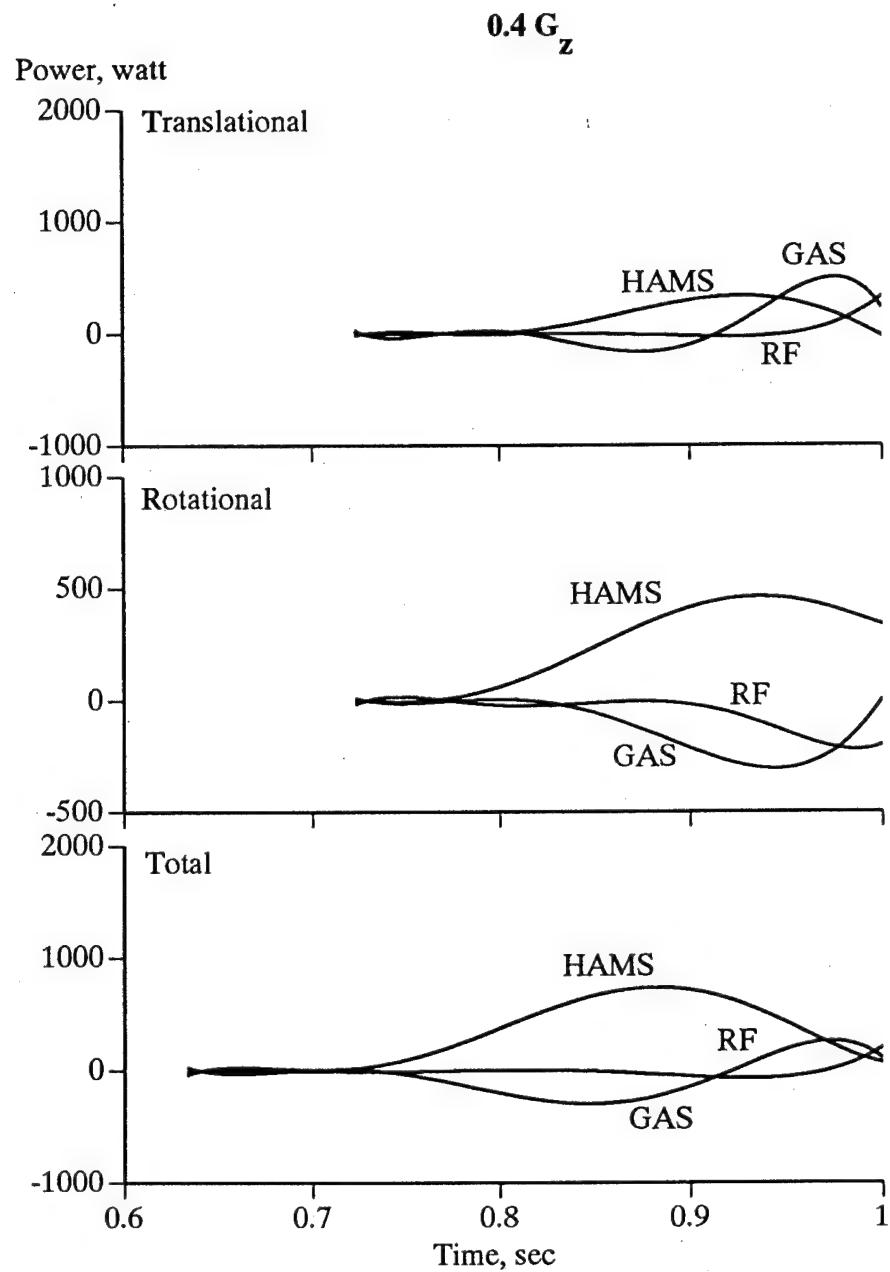
Figure 5.12 Bi-articular Muscle Power Transferred to HAT Segment at 0.4 G_z

For the uni-articular muscles, the peak translational power was always greater than the rotational power. The reverse was true for the bi-articular muscles. The uni-articular muscles provided the vast majority of the translational power required for jumping. The bi-articular muscles provided the rotational power necessary to maintain the proper orientation of the HAT segment.

The peak muscle powers transferred to the HAT segment did not vary greatly over the G_z range studied. Since the peak muscle powers transferred to the HAT segment did not vary greatly, it was expected that the muscle forces should demonstrate a similar pattern. The predicted muscle forces for VAS, UHE, GAS and HAMS for different G_z levels are presented in Figures 5.13 and 5.14.

The muscle force patterns from these four muscle groups are representative of the muscle patterns for all 20 muscles. The peak muscle force production did not increase substantially as G_z was increased. VAS had the greatest increase in peak force production, only 20% increase in peak force for a nine fold increase in G_z. As with muscle power transferred to the HAT, the muscles were activated longer rather than producing more force with increased G_z. The only major difference in muscle force between G_z levels were the muscle forces' initial values. As G_z was increased, the muscle forces required to maintain static equilibrium increased.
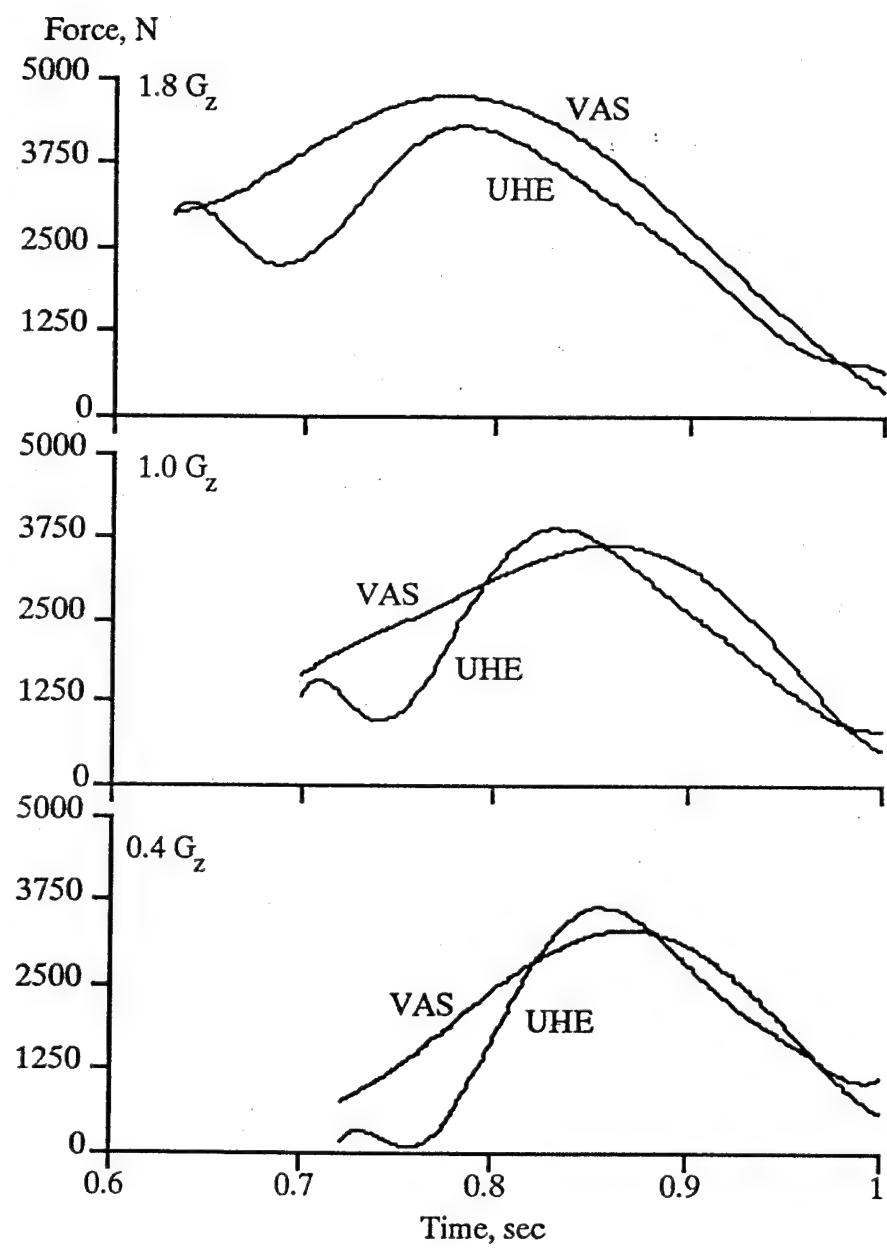
Figure 5.13 Muscle Force Generated by VAS and UHE for different G_z Levels
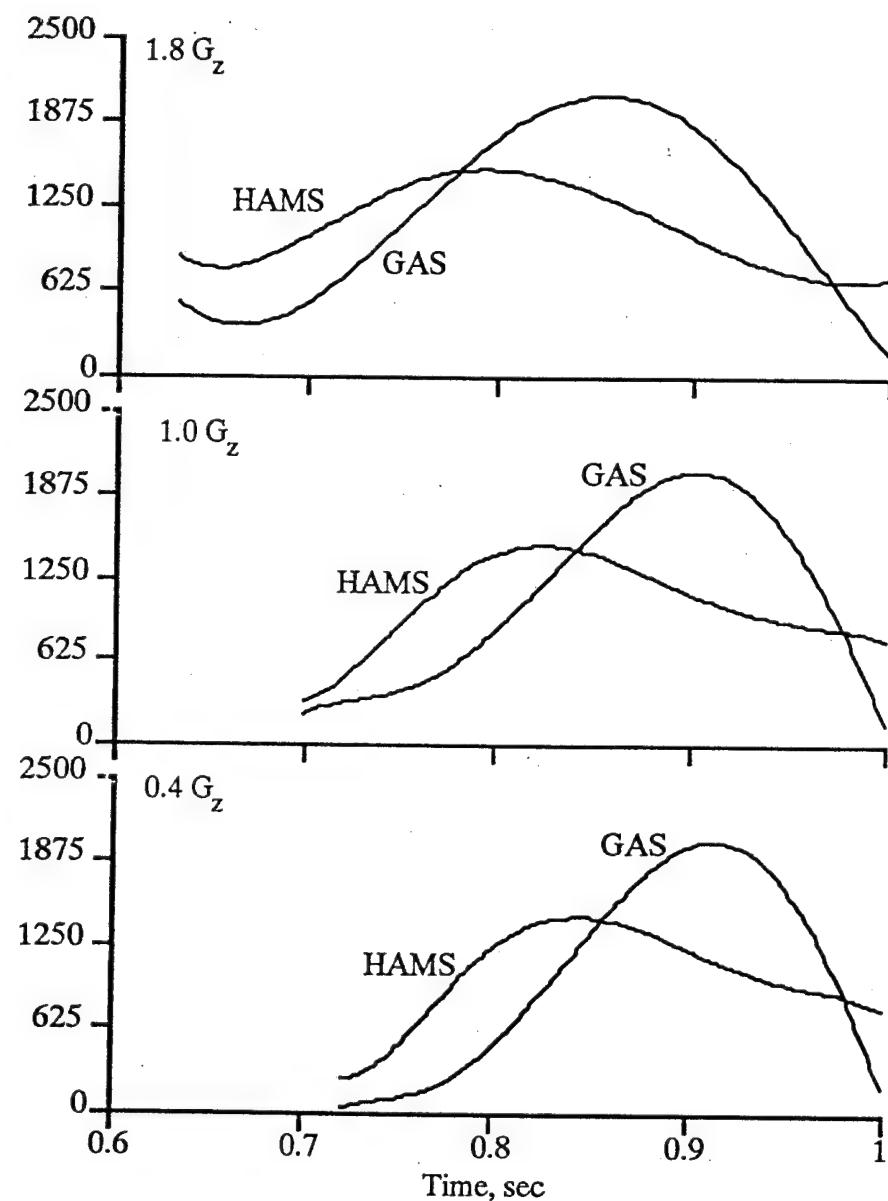
Figure 5.14 Muscle Force Generated by VAS and UHE for different G_z Levels

5.2 MUSCLE NEUROEXCITATION AND ACTIVATION

Muscle force was the result of muscle neuroexcitation-activation dynamics. The predicted neuroexcitations for GMAX (UHE), VAS, SEM/TEN (HAMS) and GAS are presented in Figure 5.15 (real time) and Figure 5.16 (normalized time). These muscles represent the major uni-articular and bi-articular muscle groups. Jumping is generally considered a bang-bang activity, muscle is either on or off. The neuroexcitation patterns are generally but not completely bang-bang and follow the same pattern across different levels of G_z with the exception of VAS. The rapid changes in VAS at the 1.8 G_z were probably the result of the t_{decay} constant in the neuroexcitation-contraction dynamics. Jumping required less than 0.35 seconds; with a 200 msec decay constant (Chapter 3), a rapid change in neuroexcitation was required to produce a small change in muscle de-activation during the jump.

From Figures 5.15 and 5.16, it would appear that the muscles were experiencing large fluctuations during jumping at all G_z levels. However, the reported muscle forces did not exhibit the same trends. This occurred because muscle force is related to muscle excitation-contraction dynamics via muscle activation dynamics (Figures 5.17 and 5.18). In real time, the muscle activation patterns, including VAS, were very similar for each G_z environment. When the muscle activations were reviewed in normalized time (Figure 5.18), muscle activations were almost identical.

Comparison of the muscle neuroexcitations and muscle activations indicated that the sequencing of muscles did not change with G_z. The same
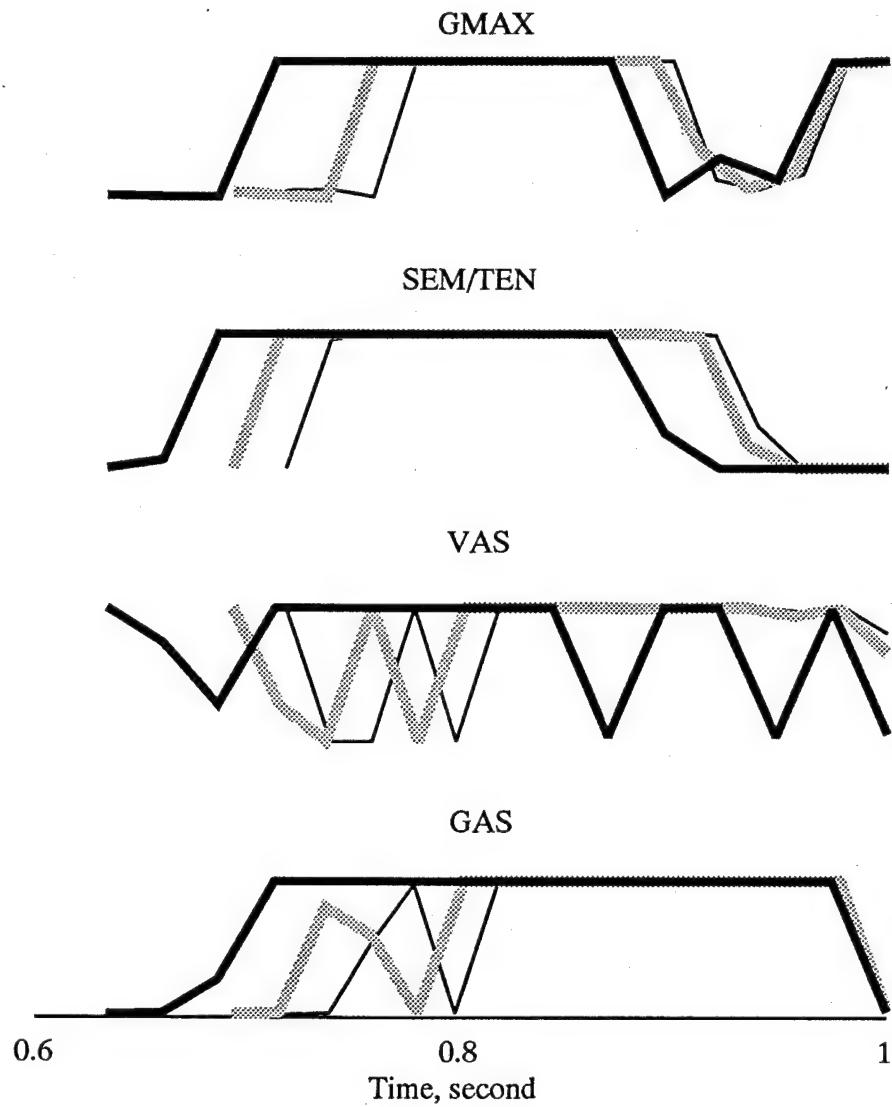
Figure 5.15 Muscle Neuroexcitations in Real Time

Heavy black line 1.8 G_z, gray line 1.0 G_z and thin black line 0.4 G_z.
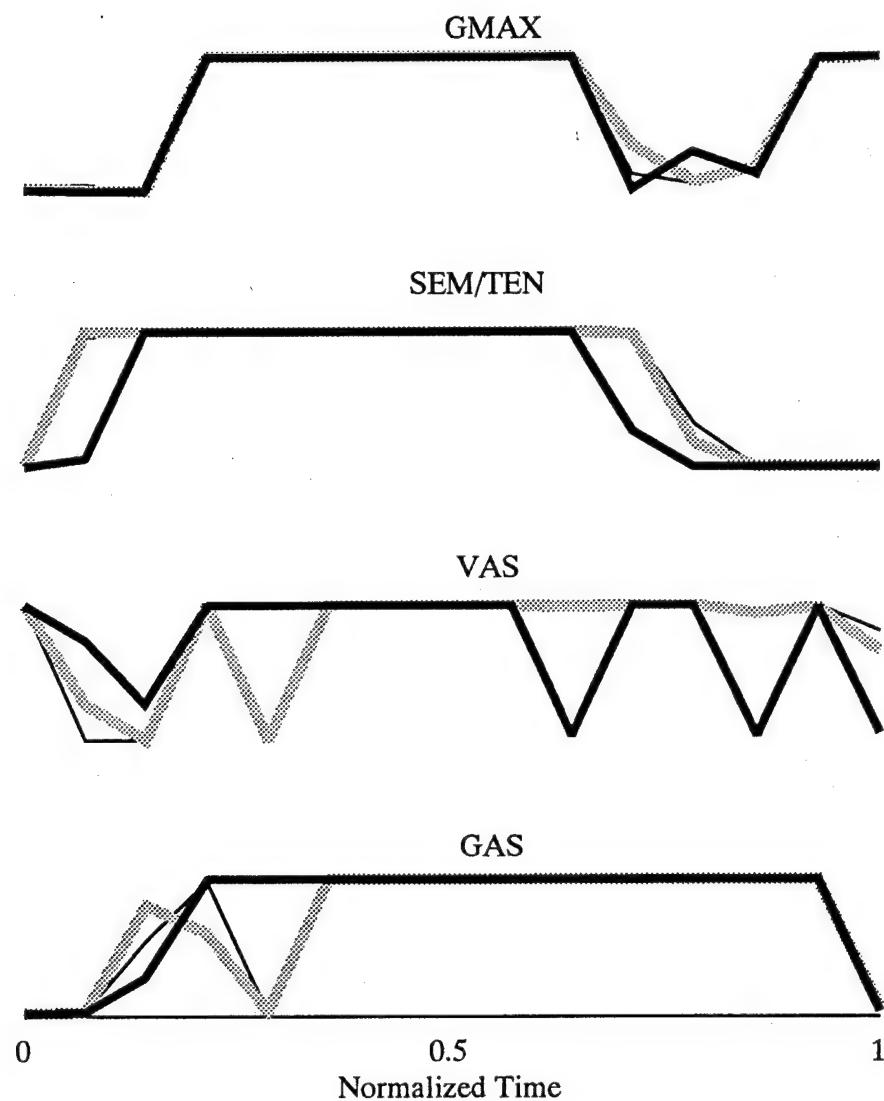
Figure 5.16 Muscle Neuroexcitations in Normalized Time

Heavy black line 1.8 G_z, gray line 1.0 G_z and thin black line 0.4 G_z.
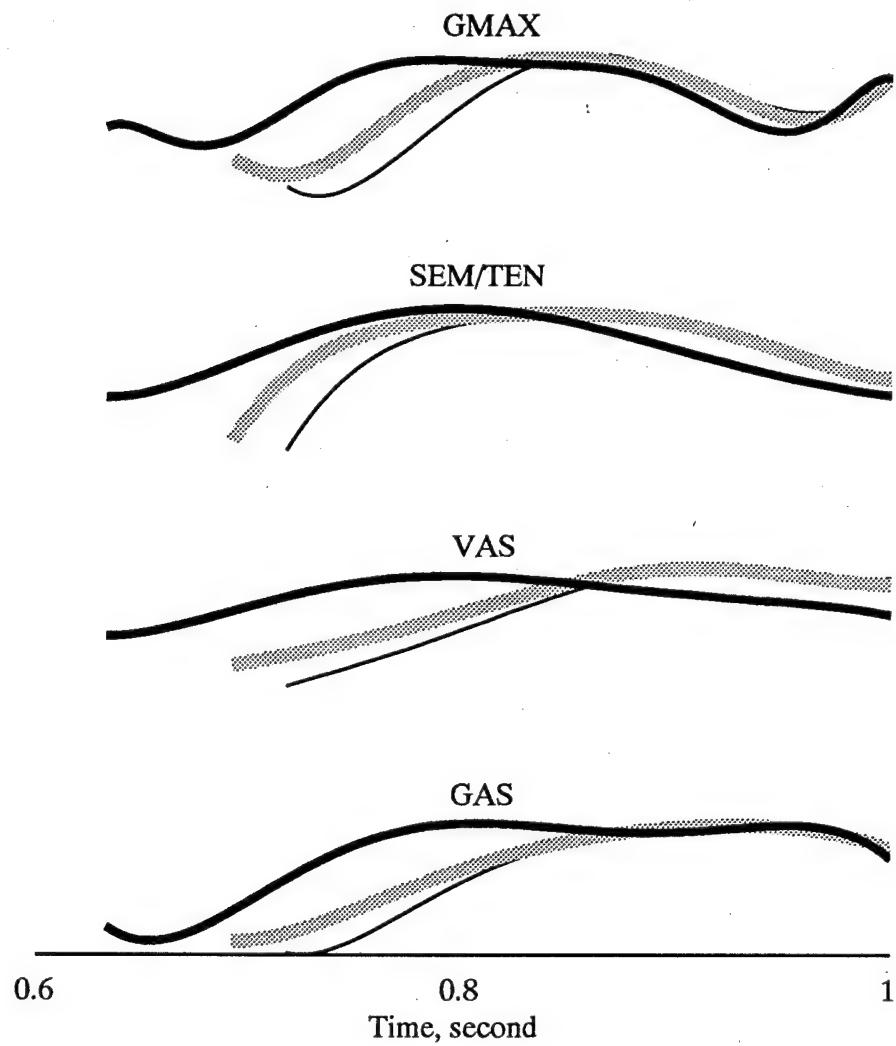
Figure 5.17 Muscle Activation in Real Time

Heavy black line 1.8 G_z, gray line 1.0 G_z and thin black line 0.4 G_z.
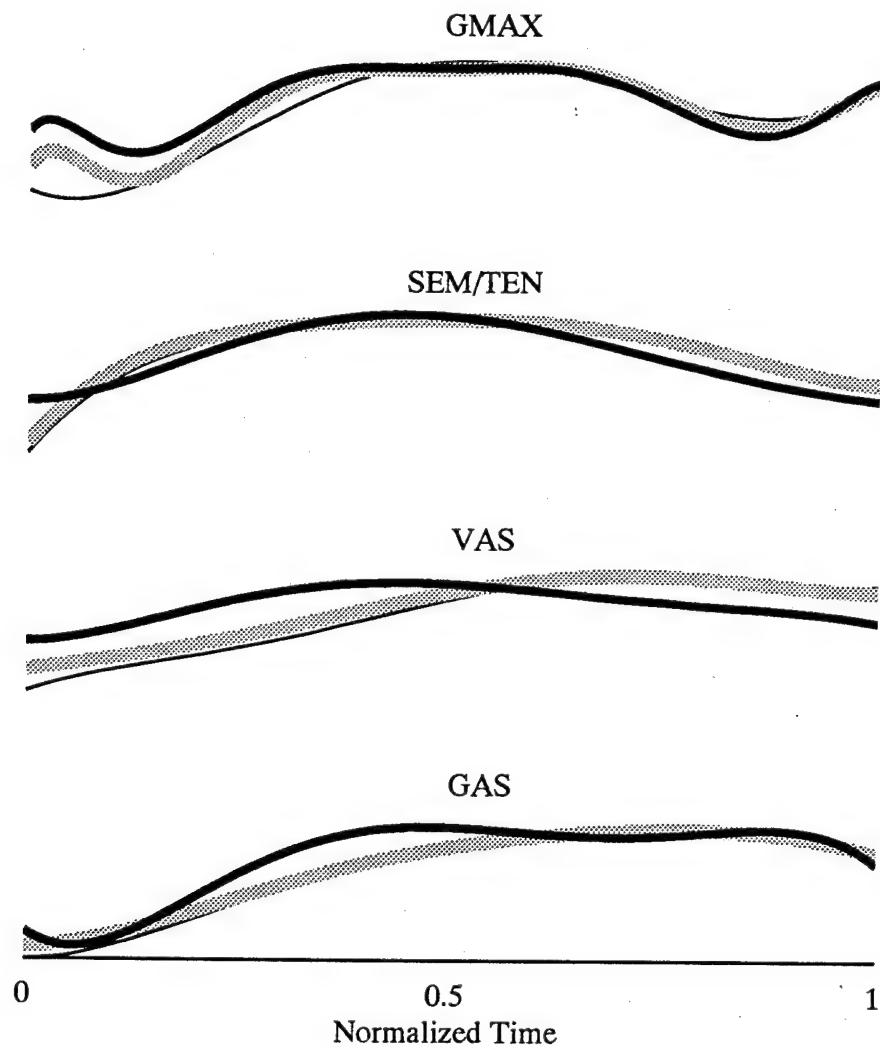
Figure 5.18 Muscle Activation in Normalized Time

Heavy black line 1.8 G_z, gray line 1.0 G_z and thin black line 0.4 G_z.

muscle activation patterns were used to achieve the motion regardless of the G_z environment during jumping. Only the time required to produce the motion changed. Also, the time of activation of a muscle, relative to all other muscles activations, remained constant. The general time histories of the muscle neuroexcitations and activations did not change with G_z. Thus, the sequencing of the muscles remained constant, i.e. if UHE was activated prior to VAS at 1.8 G_z then the same would occur at all other G_z levels.

Chapter 6: Conclusions

This study was designed to answer the research question, "how do changes in gravitational force affect jumping performance and intermuscular control?" To determine the effects of gravity on jumping performance and intermuscular control, a musculoskeletal model was used. Prior to analyzing the musculoskeletal model solutions for jumping in hypo- and hyper-gravitational environments, the musculoskeletal model was validated by comparing model solutions to experimental data collected in increased gravitational environments. The effect of gravity on jumping performance and intermuscular control are discussed in this chapter.

6.1 JUMPING PERFORMANCE

Jumping performance was divided into the following areas: jump height, energy utilized during jumping, muscle energy and power delivered to the center of mass and muscle forces generated during a jump. In this section, each of these areas will be discussed.

Intuitively, it was known that jump height would decrease in an increased gravitational environment. However, the rate of decline in jump height and changes in how the jump would be performed were not known. It was found that jump height was inversely related to gravitational force.

The total energy utilized to jump in different gravitational environments increased as gravity increased, however, the increase in energy expended was not

as great as the increase in gravity. The total energy distribution changed as gravity changed. The change in potential energy expended was the same as the change in gravity while the change in kinetic energy utilization decreased as gravity was increased. The potential energy changed directly with gravity because $^Z\overline{d}_{com}$ remained constant at take-off as gravity was altered. This finding was reasonable since it would be expected the body would be fully extended at take-off during a maximal effort jump and therefore, potential energy would be directly related to gravity. With less kinetic energy available as gravity increased, the take-off $^Z\overline{v}_{com}$ decreased and therefore, the jump height decreased. Increasing gravity also had a second detrimental effect on jump height. During flight, the only force slowing down the center of mass was gravity. Increasing gravity led to shorter flight times and more rapid slowing of the $^Z\overline{v}_{com}$. Therefore, even if take-off $^Z\overline{v}_{com}$ had remained constant as gravity increased, the jump height would have still decreased.

The energy utilized during jumping was provided by muscles. A review of the muscle activities indicated that the muscles work as six groups rather than 20 independent, non-synchronized force producing units. The peak muscle forces and muscle force time history patterns did not substantially change as gravity was altered. The only change in muscle activities related to gravity was that the muscles produced higher initial forces, to maintain static equilibrium, and were activated longer, as gravity was increased.

The muscle forces produced power and energy that was transferred to the skeletal system. The transferred muscle power followed the same trends observed in the muscle forces. The peak muscle power and the general shape of the time

history of muscle power delivered to the skeletal system did not substantially change as gravity was altered. Rather, the muscle powers were delivered to the skeletal system over a longer period of time. Since the same magnitude of muscle power was delivered over a longer period of time, the energy delivered to the skeletal system increased as gravity increased.

In general, each muscle group provided more energy for jumping to the skeletal system as gravity increased. However, the distribution of the energy between muscle groups remained relatively constant as gravity changed. The uni-articular muscles provided the translational energy needed to jump and in the process caused segment rotations. The energy provided by the bi-articular muscles was mostly rotational energy. This led to the hypothesis that the energy to translate the body segments was primarily provided by the uni-articular muscles, while the energy needed for optimal rotation of body segments was provided by the bi-articular muscles.

6.2 INTERMUSCULAR CONTROL

Intermuscular control was divided into the timing and sequencing of the neuroexcitation of the muscles and muscle activations. The timing and sequencing of the neuroexcitation of muscles indicated the muscles were activated for a longer period of time as gravity was increased. The sequencing of the muscle neuroexcitations remained constant. The same general neuroexcitation pattern for each muscle was achieved in different gravitational environments. The muscle neuroexcitation patterns were very different from the muscle force

patterns. The neuroexcitations occasionally went on-off or off-on while the muscle forces gradually increased and declined. This was the result of the muscle excitation-contraction dynamics. When observed in normalized time, it was very difficult to find any difference between a muscle's activation patterns for all gravitational levels. For jumping, the muscle neuroexcitation and activation patterns did not change with gravity. The sequencing of muscle actions remained constant as gravity changed.

6.3 FUTURE WORK

This study validated the hyper-gravitational solutions of a forward dynamics model of human jumping. However, jumping is a relatively simple, maximal effort motion with a very well-defined performance criteria. The subjects and the model started in the same position, were not allowed to countermove and finished fully extended. It should not be surprising that the experimental and predicted joint kinematics and ground reaction forces were very similar. From this study, it can be concluded that the estimates for the anthropometric properties used in the model were adequate. However, the jumping model did not adequately test the muscle controlling models due to the bang-bang nature of the activity. To determine if this type of forward dynamic modeling is useful for more practical types of problems, this modeling technique needs to be used to model a non-maximal effort activity such as rising from a chair. Therefore, the next logical step in modeling human movement would be to determine the adequacy of the muscle control models, neuroexcitations and

activation dynamics by modeling a non-ballistic, planar activity such as rising from a chair. The experimental data have already been collected and could be used to validate the model. Since the nominal anthropometric parameters have been established for the jumping model, results of the proposed study would determine the adequacy of the muscle control models, neuroexcitations and activation dynamics.

Appendix A: Human Subjects

This study required the use of the DES located at Wright-Patterson AFB. The DES is a unique piece of experimental equipment with a high relative risk for injury to human subjects. Therefore, the United States Air Force has very specific human use protocol and test procedures which must be met for all experiments. The subject consent form and test procedure were completed in March 1993 and submitted to the HURC in May 1993. With minor modification, the final human use application and test protocol were accepted in September 1993. Attached is a scanned image (size reduced) of the test plan and subject consent forms.

Protocol 93-08   1 Sep 93   Page 1

Summary

1. Title: Effects of Altered Gravitational Forces on Human
Movement

2.   Principle Investigator-   Roxanne Constable, DSN 240-3446
                              AL/ DOJE

3.   Date: TYPE: Specific   Renewal: New

4 .   Synopsis: The nature of this study involves measuring total
body movement in environments of 1.0 to1.8 Gz. The tasks
involve rising from a chair and squat jumping. The collected
data will be used to validate a musculoskeletal model which can
be used to predict human motion,

5. Previous Year's Experience :   None

6.   Attachments :

    Atch 1 - Consent Form
    Atch 2 - Curriculum Vitae

Protocol 93-08   7 Sep 93   Page2

TITLE : Effects of Altered Gravitational Forces on Human Movement

1. Project/Task/Work Unit: ILIR CT31

2. Principal Investigator: Roxanne Constable, AL/DOJE

3. Associate Investigators: Maj. David Carpenter, AFIT/CI

                                    Dr. Marcus Pandy, University of

                                    Texas, Austin

                                    Mr. John Frazier, AL/CFBS

4. Medical Consultant: Maj or Andrew Tong, SFS, AL/CFB S

                                    DSN 785-5742 , or

                                    George Potor, M.D., 785-5742

5. Facility: Dynamic Environment Simulator (DES), Bldg. 33

                Wright Patterson AFB, OH

6. Objectives: Demonstrate the potential of usinq optimal
control techniques in conjunction with musculoskeletal computer
modeling to predict human motion at different values of Gz,
Also, to determine if the use of nominal anthropometric values
for the parameters in the musculoskeletal model can produce
acceptable results when modeling human motion in an increased Gz
environment.

7. Background and Relevance : Forces in muscles and tendons and
those resulting from bone-on-bone contacts are extremely diffi-

cult to measure. Without knowledge of muscle forces, the
stresses experienced by the skeletal and muscle systems related
to human movement cannot be determined.   To determine these
forces, musculoskeletal modeling techniques need to be used.   The
ability to accurately compute musculoskeletal loading histories
is particularly important to the Air Force, where exposure to
different environments and gravitational levels can significantly
affect human performance and coordination. Modeling of musculo-
skeletal forces is complex since there are many ligaments and
muscles crossing a joint, resulting in a structurally indetermi-
nate system.   The only proven method available to resolve this
indeterminate system consists of a combination of optimal control
theory (dynamic optimization technique) and musculoskeletal
computer modeling.

In general, an optimal control solution consists of the predicted
time history of muscle activations which would achieve the
desired motion while optimizing a given performance criteria,
Once anoptimal control solution is found, the researchers have
an array of predicted values for the time histories of muscle
activation patterns, joint motion, and ground reaction forces.
The optimal control solution is validated by comparing predicted
values of muscle activation patterns, ground reaction forces and
joint motions of experimental data. Once the musculoskeletal
model solution is validated for a given motion pattern, the
optimal control solution can be further analyzed to determine

the required muscle forces, energy requirements, and intersegmen-
tal forces all of which are not obtainable from experimental
data. By incorporating these previously unknown human factors
into Air Force system design, the performance of the individual
and the system can be enhanced.

This technique for solving human motion problems is relatively
new. Dr. Marcus Pandy and colleagues have successfully applied
optimal control techniques in solving two types of human motions
at 1.0 Gz; rising from a chair and jumping. In both cases, the
human movement patterns were relatively simple motions, requiring
mostly lower extremities muscles and planar motion. To determine
if optimal control theory combined with musculoskeletal modeling
can be practically applied to Air Force needs, this method of
modeling must be demonstrated at increased Gz levels and for
different activities. Testing at increased Gz will determine if
this method of modeling human motion is applicable to an increase
Gz environment and further validate the nominal parameters used
in the model.

8.   Impact Statement: The Air Force has a need for a precise and
reliable computer model which accurately predicts musculoskeletal
loading histories and specific muscle coordination patterns in
any gravitational field. This model could be used in numerous
design settings such as aircraft seat and cockpit design and
occupational ergonomics. In the future, the muscle activation
dynamics of the model could be enhanced to study neurological
related issues such as high-G effect and vestibular feedback.

The data will have an additional application in the study of aging.

9.   Experimental Plan:

   a.   Equipment: All acceleration experimentation will be performed using the DES.   The required equipment includes a forceplate, cameras, VCRs, chair, EMG electrodes and computer system.   A forceplate will be installed in a floor which in turn will be secured in the DES cab.   Two TV cameras will be mounted in the cab to record the subject's motions.   A chair, with a strain gauge mounted on the seat pan to measure vertical seat force, will be attached to the floor directly behind the force-plate.   All signals from the forceplate, strain gauge, EMGs and cameras will be passed through slip rings to the control room where analog data will be collected by computer and video data by VCRs.

   b.   Subjects: Subjects will be members of the AL/CFBS Sus-tained Acceleration Panel and the associate investigator.   As much as possible, subjects will be selected based on weight (160-180 pounds), height (175 cm - 185 cm), and age (25-39 years old).   Informed consent (attachment 1) will be obtained from a subject prior to participation.   Subjects may terminate their participation at any point during the experiment, without preju-dice.   The study will require at least eight subjects.

Protocol 93-O8   7 Sep 93   Page 4

   c.   Duration of study :   Data collection will require up to six
weeks.

   d.   Experimental Procedures: Reflective markers and EMG
electrodes will be placed on the subjects.   They will wear shorts,
gym shoes, and a sleeveless shirt.   They will also be fitted with
a safety harness and helmet.   At 1.0 Gz, the subject will be
asked to rise from a seated position and then instructed to
perform a squat jump three times.   This motion procedure will be
repeated at each different value of Gz(i.e, 1.0, 1.2, 1.4, 1.6,
and 1.8).   After the third squat jump, the subject will be
instructed to sit while the resultant vertical acceleration is
increased.   After the desired acceleration level is obtained, the
subject will repeat the standing and jumping protocol tests.
Once the Motion protocol is finished at 1.8 Gz,   the resultant
vertical acceleration will be reduced by 0.2 Gz increments, and
the motion procedure repeated.   The subject will perform the
motion procedure a maximum of nine times; once at 1.8 Gz and
twice at 1.0, 1.2, 1.4, and 1.6 Gz for each test run.   After the
motion procedure is completed at 1.0 Gz for the second time, the
tests for that day are completed.   A total of four test days,
each with the above conditions will be conducted with each sub-
ject.

The different Gz levels will not be randomized.   At the highest
level of Gz, a great deal of energy will be needed to perform the
motions and fatigue could result.   If the highest Gz level were
tested first, it is possible the fatigue could influence the test

results at lower values of Gz. If, during the conduct of the testing, a subject is not able to stand or jump at a Gz level, testinq at higher Gz levels that day with the subject will not be attempted.

10 . Data Analysis: It will be assumed the subject pool is a homogeneous group. The results of the group will be compared to the model predictions controlling for Gz and activiliy.   Jump height and time required to perform the motion will be evaluated using confidence intervals calculated from group performance. Ground reaction forces and joint kinematics will be compared using regression analysis. To determine if fatigue occurred, the results from the increasing Gz environment will be compared to the results from the decreasing Gz environment. To determine if a learning pattern occurred for these movements, the results from the four individual test days will be compared.

11.   Medical Risks: An increase in Gz acceleration causes a shift of blood from the head to the lower parts of the body.   Due to this blood shift, loss of vision and even unconsciousness may result. These effects have been well studied and have shown to be both without permanent effects and spontaneously reversible when the acceleration is reduced. The exposures in this study are relatively low, less than 2.0 Gz, and cardiac compensation should counteract the pooling effects and no problems with loss of vision or unconsciousness are anticipated. This study requires the subject to perform whole body movement in Gz envi-

Protocol 93-08   7 Sep 93   Page 5

ronments between 1.0 and 1.8 Gz. There is little or no precedent

for tests of this nature. There is a significant risk of disori-

entation, nausea, loss of balance and falling.   A restraining

system and cab padding are being designed and tested which will

prevent injury to the subject from falling or contacting objects

in the DES cab while also allowing sufficient mobility to rise

from a chair and jump.   This test set-up will be demonstrated to

the Technical Safety Committee and approved by Mr. Naylor

(AL/CFPP) before testing will begin.

12.   References:

       a.   Generic Sustained Acceleration Protocol 83-23.

13.   Attachments:

       Atch 1 - Consent Form

       Atch 2 - Curriculum Vitae

Protocol 93-08   7 Sep 93   Page 6

INFORMATION PROTECTED BY THE PRIVACY ACT OF 1974

CONSENT FORM

TITLE :   Effects of Altered Gravitational Forces on Human Movement

1.   a. Nature: The nature of this study involves measuring

total body movement in environments of 1.0 to 1.8 Gz. The tasks

involve rising from a chair and squat jumping. The collected

data will be used to validate a musculoskeletal model which can

be used to predict human motion.

   b. Purpose: The purpose of this study is to investigate the

accuracy of a musculoskeletal model which could be used to

predict numerous types of human motions at different values of

Gz. This modeling technique is unique in that researchers using

this model can predict muscle forces, intersegmental forces

muscle coordination and neural excitation patterns associated

with human movement. In turn, this information can be used to

enhance design of Air Force systems.

   c. Your participation in this study will take about four

hours on four different days.

2.   This study will require up to 12 subjects from the Sustained

Acceleration Stress Panel. As a member of the Sustained

Acceleration Stress Panel you are invited to participate in a

study of changes in human movement resulting from increased

gravitational stress. The testing will require you to rise from
a chair and squat jump while inside the cab of the Dynamic Envi-
ronment Simulator (DES), a man-rated centrifuge. We will test
the hypothesis that human motion patterns at increased Gz can be
predicted by using optimal control theory in conjunction with
musculoskeletal modeling. This method of modeling human motion
is the only known method which allows researchers to predict
muscle forces, intersegmental forces, muscle coordination and
joint kinematics. This type of information is required to
understand the muscular and skeletal stresses involved with human
movement at any Gz.

You will be asked to participate in a whole body movement
study that requires rising from a chair and squat jumping in
environments of 1.0 to 1.8 Gz. You will be required to wear
jogging shorts, sleeveless shirt and comfortable athlete tYpe
shoes. You will have five surface electromyography (EMG) elec-
trodes attached to one leg. These electrodes will be used to
measure EMG patterns of surface muscles. A minimal amount of
skin preparation will be required for placement of the elec-
trodes. The skin will be shaved at the attachment sites and
cleaned with alcohol. The electrodes will be attached to the
skin with double face tape. You will have five reflective mark-
ers attached to your body, foot, ankle, knee, hip and shoulder.

Subject Signature and SSN_____ Date_____.

Protocol 93-08   7 Sep 93   Page 7

These markers are used in conjunction with a video system to
record your body position at all times. The reflective markers
will be attached to your with double face tape. You will
be required to wear a helmet for head protection and for communi-
cation with the principal investigator (PI). You will also be
required to wear a harness system during the entire experiment
The harness system is required to prevent falling or contacting
walls during the testing.

3 .   Experimental Risk

    a.   Acceleration:

    Physiological changes include primarily a redistribution of
the blood supply to various organs. Acceleration encountered in
the vertical direction causes a shift of blood from the head to
the lower parts of the body. Because of this blood shift, loss
of vision and even loss of consciousness may result. These
effects have been well studied and have been shown to be both
without permanent effects and spontaneously reversible when the
vertical acceleration is reduced. As noted, you will be experi-
encing only 1.8 Gz in this experiment, so loss of vision or
consciousness is considered unlikely . Effects upon the heart
include irregularities in beat rhythm (cardiac arrhythmias), most
of which are self-limiting and resolve with cessation of Gz
stress. Vary rarely a potentially serious arrhythmia develops.
If a serious arrhythmia occurs, the test will be immediately
terminated.

Small breaks in the skin capillaries (petechial hemorrhage) and bruises occasionally occur on arms, trunk or legs. These are considered to be harmless. Fractures or dislocation of the skeletal bone is possible under g-stresses but probably not at 1.8 Gz.

b. Whole Body Movement at Increased Gz

You may experience motion sickness, nausea, dizziness vertigo, vomiting, and fatigue. This study requires you to move and jump while the DES cab is moving. You could lose your orientation or balance and fall. A safety harness has been designed to allow the range of motion required for the study yet provide fall protection for the subject. The safety harness has been tested to ensure your displacement inside the cab is minimal and toensure you will not contact the cab hard structures or fall completely to the floor. In the remote event of a catastrophic failure of the harness system, you could impact into a wall or fall to the floor sustaining impact type injuries.

c. Loss of Cab Position

A remote but possible failure mode is a DES cab drive system malfunction with loss of cab position control. This could

Subject Signature and SSN_____Date_____.

Protocol 93-08   7 Sep 93   Page 8

result in the subject being exposed to lateral (Gy) or negative
(-Gz) force vectors. There are several DES system design layers
to prevent this failure mode, the force field is low (1.8 G), and
the safety harness is designed for multi-axis restraint.

4 .   Benefits to Subject: Participation in this study will pro-
vide no additional tangible benefit to you other than those
already covered in the DoD Pay and Entitlements Manual.

5 .   Alternative Procedures: No other pocedures exists which
could be safely used on human test subjects that would present
the same data this study provides.

6.   I _____, am participating
because I want to. The decision to participate in this research
study is completely voluntary. No one has coerced or intimidated
me into participating in this program.

W. Roxanne Constable, Principal Investigator (DSN 24 0-3446),
John W. Frazier, Associate Investigator (DSN 785-5742), or de-
signee has adequately answered any and all questions I have asked
about this study, about my participation, and about the proce-
dures involved. I have read these procedures as set forth above.
I understand that the PI or Maj. David R. Carpenter, co-investi-
gator 512-471-1273 ext 53, will be available to answer questions
concerning procedures throughout this study. I understand that
if significant new findings develop during the course of this
research which relate to my decision to continue participation, I

will be informed. I further understand that I may withdraw this consent at any time and discontinue further participation in this study without prejudice. I also understand that the medical consultant may terminate my participation in this study if he/she feels this to be in my best interest. I may be required to undergo certain further examinations, if in the opinion of the medical consultant, such examinations are necessary for my health or well being.

7. I have considered and accept the unlikely but theoretical possibility of the following:

a. If physical examinations and/or monitoring of physiological parameters related to this experiment are conducted, it is possible for an unknown physical defect to come to light, which may result in disqualification from flight or special duty.

b. If physical injury occurs it may possibly result in physical disqualification from flight or other special duty.

8. I understand that my entitlement to medical care or compensation in the event of injury are governed by federal laws and regulations, and that if I desire further information I may contact the Principal Investigator.

Subject Signature and SSN_____Date_____.

Protocol 93-08   7 Sep 93   Page 9

9.   I understand that for my participation in this project I
shall be entitled to payment as specified in the DoD Pay and
Entitlements Manual or as specified in current contracts.

10.   I understand that my participation in this study may be
photographed, filmed or video taped. I consent to the use of
these media for training purposes and understand that any release
of records of my participation in this study may only be dis-
closed according to federal law, including the Federal Privacy
Act, 55 U.S.C. 552a, and its implementing regulation.

11.   I have been informed that the PI and co-investigator will
use the results from this study as part of their doctoral stud-
ies.

I FULLY UNDERSTAND THAT I AM MAKING A DECISION WHETHER OR NOT TO
PARTICIPATE. MY SIGNATURE INDICATES THAT I HAVE DECIDED TO
PARTICIPATE HAVING READ THE INFORMATION PROVIDED ABOVE.

Volunteer Signature and SSN_____Date_____.

Witness Signature_____Date_____.

Principal Investigator_____Date_____.

INFORMATION PROTECTED BY THE PRIVACY ACT OF 1974

AUTHORITY: 10 U.S.C. 8012, Secretary of the Air Force; powers

and duties; delegation by; implemented by DOE 12-1, Office
Locator.

PURPOSE: To request consent for participation in approved medi -
cal research studies.   Disclosure is voluntary.

ROUTINE USE: Information may be disclosed for any of the blanket
routine uses published by the Air Force and reprinted in
AFP 12-36 and in Federal Register 52 FR 16431.

Appendix B: Force Plate

The collection of biomechanical data in the DES had never been attempted before.   Therefore, much of the data collection instrumentation had to be fabricated. This included the force plate. This Appendix includes operational characteristics of the force plate. The force plate had a unloaded, natural frequency of 2000 Hz while with a 2000 N load, the force plate frequency dropped to 500 Hz. The response of the force plate was much greater than the 8 Hz frequency related to jumping.

The calibration of the force transducers is presented in Figure B.1. The transducers had linear coefficients greater than 0.99 and a very similar response curve between transducers.

FORCE PLATE RESPONSE

$$\omega_0 = \text{frequency of force plate} = \sqrt{k/mass}$$

$$k = \text{spring constant} = \text{force}/\Delta H$$

$$\Delta H = \left(\text{force} \times L^3\right) / \left(48 \times E \times I\right)$$

$$E = \text{modulus of elasticity} = 1 \times 10^6$$

$$I = \text{moment of inertia} = \frac{mass}{12}\left(b^2 + h^2\right)$$

$b = \text{length of base}$

$h = \text{height}$

The mass is equal to;

$$mass_{force\ plate} = \rho \times \text{volume}$$

$$= \frac{2.2\text{gram}}{\text{cm}^3}\left(2100\text{cm}^3\right)\left(\frac{1\text{kg}}{1000\text{gram}}\right)$$

$$= 4.6\text{kg}$$

$$I = 557 \text{ kg} \cdot \text{cm}^2$$

$$\Delta H_{\text{force plate}} = 2.73 \times 10^{-4}\text{cm}$$

$$\omega_{\text{force plate}} = 1900 \text{ hertz}$$

With a 2000 newton vertical load,

$$\Delta H = 0.012 \text{ cm}$$

$$\omega_{\text{force plate + load}} = 456 \text{ hertz}$$

Calibration of Force Transducers
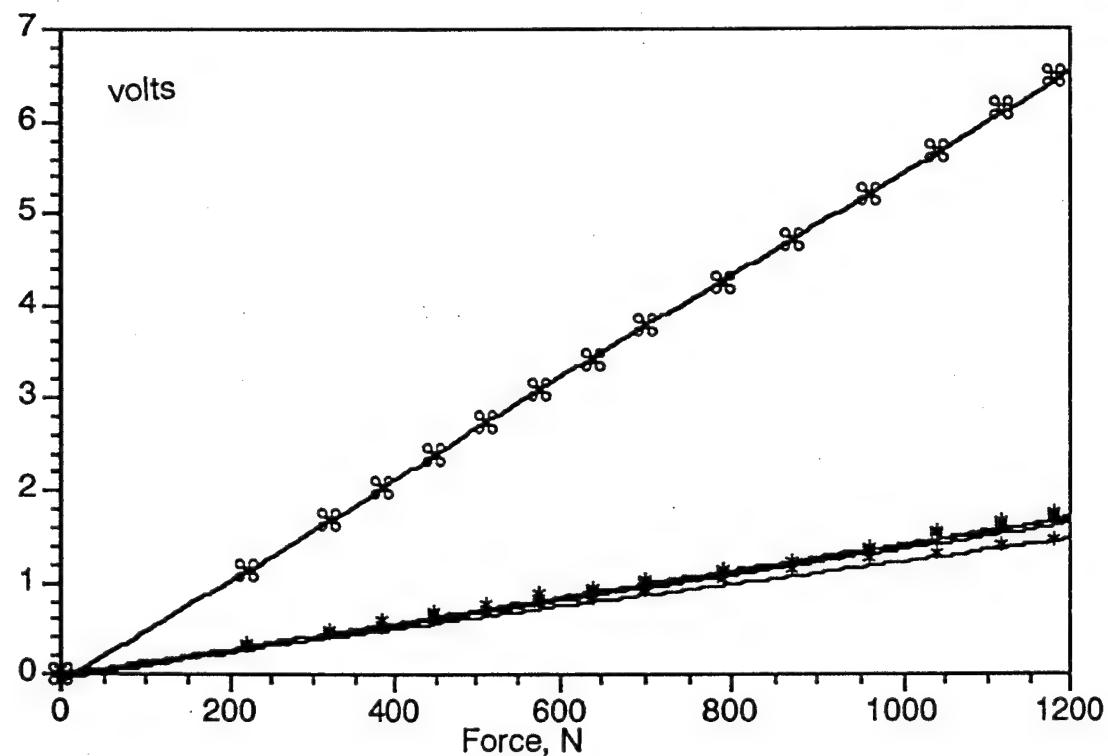
Linear regression analysis
volts = 0.0014 * force - 0.03666
or
force = 711.08 * volts + 26.07

Appendix C: Placement of EMG Electrodes

As part of this experiment, SEMG signals from gastrocnemius, semitendinosus, vastus lateralis, and gluteus maximus were collected. Each subject had three data collection rides on the DES. To minimize differences between rides in EMG signals, the EMG electrodes were placed in the same position each time.

To determine the area for placement of the EMG electrodes, Figures C-1 through C-4 were used (Delagi et al., 1975). These figures gave the general position of the four muscles of interest.
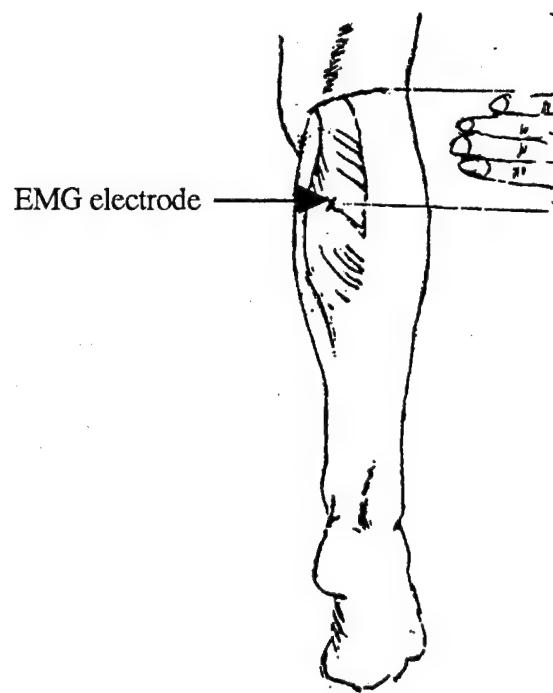
Fig. C-1 SEMG Placement for Gastrocnemius

GAS originates at the medial femoral condyle and inserts into the calcaneus
through the Achilles' tendon.
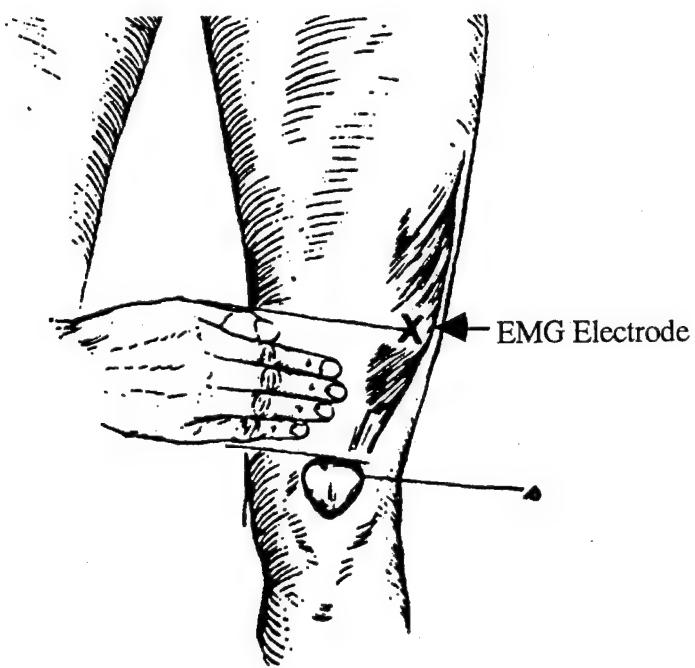
Fig. C-2 SEMG Placement for Vastus Lateralis

This muscle originates from the intertrochanteric line and inserts through the quadriceps tendon onto the tibial tubercle.
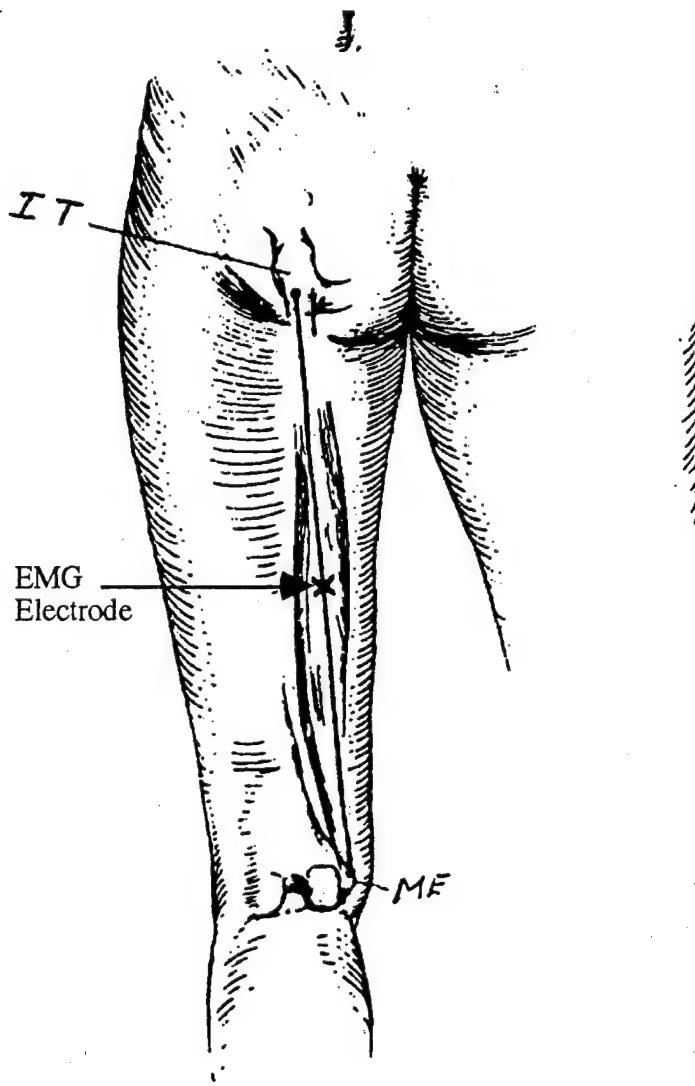
Fig C-3 SEMG Placement for Semitendinosus

This muscle originates at the ischial tuberosity (IT) and inserts on the medial condyle (ME) of the tibia. This muscle was used to represent the Hamstring muscles.
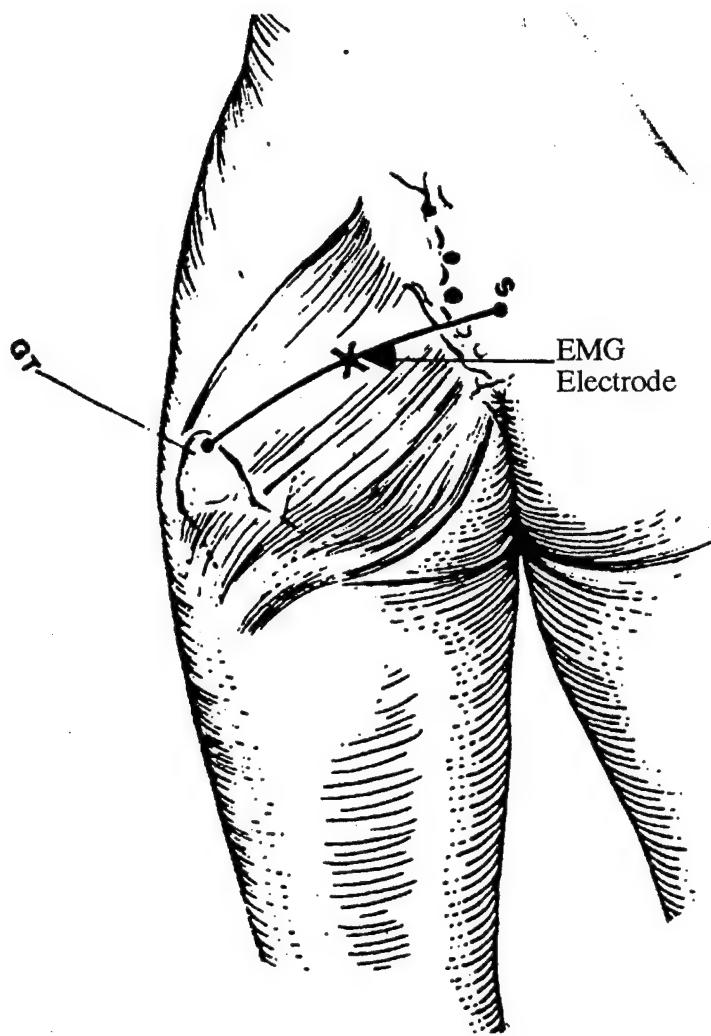
Fig. C-4 SEMG Placement for Gluteus Maximus

This muscle originates from the gluteal line and inserts into the iliotibial tract.

References

Anderson F. C. (1992) Storage and Utilization of Elastic Strain Energy During Human Jumping: An Analysis Based on the Predictions of an Experimentally Verified Optimal Control Model. Masters thesis, Dept., of Kinesiology and Health Education, The University of Texas at Austin, Austin, TX.

Anderson F. C., and Pandy M. G. (1993) Storage and Utilization of Elastic Strain Energy During Jumping. *J of Biomechanics* accepted March 1993 for publication

Anderson F. C., Ziegler J. M., Pandy M. G., and Whalen R. T. (1993) Numerical Computation of Optimal Controls for Large-Scale Musculoskeletal Systems. *ASME Adv Bioengng* 26:519-522.

Apseloff G., Girten B., Gerber N., Shepard D. R., and Matkovic V. (1992) Lack of Effect of Gallium Nitrate on Bone Density in a Rat Model of Simulated Microgravity. *Aviat Space and Environ. Med* 62:27-31

Arnaud S. B., Sherrard D. J., Maloney N., Whalen R. T., and Fung P. (1992) Effects of 1-Week Head-Down Tilt Bed Rest on Bone Formation and the Calcium Endocrine System. *Aviat Space and Environ. Med.* 62:14-20

Audu M. and Davy D. (1985) The Influence of Muscle Model Complexity in Musculoskeletal Motion Modeling. *J. Biomech Engng Med* 107:147-157

Avela, J., Santos, P.M., Kyrolainen, H. and Komi, P. V. (1994) Effects of Different Simulated Gravity Conditions on Neuromuscular Control in Drop Exercises. *Aviat Space and Environ. Med* 65:301-308

Bagian J. P. and Schafer L. E. (1992) Comparison of Current Shuttle and Pre-Challenger Flight Suit Reach Capabilities During Launch Acceleration. *Aviat Space and Environ. Med* 63:624-628

Ball T. E., Massey,B. H., Misner J. E. McKeown, B. C., and Lohman T. G. (1992) The Relative Contribution of Strength and Physique to Running and Jumping Performance of Boys 7 - 11. *J of Sports Medicine and Physical Fitness* 32(4):364-371

Beckh H., J. (1954) Experiments with Animals and Human Subjects under Sub- and Zero-Gravity Conditions During the Dive and Parabolic Flight. *Aviation Medicine* 235:241

Berry P., Berry I., and Manelfe C. (1993) Magnetic Resonance Imaging Evaluation of Lower Limb Muscles During Bed Rest--A Microgravity Simulation Model. *Aviat Space and Environ. Med.* 63:212-218

Bobbert M. F., Huijing P. A. and van Ingen Schenau G. J. (1986) An Estimation of Power Output and Work Done by the Human Triceps Surea Muscle-tendon Complex in Jumping. *J of Biomechanics* 19(11):899-906

Bobbert M. F., Huijing P. A., and van Ingen Schenau G. J. (1988) Coordination in Vertical Jumping. *J of Biomechanics* 19,887-898

Bobbert M. F. and van Ingen Schenau G. J. (1988) Coordination in Vertical Jumping. *J of Biomechanics* 21(3):249-262

Bobbert M. F. and van Ingen Schenau G. J. (1990) Mechanical Output about the Ankle Joint in Isokinetic Plantar Flexion and Jumping. *Med Sci Sports Exerc* 22(5):660-668

Bock O. (1990) Load Compensation in Human Goal-Directed Arm Movements *Behavioral Brain Research* 41:167-177

Bonde-Petterson F. (1994) Health Care During Prolonged Weightlessness in Humans. *Acta Physiol Scand* Suppl 616 150:99-102

Bovens A. M. P., van Baak M. A., Vrencken J. G. P. M., Wijnen J. A. G., and Verstappen F. T. J. (1990) Variability and Reliability of Joint Measurements. *Amer J of Sports Medicine* 18(1):58-63

Brand R. A., Pederson D. R. and Friederich J. A. (1986) The Sensitivity of Muscle Force Predictions to Changes in Physiologic Cross-sectional Area. *J of Biomechanics* 19(8):589-596

Brenton D. P., Edwards R. H. T., Grindrod S. R. and Tofts P. S. (1981) Computerized X-ray Tomography to Determine Human Muscle Size and Composition in Health and Disease. *Physiological Society* 3P

Buckle J. A., Termote L., Palmers Y., Crolla D. (1979) Computed Tomography of the Human Skeletal Muscular System. *Neuroradiology* 17:127-136

Cabri J. M. H. (1991) Isokinetic Strength Aspects of Human Joints and Muscles. *Critical Reviews in Biomedical Engineering* 19(2,3):231-259

Callister R., Callister R. J., Fleck S. J. and Dudley G. A. (1990) Physiological and Performance Responses to Overtraining in Elite Judo Athletes. *Med and Science in Sports* 22(6):816-824

Cavagna G. A., Zamboni A., Faraggiana T., and Margaria R. (1972) Jumping on the Moon: Power Output at Different Gravity Values. *Aerospace Medicine* 43(4):408-414

Cholewicki J. and McGill S. M. (1994) EMG Assisted Optimization: A Hybrid Approach for Estimating Muscle Forces in an Indeterminate Biomechanical Model. *J of Biomechanics* 27(10):1287-1289

Clauser C. (1963) Moments of Inertia and Centers of Gravity of the Living Human Body. AMRL Technical Documentary Report, 63-36. Wright-Pattterson AFB, Ohio

Clement G., Gurfinkel V. S., Lestienne F., Lipshits M. I. and Popov K.E. (1985) Changes of Posture During Transient Perturbations in Microgravity. *Aviat Space, and Environ Med* 56:666-671

Cohen M., M. (1970) Sensory-motor Adaptation and After-effects of Exposure to Increased Gravitational Forces. *Aerospace Medicine* 318-322

Colliander E. B., and Tesch P. A. (1992) Effects of Detraining Following Short Term Resistance Training on Eccentric and Concentric Muscle Strength. *Acta Physiol Scand* 144:23-29

Daigle K. (1994) The Effects of Muscle Strength on the Coordination of Rising from a Chair in Minimum Time: Predictions of an Optimal Control Model. Masters thesis, Dept. of Mechanical Engineering, The University of Texas at Austin, Austin, TX

Davies C. T. M. (1971) Human Power Output in Exercise of Short Duration in Relation to Body Size and Composition. *Ergonomics* 14(2):245-256

Davies C. T. M. and Rennie R. (1968) Human Power Output. *Nature* 217:770-771

Davis B. L. and Cavanagh P. R. (1993) Simulating Reduced Gravity: a Review of the Biomechanical Issues Pertaining to Human Locomotion. *Aviat Space and Environ Med* 64:557-567

Davy D. and Audu M. (1987) A Dynamic Optimization Technique for Predicting Muscle Forces in the Swing Phase of Gait. *J of Biomechanics* 20:187-201.

Delagi E. F., Perotto A., Iazzetti J. and Morrison D (1975) Anatomic Guide for the Electromyographer - the Limbs Thomas Books, Springfield Illinois

Delp S. (1990) Surgery Simulation: A Computer Graphics System to Analyze and Design Musculoskeletal Reconstruction of Lower Limb. Ph.D. Dissertation. Stanford University, Palo Alto, CA.

Edwards R. H. T., Young A., Hosking G. P., and Jones D. A. (1977) Human Skeletal Muscle Function: Description of Test and Normal Values *Clinical Sciences and Molecular Med* 52:283-290

Friederich J. and Brand R. (1990) Muscle Fiber Architecture in the Human Lower Limb. *J of Biomechanics* 23:91-95

Fujii N., and Moriwaki, T. (1993) Effect of Additional Weight on Muscular Power and Performance in Vertical Motion. International Society of Biomechanic, Sidney Australia

Fukashiro S. and Komi P. V. (1987) Joint Moment and Mechanical Power Flow of the Lower Limb During Vertical Jump. *Int J Sports Med* 8:15-21 Supplement

Garner B. A. (1992) A Dynamic Musculoskeletal Computer Model for Rising from a Squatting Position: A Study of Performance Criteria for Optimal Control of Non-Ballistic Human Movements. Masters thesis, Dept. of Mechanical Engineering, The University of Texas at Austin, Austin, TX.

Gerathewohl S., J., Strughold H., and Stallings H. D. (1957) Sensomotor Performance During Weightlessness, Eye Hand Coordination. *Aviation Medicine* 7:12

Gill,P.E., Murray W., and Wright M. H. (1981) Optimality Conditions In Practical Optimization. Chapter 3, Academic Press, New York.

Grassi B., Cerretelli P., Narici M. V. and Marconi C. (1991) Peak Anaerobic Power in Master Athletes. *Eur J Appl Physiol* 62:394-399

Gregorie L., Veeger H. E., Huijing P. A., van Ingen Schenau G. J. (1984) Role of Mono- and Biarticular Muscles in Explosive Movements. *Int J Sports Med* 5: 301-305

Haggmark T., Jansson E., and Svane B. (1978) Cross Sectional Area of the Thigh Muscle in Man Measured by Computed Tomography. *Scand J Clin Lab Invest* 38:355-360

Häkkinen K (1991) Force Production Characteristic of Leg Extensor, Trunk Flexor and Extensor Muscles in Male and Female Basketball Players. *J of Sports Med and Physical Fitness* 31(3):325-331

Happee R. (1994) Inverse Dynamic Optimization Including Muscular Dynamics. A New Simulation Method Applied to Goal Directed Movements. *J of Biomechanics* 27(7):953-960

Hargens A. R. (1994) Recent Bed Rest Results and Countermeasure Development at NASA. *Acta Physiol Scand, Suppl 616* 150:103-114

Hatze H. (1976) The Complete Optimization of a Human Motion. *Math Biosci* 28:99-135.

He J., Kram, R., and McMahon, T. A. (1991) Mechanics of Running Under Simulated Low Gravity. *American Physiological Society* 71(3):863-870

Heekin A. (1991) Optimal Control Solutions for Standing Up from a Seated and Static-Squat Position. Masters thesis, Dept. of Kinesiology and Health Education, The University of Texas, Austin, TX.

Herzog W., Hasler E., and Abrahamse S. K. (1991) Comparison of Knee Extensor Strength Curves Obtained Theoretically and Experimentally. *Med and Sci in Sports and Exercise* 23(1):108-114

Horstmann G. A. and Dietz V. (1990) A Basic Posture Control Mechanism: The Stabilization of the Centre of Gravity. *Electroencephalography and Clinical Neurophysiology* 76:165-176

Hortobagyi T., Katch V. L., LaChance P. F. and Behnke (1990) Relationships of Body Size, Segmental Dimensions, and Ponderal Equivalents to Muscular Strength in High Strength and Low Strength Subjects. *Int J. Sports Med* 11: 349-356

Hull D. G. (1991) Class Notes in Optimal Control Theory ASE 381 D.#, The University of Texas at Austin, Austin Texas

Igarashi M. (1988) New Facts in Space Medicine. *Acta Otolaryngol (Stockh)* Suppl. 458,103-107.

Ilyina-Kakueva E., Portugalov V. V., and Krivenkova N. P. (1976) Space Flight Effects on the Skeletal Muscles of Rats. *Aviat Space and Environ Med* 47:700-703

Jensen R. H., Smidt G. L. and Johnston R. C. (1971) A Technique for Obtaining Measurements of Force Generated by Hip Muscles. *Archives of Physical Medicine and Rehabilitation* 207-215

Jacobs R., and van Ingen Schenau J. (1992) Intermuscular Coordination in a Sprint Push-off. *J of Biomechanics* 25(9):953-965

Kannus P., Järvinen M., and Lehto M. (1991) Maximal Peak Torque as a Predictor of Angle-specific Torques of Hamstring and Quadriceps Muscles in Man. *European J. of Applied Physiology* 63:112-118

Klitgaard H., Mantoni M., Schiaffino S (1990) Function, Morphology and Protein Expression of Aging Skeletal Muscle: a Cross-sectional Study of Elderly Men with Different Training Backgrounds. *Acta Physiol Scand* 140:41-54

Knapik J. J., Wright J. E., Mawdsley R. H. and Braun J (1983) Isometric, Isotonic and Isokinetic Torque Variations in Muscle Groups Through a Range of Motion. *Physical Therapy* 63(6):938-947

Komi P. V. and Bosco C (1978) Utilization of Stored Elastic Energy in Leg Extensor Muscles by Men and Women. *Med and Science in Sports* 10(4):261-265

Koopman H. F. (1989) The Three-Dimensional Analysis and Prediction of Human Walking. Ph.D. Dissertation, Mechanical Engineering Department, University of Twente, The Netherlands

Krippendorf B. B. and Riley D. A. (1993) Distinguishing Unloading- Versus Reloading-Induced Changes in Rat Soleus Muscle. *Muscle and Nerve* 16:99-108

Kulig K., Andrews J. J. and Hay J. G. (1984) Human Strength Curves. *Exercise Sports Science Review* 12:417-466

Laubach L. L. (1969) Body Composition in Relation to Muscle Strength and Range of Joint Motion. *J Sports Med* 9:89-97

Layne C. S., and Spooner B. S. (1990) EMG Analysis of Human Postural Responses During Parabolic Flight Microgravity Episodes. *Aviat Space, and Environ Med.* 61:994-998

Lorentzon R., Elmqvist L., Sjostrom M., Fagerlund M., Fuglmeyer A. R. (1989) Thigh Musculature in Relation to Chronic Anterior Cruciate Ligament Tear: Muscle Size, Morphology, and Mechanical Output before Reconstruction. *Am J of Sports Medicine* 17(3):423-429

Loveland M. E., Kim S., Pandy M. G. and Whalen R. T. (1992) Effects of Gravity on Jumping Performance and Coordination. In Proceeding of North American Congress on Biomechanics, NACOB Annual Meeting in Chicago Il

Mandel J. (1984) The Statistical Analysis of Experimental Data. Dover Publications Inc, New York 224-239

Martin T. P., Edgerton V. R., Grindeland R. E. (1982) Influence of Spaceflight on Rat Skeletal Muscle. *J of Appl Physiol* 65:2318-2325

Maughan R. J., Watson J. S. and Weir J. (1983) Strength and Cross-sectional Area of Human Skeletal Muscle. *J Physiol* 338:37-49

May W. W. (1967) Relative Isometric Force of the Hip Abductor and Adductor Muscles. *Physical Therapy* 48(8):845-851

Mayhew J. L. and Salm P. C. (1990) Gender Differences in Anaerobic Power Tests. *Eur J Appl Physiol* 60:133-138

McCullagh P., Maughan R. J., Watson J. S., Weir J (1983) Biomechanical Analysis of the Knee in Relation to Measured Quadriceps Strength and Cross-sectional Area in Man. *J of Physiol* 346:60P

McKinley P., Pedotti A. (1992) Motor Strategies in Landing from a Jump: the Role of Skill in Execution. *Exp Brain Res* 90:427-440

Moore, T. W., Jaron D, Hrebien L, and Bender D. (1993) A Mathematical Model of G Time-Tolerance. *Aviat Space and Environ. Med.* 63:947-951

Morey E. R. and Baylink D. J. (1978) Inhibition of Bone Formation During Spaceflight. *Science* 201:1134-1141

Murray P., Maldwin D., Gardner E. M., Sepic S. B., and Downs W. J. (1977) Maximum Isometric Knee Flexor and Extensor Muscle Contractions, Normal Patterns of Torque Versus Time. *Physical Therapy* 57(6):637-643

Murray M. P. and Sepic S. B. (1970) Maximum Isometric Torque of Hip Abductor and Adductor Muscles. *Physical Therapy* 48(12):1327-1335

Narici M. V., Roi G. S., Landoni L. (1988) Force of Knee Extensor and Flexor Muscles and Cross-sectional Area Determined by Nuclear Magnetic Resonance Imaging. *Eur J of Apply Physiol* 57:39-44

Nutter J. and Thorland W. G. (1987) Body Composition and Anthropometry Correlates of Isokinetic Leg Extension Strength of Young Adult Males. *Research Quarterly* 58(1):47-51

Offenbacher E. L. (1970) Physics and the Vertical Jump. *American J of Physics* 38(7):829-836

Olson V. L., Smidt G. L. and Johnston R. C. (1972) The Maximum Torque Generated by the Eccentric, Isometric and Concentric Contractions of the Hip Abductor Muscles. *Physical Therapy* 52(2):149-157

Osternig L. R., Bates B. T., and James S. L. (1977) Isokinetic and Isometric Torque Force Relationships. *Arch Phys Med Rehabil* 58

Overend T. J., Cunningham D. A., Kramer J. F., Lefcoe M. S. and Paterson D. H. (1992) Knee Extensor and Knee Flexor Strength: Cross-sectional Area Ratios in Young and Elderly Men. *J of Gerontology* 47(6):M204-210

Pandy M., Anderson F. C., and Hull D. (1992) A Parameter Optimization Approach for the Optimal Control of Large-Scale, Musculoskeletal Systems. *J Biomech Engng* **114**, 450-460.

Pandy M. G., and Zajac, F. E. (1991) Optimal Muscular Coordination Strategies for Jumping. *J of Biomechanics* **24**,1-10.

Pandy M. G. and Zajac F. E. (1989) Dependence of Jumping Performance on Muscle Strength, Muscle-fiber Speed, and Tendon Compliance. In Issues in the Modeling and Control of Biomechanical Systems, ASME Winter Annual Meeting in San Francisco 12:59-63

Pandy M. G., Zajac F. E., Sim E. and Levine W. S. (1990) An Optimal Control Model for Maximum-height Human Jumping. *J of Biomechanics* 23(12):1185-1198

Perrine J. J. and Edgerton V. R. (1978) Muscle Force - Velocity and Power - Velocity Relationships under Isokinetic Loading. *Med Sci Sport* 10(3):159-166

Raytheon Service Company (undated) *Dynamic Environment Simulator DES User Guide* Burlington Massachusetts

Rim K., and Chao E. Y. (1969) Application of Optimization Principles in Determining the Internal Moments in Human Leg Joints During Gait. Defense Technical Information Center, Technical Report AD 699385

Roman J., A., Warren B. H., Niven J. I., and Graybeil A. (1963) Some Observations on the Behavior of a Visual Target and a Visual Afterimage During Parabolic Flight. *Aerospace Medicine* 841:845

Santschi W. R., DuBois J., and Omoto C. (1963) Moments of Inertia and Centers of Gravity of the Living Human Body. AMRL-TDR 63-36, Aerospace Medical Research Laboratories, Wright-Patterson AFB, OH (AD 410 451)

Schafer L. E. and Bagian J. P. (1993) Overhead and Forward Reach Capability During Exposure to + 1 to + 6 Gx Loads. *Aviat Space and Environ Med* 63:979-984

Schantz P., Randall-Fox E., Hutchison W., Tyden A. and Astrand P. O. (1983) Muscle Fiber Type Distribution, Muscle Cross-sectional Area and Maximal Voluntary Strength in Humans. *Acta Physiol Scand* 117:219-226

Scudder G. N. (1980) Torque Curves Produced at the Knee During Isometric and Isokinetic Exercise. *Arch Phys Med Rehabil* 61

Sekiguchi C. (1994) Issues of Health Care under Weightlessness. *Acta Physiol Scand* Suppl 616 150:89-97

Shadmehr R., Mussa-Ivaldi F. A. and Bizzi E (1993) Postural Force Fields of the Human Arm and Their Role in Generating Multijoint Movements. *J of Neuroscience* 13(1):45-52

Sim, E. (1988) The Application of Optimal Control Theory for Analysis of Human Jumping and Pedaling. Ph.D. Dissertation, Department of Electrical Engineering, University of Maryland, College Park

Sipilä S., Viitasalo J., Era P. and Suominen H (1991) Muscle Strength in Male Athletes Aged 70 - 81 Years and a Population Sample. *Eur J. Appl Physiol* 63:399-403

Smidt, G. L. (1973) Biomechanical Analysis of Knee Flexion and Extension. *J of Biomechanics* 6:79-92

van Soest A. J., Schwab A. L., Bobert M. F. and van Ingen Schenau G. J. (1993) The Influence of the Biarticularity of the Gastrocnemius Muscle on Vertical Jumping Achievement. *J of Biomechanics* 26:1-8

Spoor C. W. and van Leeuwen J. L. (1992) Knee Muscle Moment Arms from MRI and From Tendon Travel. *J of Biomechanics* 25(2):201-206

Spoor C. W. , van Leeuwen J. L., Meskers C. G. M., Titulaer A. F., and Huson A. (1990) Estimation of Instantaneous Moment Arms of Lower-Leg Muscles. *J of Biomechanics* 23(12):1247-1259

Suzuki, S., Watanabe, S., and Homma, S. (1982) EMG Activity and Kinematics of Human Cycling Movements at Different Constant Velocities. *Brain Research* 245-258

Termote J. L., Baert A., Crolla D., Palmers Y. and Bulcke J. A. (1980) Computed Tomography of the Normal and Pathologigic Muscular System. *Radiology* 137:439-444

Thornton W. E. and Rummel J. A. (1977) Muscle Deconditioning and its Prevention in Space Flight NASA SP-377, Washington D.C.

van Ingen Schenau G. J., Bobbert M. F., Huijing P. A. and Woittiez R. D. (1985) The Instantaneous Torque-angular Velocity Relationship in Plantar Flexion During Jumping. *Med Sci. Sports Exerc* 17(4):422-426

van Leeuwen J. L. and Spoor C. W. (1991) On the Role of Biarticular Muscles in Human Jumping. Letters to the Editor in *J of Biomechanics* 25:1-12

van Soest A. J., Schwab A. L., Bobbert M. F. and van Ingen Schenau G. J. (1993) The Influence of the Biarticularity of the Gastrocnemius Muscle on Vertical-Jumping Achievement. *J of Biomechanics* 26:1-8

Vanderwalle H., Peres G., and Monod H. (1987) Standard Anaerobic Exercise Tests. *Sports Medicine* 4:268-289

Vehrs P. R., Plowman S. A., and Fernhall B. Exercise During Gravity Inversion: Acute and Chronic Effects. *Arch Phys Med Rehabil* 69:950-954

Wennerberg D. (1991) Reliability of an Isokinetic Dorsiflexion and Plantar Flexion Apparatus. *Am J Sports Med* 19(5):519-522

Whalen R. (1993) Musculoskeletal Adaptation to Mechanical Forces on Earth and in Space. *Physiologist* 36:S127-S130

White A. T. and Johnson S. C. (1993) Physiological Aspects and Injury in Elite Alpine Skiers. *Sports Medicine* 15(3):170-178

Whiteside, T. C. D. (1961) Hand-Eye Coordination in Weightlessness. *Aviation Medicine* 719-725

Whinnery J. E. (1990) Recognizing +Gz-Induced Loss of Consciousness and Subject Recovery From Unconsciousness on a Human Centrifuge. *Aviat Space Environ Med* 61:406-412

Whiting W. C., Gregor R. J., Roy R. R. and Edgerton V. R. (1984) A Technique for Estimating Mechanical Work of Individual Muscles in the Cat During Treadmill Locomotion. *J of Biomechanics* 17(9):685-694

Wickiewicz T. L., Roland R. R., Powell P. L., Perrine J. J., Edgerton V. R. (1984) Muscle Architecture and Force-Velocity Relationships in Humans. *J Appl Physiol* 57:45-443

Whitsett C. (1963) Some Dynamic Response Characteristics of Weightless man. AMRL Technical Documentary Report 63-18. Wright-Patterson Air Force Base, Ohio

Winter D. A. (1990) Biomechanics and Motor Control of Human Movement. Wiley & Sons, New York

Yamaguchi G., Pandy M., and Zajac F. (1991) Dynamic Musculoskeletal Models of Human Locomotion: Perspectives on Model Formulation and Control. In Adaptability of Human Gait, Elsevier Science Publishers B.V. North Holland, .205-240

Young A., Stokes M., Round J. M. and Edwards R. H. T. (1983) The Effect of High Resistance Training on the Strength and Cross-sectional Area of the Human Quadriceps. *European J of Clinical Investigation* 13:411-417

Zajac F. E. (1989) Muscle and Tendon: Properties, Models, Scaling, and Application to Biomechanics and Motor Control. *CRC Critical Rev Biomed Engng* 17:359-411

Zajac F. E. (1993) Muscle Coordination of Movement: a Perspective. *J of Biomechanics* 26(Suppl 1):109-124

Zajac F. E. and Gordon M. E. (1991) Determining Muscle's Force and Action in Multi-articular Movement. *J Sci and Sports Med* 187-230

Zajac F. E., and Pandy M. G. (1991) On the Role of Biarticular Muscles in Human Jumping Authors' Response. *J. of Biomechanics* 25:2-3

Ziegler J. M. (1994) A Dynamic Computational Model of the Human Knee Joint with Implementation in Two Optimal Control Models. Ph.D. Dissertation, Dept of Mechanical Engineering, The University of Texas at Austin, Austin Texas

Vita

David R. Carpenter was born in Scranton Pennsylvania, 22 June 1955, to Ruth Marie Overbay Carpenter and George L. Carpenter. After completing his undergraduate work in Chemical Engineering at Pennsylvania State University in May 1979, he entered the United States Air Force as a 2nd Lieutenant. In 1985, Captain Carpenter was selected to return to Graduate School to study Industrial Hygiene at the University of Cincinnati. He graduated with a M.S. Degree in May 1987. In 1991, Captain Carpenter was again selected to return to Graduate School to study Biomechanics at the University of Texas at Austin and will Graduate with a Ph.D. in May 1995. Major Carpenter responsibilities during his Air Force career included Chief, Bioenvironmental Engineering Services, Air Force Consultant for Industrial Hygiene, Consultant to the Air Force Surgeon General for Ergonomic and Indoor Air Quality Issues, and Deputy Department Chairman, Bioenvironmental Engineering, United State Air Force School of Aerospace Medicine. Major Carpenter has received the Air Force Achievement Medal, Air Force Commendation Medal and Air Force Meritorious Service Medal. Major Carpenter has published several research articles dealing in different aspects of industrial hygiene since 1987.

Permanent address: 3801 Ebony Hollow Pass, Austin TX, 78739

This dissertation was typed by the author